UNIVERSITY OF CALIFORNIA
RIVERSIDE

Defense and Counter-Defense: Host-Induced Gene Silencing & *Phytophthora* Suppressor of RNA Silencing

A Dissertation submitted in partial satisfaction
of the requirements for the degree of

Doctor of Philosophy

in

Plant Pathology

by

Sara Dorhmi

December 2022

Dissertation Committee:
Dr. Shou-Wei Ding, Chairperson
Dr. Xuemei Chen
Dr. Meng Chen

The Dissertation of Sara Dorhmi is approved:

Committee Chairperson

University of California, Riverside

ACKNOWLEDGEMENTS

Firstly, my sincere thank you for all these years to my PhD supervisor Wenbo Ma, for being an incredibly insightful and intelligent guide in all facets of science and research. I have learned more about scientific investigation and myself than I could have possibly asked for, I am a better scientist because of it.

Thank you to my defense committee for their time, energy and years of feedback on my projects; Shou-Wei Ding, Xuemei Chen, Meng Chen. Thank you to my previous committee members Howard Judelson and Patricia Manosalva. Thank you to all those that made it possible to do my research, institutes, funding agencies and administrators. University of California – Riverside and the whole Plant Pathology Department, professors, and administrators, specifically Laura McGeehan. The Sainsbury Laboratory media services, staff, administrators, professors, and students that made the transition easier. Thank you to USDA – NIFA and TriCal for funding my research.

I would like to acknowledge and thank Chang-hyun Khang, who without his mentorship I would not have discovered my love for plant pathology and my desire to guide others.

I am forever in debt for the support, friendship and love I was given from my PhD cohort; Aidan Shands, Chien-hao Tseng, Gabriel Ortiz, Lindsey Pedroncelli-Gietzen and Nathan Riley. I am fortunate to know that I will forever have a group of incredible people by my side. I would like to acknowledge the care and friendship of those I met at UCR; Kelley Clark, Hannah Lovelace, Agustina De Francesco, Logan Collier and especially

Alexander McClelland. Thank you to all current and past members of the Ma lab for your incredible support; Yingnan Hou, Yi Zhai and Yufei Li specifically for contributions to my project, as well as Hui Li, Min Wang, Bozeng Tang, Michelle Hulin, Amelia Lovelace, Nicola Atkinson, Li Feng, Xiaodong Feng, Lena Knorr, Attilio Pascucci, Josh Bennett, Eva Hawara, Morgan Halane, Jessica Trinh, Simon Schwizer, Alexandre Leary and Min Qiu. Additionally, thank you to my mentees, Carolyne Dao and Haley Farrokhi, I have learned an incredible amount from you, thank you for letting me teach you about plant pathology.

Thank you to my friends for their support for many years, Dana Smith, Taylor Wood, Akeeme Martin, Cassie Willcoxon, Adam O'Kelley and Yuki Desouza.

Finally, I cannot begin to thank those at The Sainsbury Lab enough. To the fantastic TSLytherins for bringing me into your community especially during Covid. I want to specifically thank Mauricio Contreras for being my first friend here as well as Mikhaela Neequaye. Thank you to AmirAli Toghani, Josh Bennett, Jules Claeys, Camilla Molinari, Diana Gomez De La Cruz and Molly Bergum and many others. Your care with your time, food, kind words, support and laughter during my writing time will not be forgotten. I'd also like to thank Peter van-Esse for his time in energy in career mentorship.

DEDICATION

For some, science gives meaning to an otherwise nebulous existence. Therefore, I would like to dedicate this thesis to all those that have encouraged me, mentored me, and enriched my love for science.

Thus, I will dedicate this thesis to my family; Chifaa Dorhmi, Ewa Dorhmi, Nora Dorhmi and Zac Dorhmi who would move heaven and earth for me. I could not be a luckier daughter or sister.

Thank you to Richard Habel for being my biggest scientific cheerleader.

Lastly to Nate, despite all I have learned and accomplished, my greatest scientific discovery will always be you. I have won my own Nobel with you.

ABSTRACT OF THE DISSERTATION

Defense and Counter-Defense: Host-Induced Gene Silencing & *Phytophthora* Suppressor of RNA Silencing

by

Sara Dorhmi

Doctor of Philosophy, Graduate Program in Plant Pathology
University of California, Riverside, December 2022
Dr. Shou-Wei Ding, Chairperson

Since microorganisms first evolved to attack plants, there has been a constant evolutionary arms race. Plants evolve defensive mechanisms to protect themselves from pathogens that evolve countermeasures. One instance is host-induced gene silencing (HIGS), where small RNAs (sRNAs) endogenous to the plant confer resistance presumably by silencing their target gene(s) in the invading pathogen. The pathogen counter may be effectors such as *Phytophthora* suppressor of RNA silencing 2 (PSR2), which suppresses the sRNA processes in the plant host. This thesis aims to understand the mechanisms underlying HIGS and suppressing of HIGS by PSR2.

In chapter 1, I investigated the virulence activities of PSR2, which was previously found to be associated with the Double-stranded RNA binding protein 4 (DRB4) in *Arabidopsis thaliana*. Unpublished data in the lab also indicate that PSR2 associates with the plant Serine/Threonine protein phosphatase 2A (PP2A). I tested the hypothesis that PSR2 may regulate the phosphorylation levels of DRB4. By examining the

phosphorylation of DRB4 in Arabidopsis expressing PSR2, it appears that PSR2 may not affect the overall level of DRB4 phosphorylation. This suggests another mechanism underlies potential manipulation of DRB4 by PSR2.

In chapter 2, I tested whether small interfering RNAs (siRNAs) spawned from the pentatricopeptide repeat protein (PPR) transcripts can directly silence target genes in *Phytophthora* pathogen(s). I attempted to generate *Phytophthora capsici* mutants that contain various mutations in *Phyca_554980*, which was previously identified to be potentially targeted by *PPR*-siRNAs. I was unable to manipulate *Phyca_554980* through point mutation, replacement or overexpression. This could indicate a key role of this gene in the general fitness of *P. capsici*.

In chapter 3, I explored to enhance HIGS in soybean by introducing miRNA-PPR circuits and tested whether this approach could lead to the accumulation of *PPR*-siRNAs that confer resistance to *Phytophthora sojae*. The constructs were introduced into soybean using the *Agrobacterium rhizogenes*-mediated hairy root gene expression system. However, I was unable to detect *PPR*-siRNAs despite the production of mature miRNAs in the roots. Further investigations are required to further optimize the system.

My thesis research provides insight into plant-pathogen arms race centered on sRNA-mediated defense and counter-defense.

Table of Contents

List of Figures

General Introduction

List of Tables

Chapter 2

Chapter 3

GENERAL INTRODUCTION

Phytophthora disease

Oomycetes are a class of diverse filamentous microorganisms belonging to the Kingdom Stramenopilia (Judelson & Blanco, 2005). This group includes a destructive genus of plant pathogens called *Phytophthora*. *Phytophthora*, aptly meaning "the plant destroyer," cause devastating plant diseases such as damping off and late blight. Symptoms of *Phytophthora* disease include wilting, leaf blights, root, and fruit rots. There are currently over 100 described species of *Phytophthora* that infect a wide range of plants (Brasier, 2008). This causes billions of dollars in damage and prevention every year particularly in agriculture and horticulture, as well as in conservation and forestry (Erwin & Ribeiro, 1996; Wawra et al., 2012). *Phytophthora capsici* infects peppers and over 45 other plant species resulting in $100 million in losses annually (Bosland & Lindsey, 2008). *Phytophthora sojae* infects soybean seeds, seedlings and in favorable conditions causes stem and root rot. Modern disease management practices consist of integrated multi-level approaches including regulation of importation and trade, implementation of cultural practices such as irrigation management, and usage of resistant plant varieties in conjunction with targeted fungicide applications.

Phytophthora are hemibiotrophic pathogens. Starting the biotrophic stage, *Phytophthora* infects plant tissue by bearing reproductive structures called sporangia that produce and release single-celled flagellated motile spores called zoospores that encyst in a host cell. The cysts germinate and form hyphae to produce feeding structures in host cells called haustoria that penetrate the plant cell wall to form an intimate interaction with the host plasma membrane (Wang et al., 2018). This structure is also the site of secretion of hundreds

of proteins called effectors into the host cells. These effectors have a wide variety of jobs to aid in pathogenesis. For example, some effectors act as inhibitors of host proteases (Tian et al., 2007), to induce necrosis (Armitage et al., 2018), to suppress plant immunity (He et al., 2019; Li et al., 2020) or as RNA silencing suppressors (Qiao et al., 2013). Following the biotrophic stage, the infection enters the necrotrophic stage which leads to the death of infected plant cells and the development of disease symptoms. After host cell death, zoospores are released from sporangia and begin the infection cycle once again. *Phytophthora* may reproduce sexually or asexually. The heterothallic species require cross fertilization using A1 and A2 mating types (Galindo & Gallegly, 1960). Homothallic species are self-fertile. Some species of *Phytophthora* produce survival structures such as oospores or chlamydospores that are able to survive in soil, plant debris, and sub-optimal conditions. When environmental conditions are optimal the dormant spores germinate and form hyphae, beginning the cycle again (Figure I) (Fawke et al., 2015; Stassen & Van den Ackerveken, 2011).

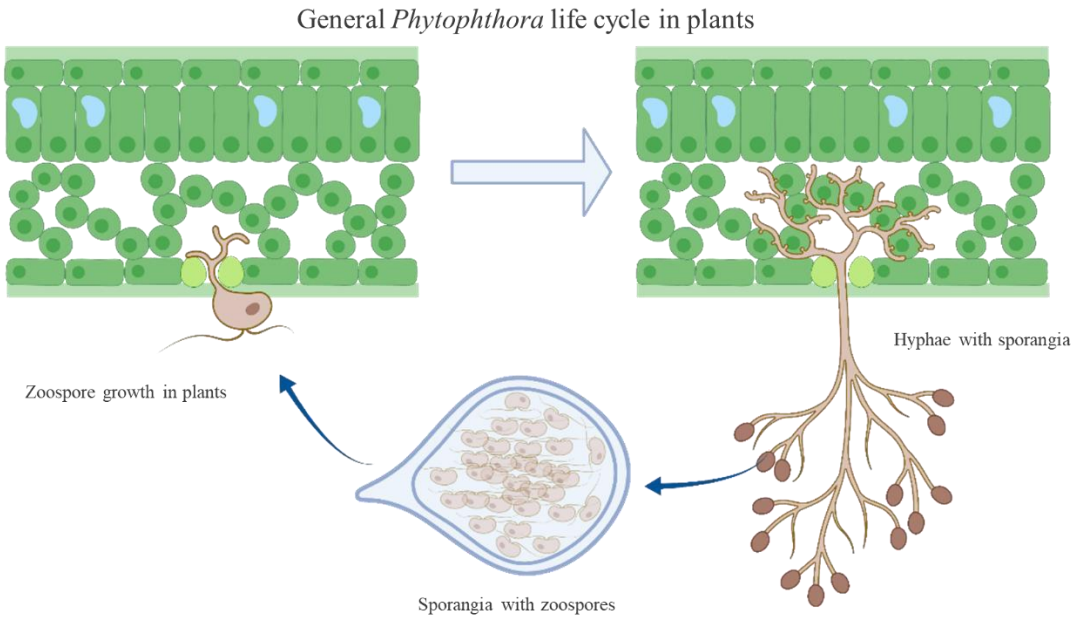

Figure I. *Phytophthora* disease cycle.

Sporangia produce motile zoospores that are released when proper environmental conditions are met. Upon coming in contact with a suitable host the zoospores encyst and subsequently germinate to produce infection hyphae. The hyphae form haustoria, from which effectors are delivered into plant cells. Hyphae may then develop into a variety of different structures depending on species and conditions. These includes sporangia (asexual, present in all species), oospores (sexual), and chlamydospores (asexual survival structure). These structures then release spores, germinate, and develop hyphae, continuing the cycle (Made with Biorender).

Plant immunity

Plants do not possess mobile immune cells or an adaptive immune system (Kumar et al., 2011). Instead, plants respond to pathogen infection using a two-tiered innate immune system that distinguishes "self" from "non-self". Initially, the plant immune system relies on pattern triggered immunity (PTI). This first line of immunity is triggered by the recognition of pathogen-associated or microbial-associated molecular patterns (PAMPS and MAMPS) by cell membrane-embedded pattern recognition receptors (Boller & He, 2009). One PAMP, Flg22, is an epitope of bacterial flagellin and is recognized by PRR Flagellin Sensing 2 (FLS2) (Felix et al., 1999). Flg22 mediates the interaction between FLS2 and the co-receptor brassinosteroid insensitive 1-associated kinase 1 (BAK1), where the three form a complex which results in transphosphorylation events, immune signaling transduction and, ultimately, plant defense (Chinchilla et al., 2007; Sun et al., 2013). A *Phytophthora infestans* PAMP, infestin 1 (Kamoun et al., 1998) leads to cell death through the recognition by a lectin-like receptor kinase protein of *Nicotiana benthamiana* (NbLRK1) (Fawke et al., 2015). The coevolution of plant and pathogen interactions has resulted in a large array of PRRs encoded in plant genomes. Though PTI provides a basal defense, successful pathogens are able to overcome it by using effectors.

Pathogen effectors translocate into host plant cells to subvert host defenses and facilitate invasion. Effector-triggered susceptibility (ETS) is the result of effectors manipulating the host target and disrupting immune signaling (Jones & Dangl, 2006; Kamoun, 2007). To counter the virulence activity of effectors, plants developed intracellular immune receptors, which are nucleotide-binding leucine-rich repeat proteins (NLR) (Biezen

& Jones, 1998; Meyers et al., 2003). Genes encoding NLRs are called the resistance genes or R genes. NLRs are evolved to recognize effector activity and trigger the second tier of plant immunity, effector-triggered immunity (ETI). ETI often leads to a localized programmed cell death called hypersensitive response (HR), which limits the spread of the pathogen from the infection site (Boller & He, 2009; Dangl et al., 2013). AvR3a is a *P. infestans* effector recognized by potato NLR gene, R3a, which triggers HR (Armstrong et al., 2005). Effectors that can trigger HR by recognition of their cognate plant NLR are sometimes called avirulence proteins (Avr). Within the gene-for-gene model described by H. H. Flor, this interaction is termed incompatible as it does not cause disease. The gene-for-gene hypothesis says for each gene that controls resistance in the host, there is a gene controlling avirulence in the pathogen. This model provided a foundation of the genetic basis in plant-pathogen interactions (Flor, 1956; Kaur et al., 2021). Building on this, the zig-zag model describes this back-and-forth phenomenon of defense and counter-defense in plants and pathogens engaged in a constant co-evolutionary arms race (Figure II). Specifically, the one for one "exchange" of pathogen associated molecular patterns (PAMPs) with PAMP triggered immunity in the host, followed by iterations of the pathogen developing effector proteins as a countermeasure, in turn selecting for hosts with R genes targeting those effector proteins, followed by new effectors, and so on (Jones & Dangl, 2006).

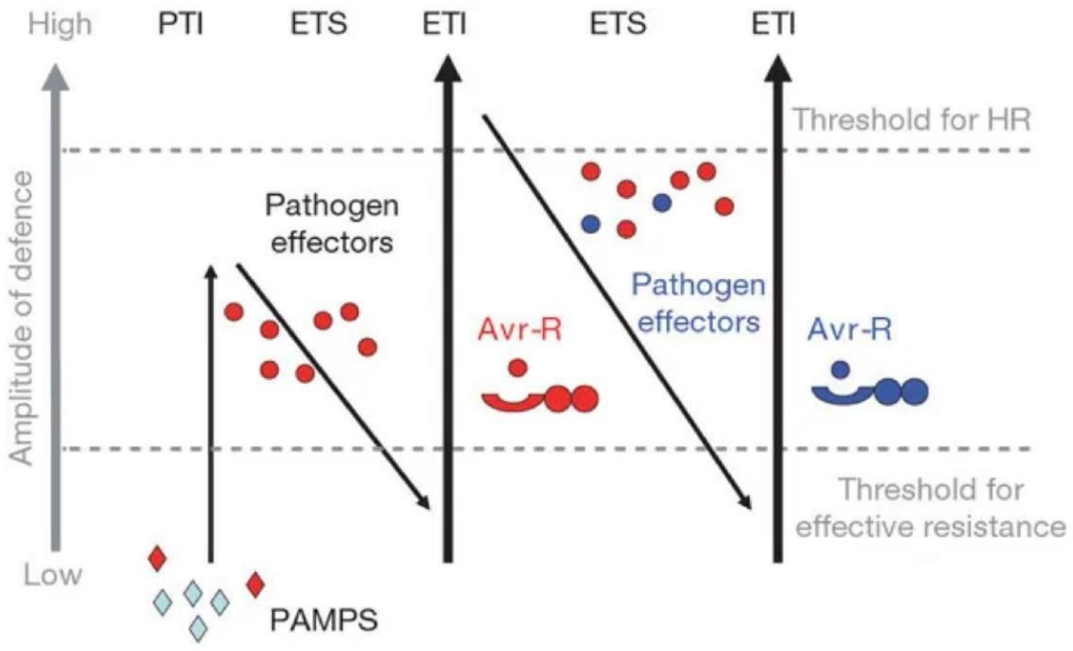

Figure II. Zigzag model of the plant immune system.

Host pattern recognition receptors (PRRs) recognize pathogen-associated molecular patterns (PAMPs) leading to PAMP-triggered immunity (PTI). Effective pathogens release effectors in order to dampen PTI, leading to effector triggered susceptibility (ETS). The host plant may develop the ability to recognize these effectors (called Avr) using resistance proteins (R), causing effector-triggered immunity (ETI), and potentially leading to the hypersensitive response (HR). This then forces selection of pathogen isolates lacking the original effector being detected by the host, and possibly the evolution of new effectors. This in turn selects for plants with novel resistance proteins, once again establishing ETI and continuing the "zig zag" pattern. (Jones and Dangl, 2006).

Small RNAs and RNA Silencing

Small RNAs (sRNA) are short (18-30 nucleotides) non-coding RNA molecules. The principal activity of sRNAs is regulating specific gene expression through sequence complementarity (Chen, 2009; Vaucheret, 2006). This activity is called RNA silencing which is a mechanism active in most eukaryotes (Kim & Rossi, 2008). In plants, the term RNA silencing involves suppression of gene expression by 21 to 24-nucleotide (nt) sRNAs produced by Dicer enzymes. There are two major small RNAs classes in plants, microRNAs (miRNAs) and small interfering RNAs (siRNAs), which are generated from distinct precursors and pathways. These sRNAs mediate post-transcriptional gene silencing (PTGS) through RNA cleavage and/or translation inhibition or transcriptional gene silencing (TGS) through RNA-dependent DNA methylation and/or histone modification (Kim et al., 2014). The latter has been involved in epigenetic events that lead to the suppression of repetitive sequence such as transposable elements (Hollister & Gaut, 2009).

miRNAs

A plant genome commonly encodes hundreds of miRNAs by the *MIRNA* (*MIR*) genes, many of which are organized in *MIR* families (Wang et al., 2019). Plant miRNAs are crucial to plant development and in stress response (Vaucheret et al., 2014; Sunkar et al., 2012). MiRNAs are normally 21-22 nucleotides in length and derived from single-stranded primary miRNA transcripts (pri-miRNAs) transcribed from *MIR* genes by RNA polymerase II (Budak & Akpinar, 2015). The pri-miRNAs can range from 60 nt to over 500 nt and include hairpin-like structures, which can be identified and are processed by Dicer-like RNAse III endonuclease (DCL) (Samarfard et al., 2022) into short stem-loop structures

called pre-miRNA together with a double stranded RNA-binding protein (HYL1) and a zinc finger protein SERRATE (SE) (Fang & Spector, 2007; Zhu, 2008). These pre-miRNAs are further processed into miRNA duplexes with 3’ overhangs after a second cleavage by DCL (Rogers & Chen, 2013; Kim, 2005)

The miRNA*/miRNA duplexes, also known as the guide strand/passenger strand, are subsequently methylated by the small RNA methyltransferase HEN1 and are transported to the cytoplasm. The guide strand is loaded onto an Argonaute (AGO) protein, while the passenger strand is ejected and degraded (Wang et al., 2019). AGO forms an effector complex called RNA-induced silencing complex (RISC), in which thetarget genes are silenced by directing mRNA cleavage or translation repression (Figure IIIa) (Gu et al., 2012; Rogers & Chen, 2013; Pratt & MacRae, 2009).

siRNAs

Unlike miRNAs, siRNAs are generated from long double-stranded RNA (dsRNA) precursors produced by RNA-dependent RNA polymerases (RdRPs). SiRNA precursors can be exogenous, such as those from viruses and inverted repeats, or endogenous transcripts. There are several classes of siRNAs including heterochromatic siRNA, natural antisense transcript-derived siRNA, repeat-associated siRNA, and trans-acting siRNA (Borges & Martienssen, 2015). Biogenesis of siRNAs begins with recognition of the dsRNAs by one of several different DCL proteins (DCL1-4). They then cleave the dsRNAs into different classes of siRNAs based on size (Margis et al., 2006). One strand of the siRNA duplex is then loaded into an AGO protein for target gene silencing (Figure IIIa) (Khraiwesh et al., 2012; Petri et al., 2011). SiRNAs are also essential for both plant development and immunity.

A.

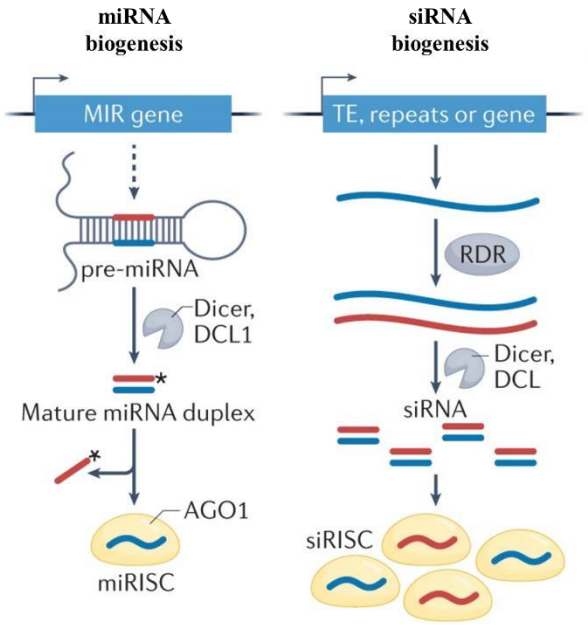
miRNA biogenesis
siRNA biogenesis
MIR gene
TE, repeats or gene
pre-miRNA
RDR
Dicer, DCL1
Dicer, DCL
Mature miRNA duplex
siRNA
AGO1
siRISC
miRISC

B.

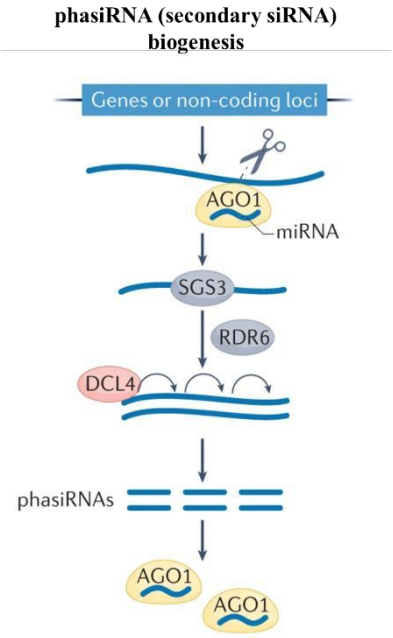
phasiRNA (secondary siRNA) biogenesis
Genes or non-coding loci
AGO1
miRNA
SGS3
RDR6
DCL4
phasiRNAs
AGO1
AGO1

Figure III Small RNA biogenesis.

A. miRNA biogenesis (left), miRNA precursors are *MIR* transcripts that form stem loop structures which are then processed by Dicer and form a mature miRNA duplex. siRNA biogenesis (right), siRNA precursors are derived from dsRNA through RdRP then cut into 21-24 nt fragments. Both are loaded into AGO protein and incorporated into RISC for post-translational gene regulation. **B.** Phased secondary siRNA biogenesis can start from coding or non-coding loci, then triggered by a miRNA for an initial cleavage. RDR6 and SGS3 then generate a long dsRNA which is then cleaved by DCLs. (Adapted from Chen and Rechavi, 2021).

Secondary siRNAs

A class of siRNAs that are of increasing interest are called secondary siRNAs, where, unlike siRNAs, their production is triggered by specific miRNAs. The "trigger" miRNA, often 22 nt in length, initiates a cleavage of a primary RNA transcribed from coding or noncoding genes. The cleavage products are fully or partially converted by RDR6 accompanied by suppressor of gene silencing 3 (SGS3) to generate a long dsRNA precursor (Rajeswaran & Pooggin, 2012). This precursor is then cleaved by DCLs to produce 21-22 nucleotide siRNAs. Since these RNA precursors are processively cleaved, a phased alignment of small RNAs called phased siRNAs (phasiRNA) are generated (Figure IIIb). Loci that spawn phasiRNAs are called PHAS loci (Arikit et al., 2014). Some phasiRNAs have been shown to regulate coding genes through mRNA cleavage in trans (Fei et al., 2013), which were named trans-acting siRNAs (tasiRNAs). TasiRNAs regulate mRNA at complementary target sites, like many miRNAs (Allen et al., 2005).

There are several primary targets of miRNAs that would generate secondary siRNA, such as the non-coding trans-acting siRNAs generating loci (TAS) and some protein-coding genes like pentatricopeptide repeat (PPR) proteins and NLR (Allen et al., 2005; Zhai et al., 2011). *PPR* genes form a large family of proteins conserved in plants (O'Toole et al., 2008). Over 400 proteins that have been identified in the rice and Arabidopsis genome (Chen et al., 2018). Many *PPR* genes can be targeted for secondary siRNA production by miRNAs which may then regulate other genes (Xia et al., 2013). Some PPRs in Arabidopsis interact with mitochondria and other organelles which are necessary for plant defense by producing salicylic acid and reactive oxygen species (Koprivova et al., 2010; Schwarzländer &

Finkemeier, 2013). They are also widely considered to be involved in RNA regulation and processing (Wang et al., 2021).

Small RNAs in plant immunity

The plant immune system consists of two categories: pattern triggered immunity (PTI) provoked by pathogen molecular patterns and effector triggered immunity (ETI) induced by pathogen effectors (Jones & Dangl, 2006). miRNAs and siRNAs can both regulate both branches of this innate immunity. MiRNAs have been shown to play an important role in plant development, such as miR393, a microRNA that targets auxin receptors (Navarro et al., 2006). They have also been shown to have a role in PTI and ETI to positively regulate resistance against bacterial, fungal and other pathogen invasions. Overexpression of miR393 enhances resistance to virulent pathogens such as *Pseudomonas syringae* (Navarro et al., 2006) and promotes soybean defense against *Phytophthora sojae* (Wong et al., 2014). Down-regulation of miR156, miR159, miR164, and miR168 in plants infected with powdery mildew fungi resulted in the upregulation of the corresponding signal transduction, stress response and oxidative stress response genes (Chen & Cao, 2015; Cui et al., 2020). These results suggest miRNAs can regulate plant immunity.

siRNAs also have a role in plant immunity. For instance, siRNAs can regulate gene expression reprogramming during plant defense as a response to bacterial or viral infection (Katiyar-Agarwal et al., 2006; Wang et al., 2011). Emerging evidence has suggested that siRNAs also have a role in regulating the expression of NLRs (Deng et al., 2018; Leonetti et al., 2021). Furthermore, plant sRNA silencing machinery targets viral dsRNAs, and produces

virus-derived siRNAs to silence viral genes in a natural antiviral process (Hamilton & Baulcombe, 1999).

Host-induced gene silencing (HIGS)

As RNA silencing can act in a non-cell autonomous manner (Fagard & Vaucheret, 2000), it has been suggested that sRNAs may act as mobile molecules and silence target genes in recipient cells (Molnar et al., 2011). Cell-to-cell trafficking, both local and systemic, have been well documented in sRNAs (Liu & Chen, 2018). Small RNAs may also translocate from plant cells into some pathogens. This process is called host-induced gene silencing (HIGS) involving RNAi where small RNAs endogenous to plants but complementary to a pathogen gene, induce the silencing of pathogen genes to confer host resistance (Qiao et al., 2021). The first example of HIGS naturally occurring in a plant pathosystem was found in cotton and the fungal pathogen *Verticillium dahliae*. During infection, the production of miR166 and miR159 were increased in cotton plants and also detected in the hyphae of *V. dahliae*, which resulted in target gene silencing in the fungus. Two fungal genes, *cysteine protease* (*Clp-1*) and *hydroxylase* (*Hic-15*) were found to be silenced by miR166 and miR159 respectively (Zhang et al., 2016).

In addition to miRNAs, secondary siRNAs are also suggested to be players in HIGS. Two Arabidopsis-originating tasiRNAs were shown to silence target genes in the fungal pathogen *Botrytis cinerea* suggesting that secondary siRNAs could also silence pathogen genes during infection (Cai et al., 2018). Furthermore, secondary siRNAs from a pool generated from *PPR* gene transcripts can potentially target genes in *P. capsici*, one of these genes is required for sporulation and the full virulence of *P. capsici* (Hou et al., 2019). An

important piece of evidence supporting a role of secondary siRNAs in plant defense is the identification and characterization of *Phytophthora* and fungal effectors that can suppress this particular sRNA pathway in plants. The *Phytophthora* effector PSR2 effects the accumulation of siRNAs produced from *TAS1*, *TAS2*, and *PPR* transcripts in *Arabidopsis thaliana* (Hou et al., 2019). In addition, the rust fungus *Puccinia graminis* f. sp. *tritici* effector PgtSR1, also reduced siRNA production (Yin et al., 2019).

HIGS has been used to confer resistance to various fungal and oomycete pathogens. The oomycete *Bremia lactucae* causes downy mildew of lettuce. Transgenic lettuce plants, expressing inverted repeats of fragments of either the *HAM34* or *Cellulose Synthase* (*CES1*) genes of *B. lactucae*, decreased the expression of these genes which resulted in considerably reduced growth and lack of sporulation of *B. lactucae* (Govindarajulu et al., 2015). The HIGS mechanism has also been used to suppress fungal diseases like *Fusarium* through generating dsRNA complementary to fungal cytochrome P450 lanosterol C-14α-demethylase (CYP51) genes. As these target genes are essential for ergosterol biosynthesis, it resulted in reduced virulence and modification of fungal morphology similar to what is seen after treatment with the CYP51 enzyme-targeting fungicide tebuconazole (Koch et al., 2013). Additionally, HIGS has been successfully introduced as a crop disease prevention in tobacco against the root-knot nematode *Meloidogyne incognita* by targeting a gene coding for splicing factor and another coding for integrase (Yadav et al., 2006). These studies corroborate that HIGS can be a successful strategy to improve plant resistance to disease.

REFERENCES

A, G., J, & Gallegly, M. E. (1960). The nature of sexuality in Phytophthora infestans. *Phytopathology*, *50*, 123–128.

Allen, E., Xie, Z., Gustafson, A. M., & Carrington, J. C. (2005). MicroRNA-Directed Phasing during Trans-Acting siRNA Biogenesis in Plants. *Cell*, *121*(2), 207–221. https://doi.org/10.1016/j.cell.2005.04.004

Arikit, S., Xia, R., Kakrana, A., Huang, K., Zhai, J., Yan, Z., Valdés-López, O., Prince, S., Musket, T. A., Nguyen, H. T., Stacey, G., & Meyers, B. C. (2014). An Atlas of Soybean Small RNAs Identifies Phased siRNAs from Hundreds of Coding Genes. *The Plant Cell*, *26*(12), 4584–4601. https://doi.org/10.1105/tpc.114.131847

Armitage, A. D., Lysøe, E., Nellist, C. F., Lewis, L. A., Cano, L. M., Harrison, R. J., & Brurberg, M. B. (2018). Bioinformatic characterisation of the effector repertoire of the strawberry pathogen Phytophthora cactorum. *PLOS ONE*, *13*(10), e0202305. https://doi.org/10.1371/journal.pone.0202305

Armstrong, M. R., Whisson, S. C., Pritchard, L., Bos, J. I. B., Venter, E., Avrova, A. O., Rehmany, A. P., Böhme, U., Brooks, K., Cherevach, I., Hamlin, N., White, B., Fraser, A., Lord, A., Quail, M. A., Churcher, C., Hall, N., Berriman, M., Huang, S., … Birch, P. R. J. (2005). An ancestral oomycete locus contains late blight avirulence gene *Avr3a* , encoding a protein that is recognized in the host cytoplasm. *Proceedings of the National Academy of Sciences*, *102*(21), 7766–7771. https://doi.org/10.1073/pnas.0500113102

Biezen, E. A. van der, & Jones, J. D. G. (1998). The NB-ARC domain: A novel signalling motif shared by plant resistance gene products and regulators of cell death in animals. *Current Biology*, *8*(7), R226–R228. https://doi.org/10.1016/S0960-9822(98)70145-9

Boller, T., & He, S. Y. (2009). Innate immunity in plants: An arms race between pattern recognition receptors in plants and effectors in microbial pathogens. *Science (New York, N.Y.)*, *324*(5928), 742–744. https://doi.org/10.1126/science.1171647

Borges, F., & Martienssen, R. A. (2015). The expanding world of small RNAs in plants. *Nature Reviews. Molecular Cell Biology*, *16*(12), 727–741. https://doi.org/10.1038/nrm4085

Bosland, P. W., & Lindsey, D. L. (Eds.). (n.d.). A seedling screen for phytophthora root rot of pepper, Capsicum annuum. *PLANT DISEASE*.

Brasier, C. M. (2008). The biosecurity threat to the UK and global environment from international trade in plants. *Plant Pathology*, *57*(5), 792–808. https://doi.org/10.1111/j.13653059.2008.01886.x

Budak, H., & Akpinar, B. A. (2015). Plant miRNAs: Biogenesis, organization and origins. *Functional & Integrative Genomics*, *15*(5), 523–531. https://doi.org/10.1007/s10142-015

Chen, L., Li, Y., Li, C., Shi, Y., Song, Y., Zhang, D., Li, Y., & Wang, T. (2018). Genome wide analysis of the pentatricopeptide repeat gene family in different maize genomes and its important role in kernel development. *BMC Plant Biology*, *18*(1), 366. https://doi.org/10.1186/s12870-018-1572-2

Chen, M., & Cao, Z. (2015). Genome-wide expression profiling of microRNAs in poplar upon infection with the foliar rust fungus Melampsora larici-populina. *BMC Genomics*, *16*, 696. https://doi.org/10.1186/s12864-015-1891-8

Chen, X. (2009). Small RNAs and their roles in plant development. *Annual Review of Cell and Developmental Biology*, *25*, 21–44. https://doi.org/10.1146/annurev.cellbio.042308.113417

Chinchilla, D., Zipfel, C., Robatzek, S., Kemmerling, B., Nürnberger, T., Jones, J. D. G., Felix, G., & Boller, T. (2007). A flagellin-induced complex of the receptor FLS2 and BAK1 initiates plant defence. *Nature*, *448*(7152), 497–500. https://doi.org/10.1038/nature05999

Cui, C., Wang, J.-J., Zhao, J.-H., Fang, Y.-Y., He, X.-F., Guo, H.-S., & Duan, C.-G. (2020). A Brassica miRNA Regulates Plant Growth and Immunity through Distinct Modes of Action. *Molecular Plant*, *13*(2), 231–245. https://doi.org/10.1016/j.molp.2019.11.010

Dangl, J. L., Horvath, D. M., & Staskawicz, B. J. (2013). Pivoting the plant immune system from dissection to deployment. *Science (New York, N.Y.)*, *341*(6147), 746–751. https://doi.org/10.1126/science.1236011

Deng, Y., Wang, J., Tung, J., Liu, D., Zhou, Y., He, S., Du, Y., Baker, B., & Li, F. (2018). A role for small RNA in regulating innate immunity during plant growth. *PLOS Pathogens*, *14*(1), e1006756. https://doi.org/10.1371/journal.ppat.1006756

Erwin, D. C., & Ribeiro, O. K. (1996). Phytophthora diseases worldwide. *Phytophthora Diseases Worldwide*. https://www.cabdirect.org/cabdirect/abstract/19971001256

Fagard, M., & Vaucheret, H. (2000). (TRANS)GENE SILENCING IN PLANTS: How Many Mechanisms? *Annual Review of Plant Physiology and Plant Molecular Biology*, *51*, 167–194. https://doi.org/10.1146/annurev.arplant.51.1.167

Fang, Y., & Spector, D. L. (2007). Identification of nuclear dicing bodies containing proteins for microRNA biogenesis in living Arabidopsis plants. *Current Biology: CB*, *17*(9), 818–823. https://doi.org/10.1016/j.cub.2007.04.005

Fawke, S., Doumane, M., & Schornack, S. (2015). Oomycete Interactions with Plants: Infection Strategies and Resistance Principles. *Microbiology and Molecular Biology Reviews : MMBR*, *79*(3), 263–280. https://doi.org/10.1128/MMBR.00010-15

Fei, Q., Xia, R., & Meyers, B. C. (2013). Phased, Secondary, Small Interfering RNAs in Posttranscriptional Regulatory Networks. *The Plant Cell*, *25*(7), 2400–2415. https://doi.org/10.1105/tpc.113.114652

Felix, G., Duran, J. D., Volko, S., & Boller, T. (1999). Plants have a sensitive perception system for the most conserved domain of bacterial flagellin. *The Plant Journal: For Cell and Molecular Biology*, *18*(3), 265–276. https://doi.org/10.1046/j.1365-313x.1999.00265.x

Flor, H. H. (1956). The Complementary Genic Systems in Flax and Flax Rust**Joint contribution from the Field Crops Research Branch, Agricultural Research Service, United States Department of Agriculture and the North Dakota Agricultural Experiment Station. In M. Demerec (Ed.), *Advances in Genetics* (Vol. 8, pp. 29–54). Academic Press. https://doi.org/10.1016/S0065-2660(08)60498-8

Govindarajulu, M., Epstein, L., Wroblewski, T., & Michelmore, R. W. (2015). Host-induced gene silencing inhibits the biotrophic pathogen causing downy mildew of lettuce. *Plant Biotechnology Journal*, *13*(7), 875–883. https://doi.org/10.1111/pbi.12307

Gu, S., Jin, L., Huang, Y., Zhang, F., & Kay, M. A. (2012). Slicing-independent RISC activation requires the argonaute PAZ domain. *Current Biology: CB*, *22*(16), 1536–1542. https://doi.org/10.1016/j.cub.2012.06.040

Hamilton, A. J., & Baulcombe, D. C. (1999). A species of small antisense RNA in posttranscriptional gene silencing in plants. *Science (New York, N.Y.)*, *286*(5441), 950–952. https://doi.org/10.1126/science.286.5441.950

He, Q., McLellan, H., Hughes, R. K., Boevink, P. C., Armstrong, M., Lu, Y., Banfield, M. J., Tian, Z., & Birch, P. R. J. (2019). Phytophthora infestans effector SFI3 targets potato UBK to suppress early immune transcriptional responses. *The New Phytologist*, *222*(1), 438–454. https://doi.org/10.1111/nph.15635

Hollister, J. D., & Gaut, B. S. (2009). Epigenetic silencing of transposable elements: A tradeoff between reduced transposition and deleterious effects on neighboring gene expression. *Genome Research*, *19*(8), 1419. https://doi.org/10.1101/gr.091678.109

Hou, Y., Zhai, Y., Feng, L., Karimi, H. Z., Rutter, B. D., Zeng, L., Choi, D. S., Zhang, B., Gu, W., Chen, X., Ye, W., Innes, R. W., Zhai, J., & Ma, W. (2019). A Phytophthora Effector Suppresses Trans-Kingdom RNAi to Promote Disease Susceptibility. *Cell Host & Microbe*, *25*(1), 153-165.e5. https://doi.org/10.1016/j.chom.2018.11.007

Jones, J. D. G., & Dangl, J. L. (2006). The plant immune system. *Nature*, *444*(7117), Article 7117. https://doi.org/10.1038/nature05286

Judelson, H. S., & Blanco, F. A. (2005). The spores of Phytophthora: Weapons of the plant destroyer. *Nature Reviews. Microbiology*, *3*(1), 47–58. https://doi.org/10.1038/nrmicro1064

Rogers, K., & Chen, Xuemei. (2013). Biogenesis, turnover, and mode of action of plant microRNAs. *The Plant Cell*, *25*(7). https://doi.org/10.1105/tpc.113.113159

Kamoun, S. (2007). Groovy times: Filamentous pathogen effectors revealed. *Current Opinion in Plant Biology*, *10*(4), 358–365. https://doi.org/10.1016/j.pbi.2007.04.017

Kamoun, S., van West P, Vleeshouwers, V., de Groot KE, & Govers, F. (1998). Resistance of nicotiana benthamiana to phytophthora infestans is mediated by the recognition of the elicitor protein INF1. *The Plant Cell*, *10*(9), 1413–1426.

Katiyar-Agarwal, S., Morgan, R., Dahlbeck, D., Borsani, O., Villegas, A., Zhu, J.-K., Staskawicz, B. J., & Jin, H. (2006). A pathogen-inducible endogenous siRNA in plant immunity. *Proceedings of the National Academy of Sciences*, *103*(47), 18002–18007. https://doi.org/10.1073/pnas.0608258103

Kaur, B., Bhatia, D., & Mavi, G. S. (2021). Eighty years of gene-for-gene relationship and its applications in identification and utilization of R genes. *Journal of Genetics*, *100*, 50.

Khraiwesh, B., Zhu, J.-K., & Zhu, J. (2012). Role of miRNAs and siRNAs in biotic and abiotic stress responses of plants. *Biochimica et Biophysica Acta*, *1819*(2), 137–148. https://doi.org/10.1016/j.bbagrm.2011.05.001

Kim, D. H., & Rossi, J. J. (2008). RNAi mechanisms and applications. *BioTechniques*, *44*(5), 613–616. https://doi.org/10.2144/000112792

Kim, V. N. (2005). MicroRNA biogenesis: Coordinated cropping and dicing. *Nature Reviews Molecular Cell Biology*, *6*(5), 376–385. https://doi.org/10.1038/nrm1644

Kim, Y. J., Maizel, A., & Chen, X. (2014). Traffic into silence: Endomembranes and posttranscriptional RNA silencing. *The EMBO Journal*, *33*(9), 968–980. https://doi.org/10.1002/embj.201387262

Koch, A., Kumar, N., Weber, L., Keller, H., Imani, J., & Kogel, K.-H. (2013). Host-induced gene silencing of cytochrome P450 lanosterol C14α-demethylase-encoding genes confers strong resistance to Fusarium species. *Proceedings of the National Academy of Sciences of the United States of America*, *110*(48), 19324–19329. https://doi.org/10.1073/pnas.1306373110

Koprivova, A., des Francs-Small, C. C., Calder, G., Mugford, S. T., Tanz, S., Lee, B.-R., Zechmann, B., Small, I., & Kopriva, S. (2010). Identification of a pentatricopeptide repeat protein implicated in splicing of intron 1 of mitochondrial nad7 transcripts. *The Journal of Biological Chemistry*, *285*(42), 32192–32199. https://doi.org/10.1074/jbc.M110.147603

Kumar, H., Kawai, T., & Akira, S. (2011). Pathogen Recognition by the Innate Immune System. *International Reviews of Immunology*, *30*(1), 16–34. https://doi.org/10.3109/08830185.2010.529976

Leonetti, P., Stuttmann, J., & Pantaleo, V. (2021). Regulation of plant antiviral defense genes via host RNA-silencing mechanisms. *Virology Journal*, *18*, 194. https://doi.org/10.1186/s12985-021-01664-3

Li, Q., Wang, J., Bai, T., Zhang, M., Jia, Y., Shen, D., Zhang, M., & Dou, D. (2020). A Phytophthora capsici effector suppresses plant immunity via interaction with EDS1. *Molecular Plant Pathology*, *21*(4), 502–511. https://doi.org/10.1111/mpp.12912

Liu, L., & Chen, X. (2018). Intercellular and systemic trafficking of RNAs in plants. *Nature Plants*, *4*(11), Article 11. https://doi.org/10.1038/s41477-018-0288-5

Margis, R., Fusaro, A. F., Smith, N. A., Curtin, S. J., Watson, J. M., Finnegan, E. J., & Waterhouse, P. M. (2006). The evolution and diversification of Dicers in plants. *FEBS Letters*, *580*(10), 2442–2450. https://doi.org/10.1016/j.febslet.2006.03.072

Meyers, B. C., Kozik, A., Griego, A., Kuang, H., & Michelmore, R. W. (2003). Genome-Wide Analysis of NBS-LRR–Encoding Genes in Arabidopsis[W]. *The Plant Cell*, *15*(4), 809–834. https://doi.org/10.1105/tpc.009308

Molnar, A., Melnyk, C., & Baulcombe, D. C. (2011). Silencing signals in plants: A long journey for small RNAs. *Genome Biology*, *12*(1), 215. https://doi.org/10.1186/gb-2010-1112-219

Navarro, L., Dunoyer, P., Jay, F., Arnold, B., Dharmasiri, N., Estelle, M., Voinnet, O., & Jones, J. D. G. (2006). A plant miRNA contributes to antibacterial resistance by repressing auxin signaling. *Science (New York, N.Y.)*, *312*(5772), 436–439. https://doi.org/10.1126/science.1126088

O'Toole, N., Hattori, M., Andres, C., Iida, K., Lurin, C., Schmitz-Linneweber, C., Sugita, M., & Small, I. (2008). On the Expansion of the Pentatricopeptide Repeat Gene Family in Plants. *Molecular Biology and Evolution*, *25*(6), 1120–1128. https://doi.org/10.1093/molbev/msn057

Petri, S., Dueck, A., Lehmann, G., Putz, N., Rüdel, S., Kremmer, E., & Meister, G. (2011). Increased siRNA duplex stability correlates with reduced off-target and elevated on-target effects. *RNA*, *17*(4), 737–749. https://doi.org/10.1261/rna.2348111

Pratt, A. J., & MacRae, I. J. (2009). The RNA-induced silencing complex: A versatile genesilencing machine. *The Journal of Biological Chemistry*, *284*(27), 17897–17901. https://doi.org/10.1074/jbc.R900012200

Qiao, Y., Liu, L., Xiong, Q., Flores, C., Wong, J., Shi, J., Wang, X., Liu, X., Xiang, Q., Jiang, S., Zhang, F., Wang, Y., Judelson, H. S., Chen, X., & Ma, W. (2013). Oomycete pathogens encode RNA silencing suppressors. *Nature Genetics*, *45*(3), 330–333. https://doi.org/10.1038/ng.2525

Qiao, Y., Xia, R., Zhai, J., Hou, Y., Feng, L., Zhai, Y., & Ma, W. (2021). Small RNAs in Plant Immunity and Virulence of Filamentous Pathogens. *Annual Review of Phytopathology*, *59*. https://doi.org/10.1146/annurev-phyto-121520-023514

Rajeswaran, R., & Pooggin, M. M. (2012). RDR6-mediated synthesis of complementary RNA is terminated by miRNA stably bound to template RNA. *Nucleic Acids Research*, *40*(2), 594–599. https://doi.org/10.1093/nar/gkr760

Samarfard, S., Ghorbani, A., Karbanowicz, T. P., Lim, Z. X., Saedi, M., Fariborzi, N., McTaggart, A. R., & Izadpanah, K. (2022). Regulatory non-coding RNA: The core defense mechanism against plant pathogens. *Journal of Biotechnology*, *359*, 82–94. https://doi.org/10.1016/j.jbiotec.2022.09.014

Schwarzländer, M., & Finkemeier, I. (2013). Mitochondrial Energy and Redox Signaling in Plants. *Antioxidants & Redox Signaling*, *18*(16), 2122–2144. https://doi.org/10.1089/ars.2012.5104

Stassen, J. H., & Van den Ackerveken, G. (2011). How do oomycete effectors interfere with plant life? *Current Opinion in Plant Biology*, *14*(4), 407–414. https://doi.org/10.1016/j.pbi.2011.05.002

Sun, Y., Li, L., Macho, A. P., Han, Z., Hu, Z., Zipfel, C., Zhou, J.-M., & Chai, J. (2013). Structural basis for flg22-induced activation of the Arabidopsis FLS2-BAK1 immune complex. *Science (New York, N.Y.)*, *342*(6158), 624–628. https://doi.org/10.1126/science.1243825

Sunkar, R., Li, Y.-F., & Jagadeeswaran, G. (2012). Functions of microRNAs in plant stress responses. *Trends in Plant Science*, *17*(4), 196–203. https://doi.org/10.1016/j.tplants.2012.01.010

Tian, M., Win, J., Song, J., van der Hoorn, R., van der Knaap, E., & Kamoun, S. (2007). A Phytophthora infestans Cystatin-Like Protein Targets a Novel Tomato Papain-Like Apoplastic Protease. *Plant Physiology*, *143*(1), 364–377. https://doi.org/10.1104/pp.106.090050

Valencia-Sanchez, M. A., Liu, J., Hannon, G. J., & Parker, R. (2006). Control of translation and mRNA degradation by miRNAs and siRNAs. *Genes & Development*, *20*(5), 515–524. https://doi.org/10.1101/gad.1399806

Vaucheret, H. (2006). Post-transcriptional small RNA pathways in plants: Mechanisms and regulations. *Genes & Development*, *20*(7), 759–771. https://doi.org/10.1101/gad.1410506

Vaucheret, H., Vazquez, F., Crété, P., & Bartel, D. P. (2004). The action of ARGONAUTE1 in the miRNA pathway and its regulation by the miRNA pathway are crucial for plant development. *Genes & Development*, *18*(10), 1187–1197. https://doi.org/10.1101/gad.1201404

Voinnet, O. (2009). Origin, biogenesis, and activity of plant microRNAs. *Cell*, *136*(4), 669–687. https://doi.org/10.1016/j.cell.2009.01.046

Wang, J., Mei, J., & Ren, G. (2019). Plant microRNAs: Biogenesis, Homeostasis, and Degradation. *Frontiers in Plant Science*, *10*. https://www.frontiersin.org/articles/10.3389/fpls.2019.00360

Wang, M., Weiberg, A., Dellota, E., Yamane, D., & Jin, H. (2017). Botrytis small RNA BcsiR37 suppresses plant defense genes by cross-kingdom RNAi. *RNA Biology*, *14*(4), 421–428. https://doi.org/10.1080/15476286.2017.1291112

Wang, S., Welsh, L., Thorpe, P., Whisson, S. C., Boevink, P. C., & Birch, P. R. J. (2018). The *Phytophthora infestans* Haustorium Is a Site for Secretion of Diverse Classes of Infection-Associated Proteins. *MBio*, *9*(4), e01216-18. https://doi.org/10.1128/mBio.0121618

Wang, X., An, Y., Xu, P., & Xiao, J. (2021). Functioning of PPR Proteins in Organelle RNA Metabolism and Chloroplast Biogenesis. *Frontiers in Plant Science*, *12*. https://www.frontiersin.org/articles/10.3389/fpls.2021.627501

Wang, X.-B., Jovel, J., Udomporn, P., Wang, Y., Wu, Q., Li, W.-X., Gasciolli, V., Vaucheret, H., & Ding, S.-W. (2011). The 21-Nucleotide, but Not 22-Nucleotide, Viral Secondary Small Interfering RNAs Direct Potent Antiviral Defense by Two Cooperative Argonautes in Arabidopsis thaliana. *The Plant Cell*, *23*(4), 1625–1638. https://doi.org/10.1105/tpc.110.082305

Wawra, S., Belmonte, R., Löbach, L., Saraiva, M., Willems, A., & van West, P. (2012). Secretion, delivery and function of oomycete effector proteins. *Current Opinion in Microbiology*, *15*(6), 685–691. https://doi.org/10.1016/j.mib.2012.10.008

Wong, J., Gao, L., Yang, Y., Zhai, J., Arikit, S., Yu, Y., Duan, S., Chan, V., Xiong, Q., Yan, J., Li, S., Liu, R., Wang, Y., Tang, G., Meyers, B. C., Chen, X., & Ma, W. (2014). Roles of small RNAs in soybean defense against Phytophthora sojae infection. *The Plant Journal*, *79*(6), 928–940. https://doi.org/10.1111/tpj.12590

Wu, H., Li, B., Iwakawa, H., Pan, Y., Tang, X., Ling-hu, Q., Liu, Y., Sheng, S., Feng, L., Zhang, H., Zhang, X., Tang, Z., Xia, X., Zhai, J., & Guo, H. (2020). Plant 22-nt siRNAs mediate translational repression and stress adaptation. *Nature*, *581*(7806), Article 7806. https://doi.org/10.1038/s41586-020-2231-y

Xia, R., Meyers, B. C., Liu, Z., Beers, E. P., Ye, S., & Liu, Z. (2013). MicroRNA Superfamilies Descended from miR390 and Their Roles in Secondary Small Interfering RNA Biogenesis in Eudicots. *The Plant Cell*, *25*(5), 1555–1572. https://doi.org/10.1105/tpc.113.110957

Yadav, B. C., Veluthambi, K., & Subramaniam, K. (2006). Host-generated double stranded RNA induces RNAi in plant-parasitic nematodes and protects the host from infection. *Molecular and Biochemical Parasitology*, *148*(2), 219–222. https://doi.org/10.1016/j.molbiopara.2006.03.013

Yin, C., Ramachandran, S. R., Zhai, Y., Bu, C., Pappu, H. R., & Hulbert, S. H. (2019). A novel fungal effector from Puccinia graminis suppressing RNA silencing and plant defense responses. *New Phytologist*, *222*(3), 1561–1572. https://doi.org/10.1111/nph.15676

Zhai, J., Jeong, D.-H., De Paoli, E., Park, S., Rosen, B. D., Li, Y., González, A. J., Yan, Z., Kitto, S. L., Grusak, M. A., Jackson, S. A., Stacey, G., Cook, D. R., Green, P. J., Sherrier, D. J., & Meyers, B. C. (2011). MicroRNAs as master regulators of the plant NB-LRR defense gene family via the production of phased, trans-acting siRNAs. *Genes & Development*, *25*(23), 2540–2553. https://doi.org/10.1101/gad.177527.111

Zhang, T., Zhao, Y.-L., Zhao, J.-H., Wang, S., Jin, Y., Chen, Z.-Q., Fang, Y.-Y., Hua, C.-L., Ding, S.-W., & Guo, H.-S. (2016). Cotton plants export microRNAs to inhibit virulence gene expression in a fungal pathogen. *Nature Plants*, *2*(10), 16153. https://doi.org/10.1038/nplants.2016.153

Zhu, J.-K. (2008). Reconstituting plant miRNA biogenesis. *Proceedings of the National Academy of Sciences of the United States of America*, *105*(29), 9851–9852. https://doi.org/10.1073/pnas.0805207105

Chapter 1

Characterization of *Phytophthora* Suppressor of RNA Silencing 2 (PSR2)

ABSTRACT

Phytophthora produces hundreds of effectors with a diversity of virulence functions. One such effector, *Phytophthora* suppressor of RNA silencing 2 (PSR2), can suppress RNA silencing in plants. However, its role in silencing suppression is not fully known. In this chapter I aimed to understand the basic biology of PSR2 including its virulence mechanism and subcellular localization during infection. PSR2 has been reported to interact with the double-stranded RNA binding protein 4 (DRB4) in Arabidopsis. Our unpublished data also suggest that PSR2 associates with the host Ser/Thr protein phosphatase 2A (PP2A). Given that PSR2 may interact with both DRB4 and PP2A, I hypothesized that PSR2 could regulate the phosphorylation status of DRB4 through the PP2A activity. Although I was able to detect DRB4 phosphorylation, which was not found previously, the overall phosphorylation level of DRB4 did not exhibit an obvious change in Arabidopsis plants expressing PSR2. Furthermore, DRB4 regulates siRNA biogenesis by partnering with DCL4. I therefore examined whether PSR2 may affect the DRB4-DCL4 interaction. My results show that DRB4 could still associate with DCL4 in the presence of PSR2. In addition, I applied an effector visualization system to PSR2 in order to visualize its localization during infection. Though some fluorescence was observed using a transient system in *Nicotiana benthamiana*, introducing this approach into *P. capsici* was unsuccessful. Taken together, these research activities provide new information in our understanding of PSR2 functions and contribute to a general understanding of the virulence mechanisms employed by filamentous pathogens.

INTRODUCTION

Phytophthora effectors

Every *Phytophthora* species produces hundreds of effectors that they rely on to become pathogenic. Some effectors function inside the host cells to support pathogen colonization and disease development. It is still largely a mystery how effectors are trafficked into plant cells and how they promote disease once inside the host cell. *Phytophthora* effectors are separated into two classes based on their N-terminal host-targeting motif following the secretion signal peptide. Two motifs that may be involved in effector translocation have been reported: LFLAK in CRN (Crinkler or crinkling- and necrosisinducing protein) effectors and RxLR (Arg-any amino acid-Leu-Arg) (Haas et al., 2009). The CRN effectors are found in most plant pathogenic oomycetes (Haas et al., 2009; Schornack et al., 2010; Stam et al., 2013) while all the known Avr effectors have the RxLR domain, which is typically followed by another Glu, Glu, Arg (EER) domain. It is commonly accepted that RxLR effectors can enter the plant cell in an RxLR-dependent manner.

Our lab investigated RxLR effectors in *P. sojae* that can suppress RNA silencing in plants. A functional screen was conducted on 59 *P. sojae* RxLR effectors (Qiao et al., 2013). Individual effectors and green fluorescent protein (GFP) genes were co-expressed through *Agrobacterium tumefaciens*-mediated transient expression in the leaves of *Nicotiana benthamiana* 16C, which constitutively expresses GFP. SiRNAs induced by external *GFP* introduced by Agro-infiltration lead to silence the *GFP* genes and absence of green fluorescence. Bright fluorescence would be detected if the siRNA-mediated *GFP* silencing could be suppressed by candidate RxLR effectors co-expressed in the same leaf areas.

Through this assay they found that PsAvh18 and PsAvh146 suppressed *GFP* silencing (Qiao et. al 2013). These effectors are now known as *Phytophthora* suppressors of RNA silencing (PSR) 1 and 2, respectively.

PSR2 and LWY effector structure

Sequence analysis of RxLR effectors identified three motifs which are termed W, Y and L after their conserved amino acid sequence (Jiang et al., 2008). W and Y motifs are often co-occur to form a WY motif, which are sometimes arranged as tandem repeats (Win et al., 2012). Structural analysis of *PSR2* revealed that it has seven tandem repeats of one WY motif and six LWY motifs. Each LWY unit forms a highly conserved fold of five α-helices and neighboring units are concatenated through a rigid linkage, which creates a stick-like overall structure (Figure 1.1). Remarkably, analysis of five *Phytophthora* species revealed as many as 293 RxLR effectors that form a PSR2-like architecture, which includes a WY motif as the beginning unit, followed by various numbers of LWY units (He et al., 2019). Functional analysis demonstrates that individual WY/LWY units have differential contributions to the RNA silencing suppression activity of PSR2. This suggests that the LWY motifs are both structural and functional modules and may be used in *Phytophthora* as a building block for effector evolution. From five *Phytophthora* genomes, a substantial percentage (26–58%) of RxLR effectors contain LWY motifs (He et. al 2019). It has been proposed that the WY/LWY tandem repeats can promote effector family expansion and thereby contribute to the large effector repertoire in *Phytophthora* species (Dong & Ma, 2021). The conservation and prevalence of these linear structure suggest an important role in enabling virulence activity and *Phytophthora* effector evolution; this could enhance the

fitness of *Phytophthora* during the host pathogen arms race. My hypothesis was that this structural module may promote effector function by facilitating delivery into host cells. To test my hypothesis, I ventured to visualize the delivery/localization of PSR2 into plant cells using a split-GFP approach.

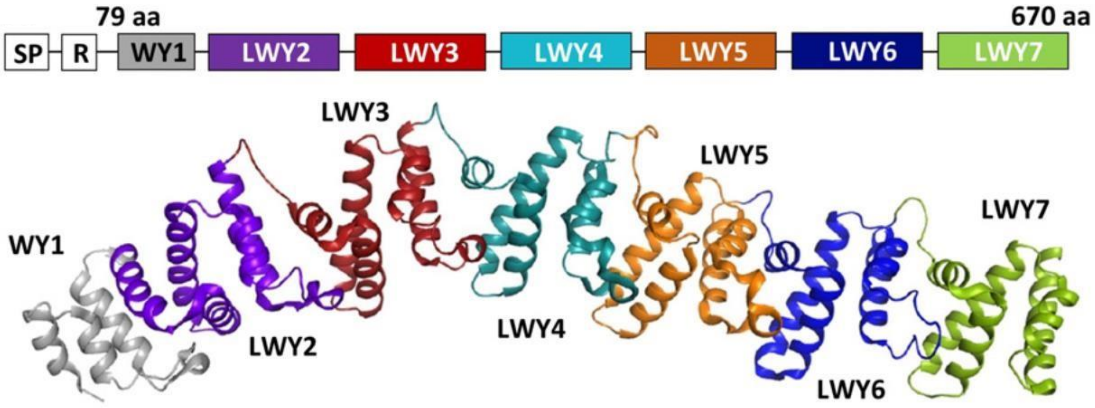

Figure 1.1 Schematic of PSR2 domain organization and crystal structure.

PSR2 has a WY1-(LWY)6 architecture and an overall stick-like shape (Figure from He et al., 2019).

Effector secretion

A missing factor in effector studies is that for many pathogens the effector secretion/translocation mechanisms are unknown. However, what little we do know about Phytophthora effector translocation comes from studies of the RxLR-dEER motif which has been suggested to be closely associated to the movement of effectors into the plant cells (Win & Kamoun, 2008). A RxLR mutant of the *P. infestans* effector Avr3a showed accumulation in apoplastic space instead of the host cytoplasm suggesting that lack of RxLR resulted in reduced translocation of the effector into the host cell (Morgan & Kamoun, 2007). Additionally, mutation at the RxLR motif also abolished the ability of the effector to trigger hypersensitive response, consistent with the assumption that without the motif the effector could not be delivered into the host cell (Whisson et al., 2007). Some evidence suggested that the RxLR motif may mediate effector entry into host cells by binding to phosphatidyl inositol phosphates (PIPs) on the surface of the plant plasma membrane, which subsequently stimulates endocytosis of the effectors into plant cells (Kale et al., 2010). However contrary evidence finds that mutations in the RxLR did not lead to any disruption in effector interaction with PIPs (Yaeno et al., 2011). More recent findings found RxLR motif cleavage prior to secretion. Additionally, it has been proposed that the RxLR motif may be involved in effector secretion instead of host cell entry (Wawra et al., 2017). Studying effector translocation is challenging, at least in part due to the fact that it is exceedingly difficult to visualize effector trafficking. This represents a major roadblock in effector research, as there is a lack of fluorescent constructs of a fusion protein that allow detection of the effectors from inside the pathogen until translocation into the plant cells during infection.

Effector visualization strategies

Effector cytological studies and their tools allow the determination of critical cellular events leading to pathogen infection. Studying cell biology through visualization reveals effector localization which hints to characterization, interaction as well as the functions of plant targets. A commonly used method to visualize protein localization is by fusion of a fluorescent protein tag. However, visualization of effectors has been described but the evidence is very infrequent. One of the first effectors to be visualized using fluorescent fusion proteins was in the *Ralstonia solanacearum* effector Pop2, which was identified as the avirulence protein recognized by an *Arabidopsis* resistance gene (RRS1-1) (Deslandes et al., 2003). Some early fluorescent fusion protein examples that examined secretion and localization include *Phytophthora infestans* RxLR effector Avr3a. By fusing to mRFP, Avr3a was found to localized in the haustoria and the extra-haustorial matrix during infection (Whisson et al., 2007). Another example is the cytoplasmic effector PWL2 of the fungal pathogen *Magnaporthe oryzae*. PWL2 fused with a nuclear localization signal and a fluorescence protein showed fluorescence in the nuclei of plant host cells nearby the fungal invasive hyphae. This study provided insights into the timing of effector delivery and effector cell-to-cell movement as the fluorescence was observed in the plant cell nuclei after ~28 hours post inoculation (Khang et al., 2010).

Split fluorescent protein assays

The average size of a fluorescent protein is around 28 kDa, which may have steric effects for protein folding or targeting thus interfering with effector function (Snapp, 2005). To address this, assays using split fluorescent proteins have been used as a work-around.

Bimolecular fluorescence complementation, an assay using split fluorescent proteins which combine to fluoresce, was first developed in mammalian cells (Ghosh et al., 2000; Hu & Kerppola, 2003) and used later for phytopathological assays (Lee & Gelvin, 2014). One such system makes use of splitting GFP's 11 beta-barrel sheets. In a method called "the strand system", effectors were fused with a GFP_{11} tag and expressed in the bacterial pathogen *Pseudomonas syringae* (Henry et al., 2017). The bacteria were then used to inoculate plants expressing the remainder of the GFP protein, GFP_{1-10}. Delivery of the effector-GFP_{11} during infection could potentially be detected by observing green fluorescence after the self-assembling of GFP to produce a full-length protein. Using this system, the *P. syringae* type III effectors AvrPtoB and AvrPto were visualized in Arabidopsis cells (Henry et al., 2017) (Figure 1.2).

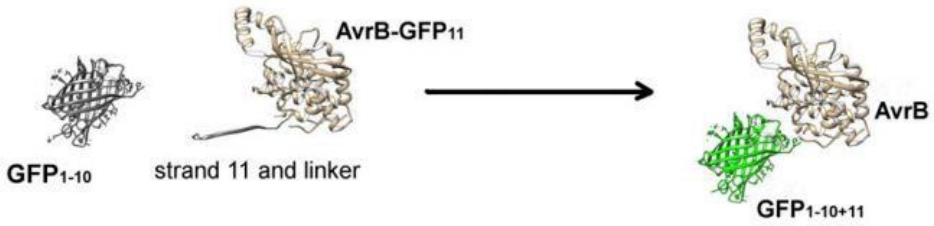

Figure 1.2 Schematic illustration of a GFP strand system, which was developed to visualize effector delivery during infection.

GFP_{1-10} strands are constitutively expressed in plant cells. The GFP_{11} strand is fused to an effector through a linker and the fusion protein would be introduced in the pathogen. If the effector-fusion protein can be delivered by the pathogen, during infection, into the plant cell, both GFP components are present together and spontaneously combine, which produce the full-length fluorescence protein (Image from Henry et al., 2017).

PSR2 associates with Double stranded RNA binding protein 4 (DRB4) in Arabidopsis

Our lab endeavored to characterize the PSR2 effector, especially its interacting proteins in plant cells. Using a yeast two-hybrid assay, an Arabidopsis cDNA library was screened. From that assay, five candidates were DNA-binding and ten were RNA-binding. These results could suggest that PSR2 may interact with nucleic-acid binding proteins in plants. One of the candidates found as potential interactors with PSR2 was double stranded RNA binding 4 (DRB4). DRB4 is essential for the accumulation of 21-nt secondary siRNAs in Arabidopsis (Fukudome et al., 2011). TasiRNA accumulation was abolished in *drb4* mutant plants (Fukudome et al., 2011; Nakazawa et al., 2007). Because PSR2 expression led to largely reduced accumulation of 21-nt secondary siRNAs spawned from *PPR*, *TAS1* and *TAS2* in Arabidopsis, we were particularly interested in DRB4 as a potential virulence target of PSR2 (Zhai, 2018). Both *drb4* mutant plants and PSR2 transgenic plant *PSR2-5* have similar developmental phenotypes of slightly long and curled leaves. They also both exhibited hypersusceptibility to *P. capsici* (Hou et al., 2019). Furthermore, both *drb4* mutant and *PSR2-5* plants showed reduced accumulation of secondary siRNAs from the abovementioned RNAs (Hou et al., 2019). Using truncates of PSR2, a previous PhD student Dr. Yi Zhai determined that the N-terminal fragment of PSR2 including WY1 and LWY2 are required for interaction with DRB4. Deletions of PSR2 WY1 or LWY2 largely reduced the RNA silencing suppression activity, further suggesting that this interaction is important for PSR2 functions in plant cells (Figure 1.3a). Additionally, WY1 and LWY2 are both necessary and by themselves sufficient for the virulence activities of PSR2 (Figure 1.3b). (Hou et al., 2019). These results show that DRB4 is a promising target of PSR2.

PSR2 association with DRB4 was confirmed *in planta* using co-immunoprecipitation (Hou et al., 2019). Additionally, a BiFC assay and a PSR2-GFP fusion assay demonstrates PSR2 co-localizes with DRB4 in the nucleus when co-expressed in *N. benthamiana* (Hou et al., 2019). DRB4 has two double-stranded RNA binding motifs (dsRBMs) that are required for its function in siRNA processing. DRB4 mutants with one or two of the dsRMB motifs deleted showed that these motifs are required for the association with PSR2 (Figure 1.3c) (Hou et al., 2019). Because dsRMB motifs are also required for the interaction of DRB4 with DCL4, which possesses the nuclease activity to generate 21-nt secondary siRNAs from the dsRNA precursors (Fukudome et al., 2011). DRB4 is generally located in the nucleus and the nuclear localization of DCL4 requires DRB4 protein (Pumplin et al., 2016). As such, the interaction of DRB4-DCL4 has been reported to be in the nucleus of Arabidopsis (Zhu et al., 2013). It is therefore interesting to test whether PSR2 may interfere with siRNA production through disrupting DRB4-DCL4 interaction.

A.

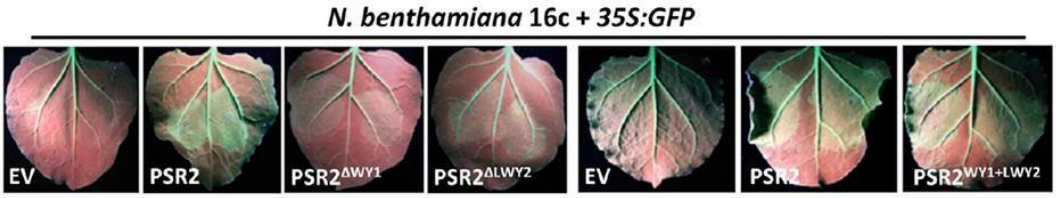
N. benthamiana 16c + 35S:GFP
EV
PSR2
PSR2ΔWY1
PSR2ΔLWY2
EV
PSR2
PSR2WY1+LWY2

B.

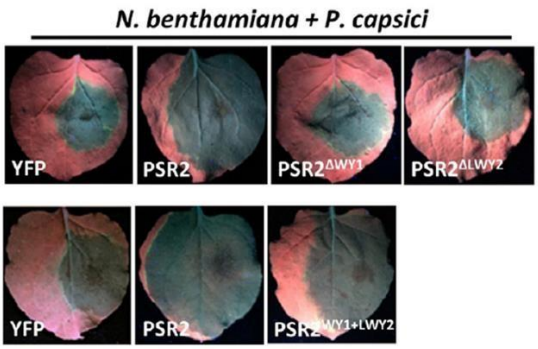
N. benthamiana + P. capsici
YFP
PSR2
PSR2ΔWY1
PSR2ΔLWY2
YFP
PSR2
PSR2WY1+LWY2

C.

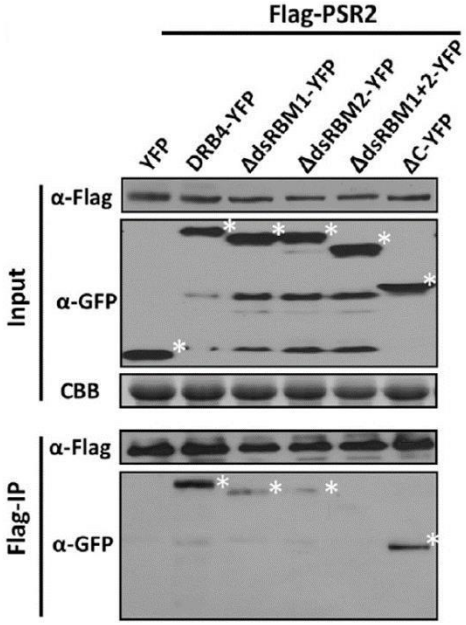
Flag-PSR2
YFP
DRB4-YFP
ΔdsRBM1-YFP
ΔdsRBM2-YFP
ΔdsRBM1+2-YFP
ΔC-YFP
Input
α-Flag
α-GFP
CBB
Flag-IP
α-Flag
α-GFP

Figure 1.3 PSR2 associates with DRB4 in Arabidopsis.

A. Deletions of PSR2 WY1 or LWY2 largely reduced the RNA silencing suppression activity. *N. benthamiana* 16c leaves were co-infiltrated with *Agrobacterium* 35S:GFP and 35S:PSR2 constructs. Images were taken 5 dpi. **B.** WY1 and LWY2 are necessary and sufficient for the virulence activities of PSR2. PSR2 and its truncates were expressed in *N. benthamiana* leaves, which were then inoculated with *P. capsici*. Lesions were examined at 3 dpi. **C.** Western blot image of the two dsRBM of DRB4 can mediate interaction with PSR2. FLAG-PSR2, DRB4-YFP, and DRB4 truncates were transiently expressed in *N. benthamiana*. PSR2 was pulled down using anti-FLAG agarose. Asterisk (*) show corresponding protein band. Coomassie brilliant blue
(CBB) was used as a protein gel stain as a loading control. (Image from Hou et al., 2019)

PSR2 also associates with a host protein phosphatase

Further PSR2-interacting protein analysis using IP-MS revealed an interaction of PSR2 with the Ser/Thr protein phosphatase 2 A (PP2A) in Arabidopsis (Dr. Ariel Kuan, PhD thesis). PP2A is a conserved phosphatase that regulates many critical cellular processes by dephosphorylation of particular proteins (Seshacharyulu et al., 2013; Virshup & Shenolikar, 2009). One third of all proteins in an eukaryotic cell are thought to experience phosphorylation on the hydroxylated sidechains of serine, threonine or tyrosine residues (Ghelis, 2011) and a majority of Ser/Thr dephosphorylation depends on PP2A.
Given the observation that PSR2 may interact with both DRB4 and PP2A, I hypothesized that PSR2 could manipulate the phosphorylation levels of DRB4 through the PP2A activity, which may subsequently affect the function of DRB4 in siRNA production. In this chapter, I investigated whether DRB4 can be phosphorylated and if yes, whether PSR2 affects DRB4 phosphorylation to better understand the relationship between these components.

In this chapter, I characterized the cellular function of PSR2 through visualization of effector delivery and virulence activity via interactions with DRB4 and PP2A. This research advances the understanding of effector biology in *Phytophthora*.

RESULTS

Generation of the PSR2-GFP$_{11}$ fusion protein

I used a green fluorescence protein (GFP) strand method to detect PSR2 delivery during natural infection. As mentioned before, due to the bulky size of fluorescent proteins, tagging a full-length fluorescent protein to effectors may interfere with protein trafficking through the secretion system(s) (Snapp, 2005). Indeed, detection of fluorescence-tagged effectors in host cells is rarely successful. In the GFP strand method, the 1-10 strands of GFP are expressed in plants as a transgene, and only the 11th strand is fused to an effector. As a proof of concept, I first co-expressed GFP$_{1-10}$ and PSR2-GFP$_{11}$ in *N. benthamiana* through an *Agrobacterium tumefaciens* infiltration assay.

To generate the *A. tumefaciens* strains, I cloned a full length *PSR2* with a C-terminally fused *GFP$_{11}$* and linker strand. Sequence encoding PSR2 without its signal peptide (ΔspPSR2 from here-on) (Figure 1.4a) was also fused to *GFP$_{11}$* as a control of effector translocation (Figure 1.4b). After co-expressing in *N. benthamiana*, both the ΔspPSR2-GFP$_{11}$ and PSR2- GFP$_{11}$ showed GFP fluorescence lining the cell membrane and a few nuclei (Figure 1.5c and 1.5d). By itself, expression of *GFP$_{1-10}$* showed low GFP signal as background fluorescence (Figure 1.5b). The positive control, a full length GFP, exhibited fluorescence in the cytoplasm, nucleus, and cell membrane (Figure 1.5a). This transient expression assay was performed twice with similar results.

A.

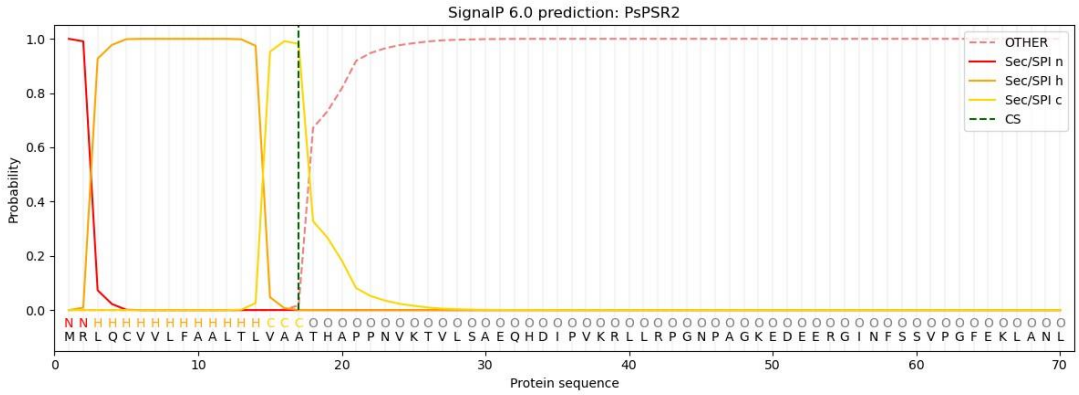

B.

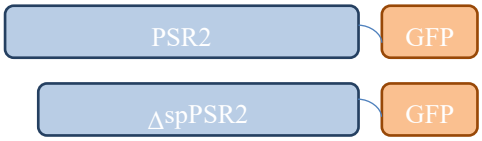

Figure 1.4 *Agrobacterium tumefaciens* constructs *PSR2*-GFP$_{11}$.

A. Prediction of an N-terminal secretion signal peptide of PSR2 (SignalP 6.0). **B.** Representation of the PSR2 constructs. Full length PSR2 (top) and a truncate without the predicted signal peptide (bottom) are C-terminal tagged with an eleven amino acid linker and GFP$_{11}$.

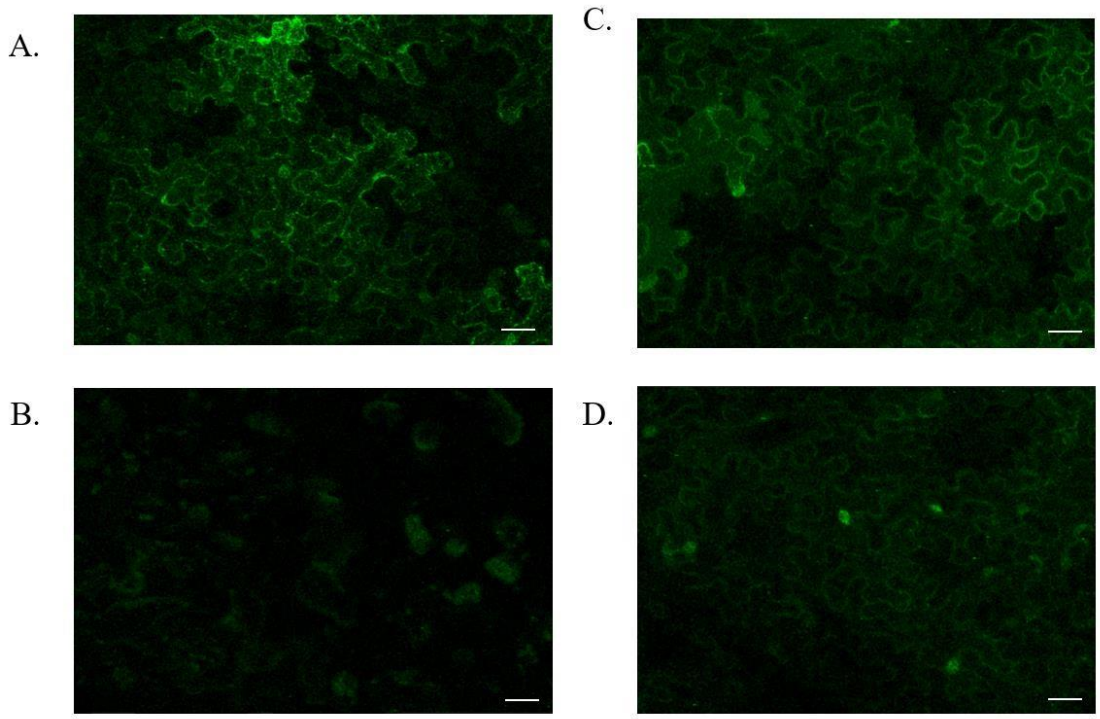

Figure 1.5 Microscopy analysis of *N. benthamiana* leaves expressing PSR2-GFP$_{11}$ with GFP$_{1-10}$.

A. Full length GFP used as a positive control. **B.** GFP$_{1-10}$ used as a negative control to show background fluorescence. **C.** ΔspPSR2-GFP$_{11}$ co-expressed with GFP$_{1-10}$. **D.** PSR2GFP$_{11}$ co-expressed with GFP$_{1-10}$. Scale bars, 5μm.

Generation of *P. capsici* transformants expressing *PSR2-GFP$_{11}$*

Next, I intended to generate a *PSR2-GFP$_{11}$* expressing *P. capsici* strain to visualize potential translocation of PSR2. *P. capsici* was used because it had been successfully transformed previously (Dunn et al., 2013; Feng et al., 2014; Hou et al., 2019). I cloned the *ΔspPSR2-GFP$_{11}$* and *PSR2- GFP$_{11}$* fragments into a *Phytophthora* expression vector, pTOR. The recombinant plasmids were then introduced into *P. capsici* using a PEG-mediated protoplast transformation system (Judelson et al., 1991). Each of these plasmids was co-transformed with another plasmid carrying *tdTomato* to facilitate the screening of transformants. If a hyphal colony expressed red fluorescence, the plasmid carrying *ΔspPSR2GFP$_{11}$* or *PSR2- GFP$_{11}$* that was co-transformed would be more likely to have also been introduced into the same protoplast (Figure 1.6). In addition to the red fluorescence, the antibiotic gentamicin B1, G418, was used to select for transformed individuals.

After two transformation experiments, I subcultured 120 colonies for *PSR2-GFP$_{11}$* and 115 for *ΔspPSR2-GFP$_{11}$*. All these colonies grew on G418-containing media. After screening each colony for red fluorescence, five candidates for *PSR2-GFP$_{11}$* and four for *ΔspPSR2-GFP$_{11}$* were further pursued (Figure 1.6). Those samples were used for western blotting to examine whether PSR2 proteins were expressed. Disappointingly, none of the colonies showed a band at around the expected PSR2 size of 70 kDa when using an anti-PSR2 antibody (Figure 1.7a). In order to investigate why PSR2 proteins were not detectable in the transformants, I examined the transcript levels of *PSR2* using RT-PCR (Figure 1.7b). My results show that *PSR2* was expressed but did not produce proteins detectable by the anti-PSR2 antibody.

I also attempted to detect the delivery of *P. syringae* effectors AvrPto and AvrPtoB using the *Arabidopsis* GFP_{1-10} expressing line during bacterial infection, as reported by Henry et al., 2017. Using confocal microscopy, both wildtype *A. thaliana*, *Col-0* and transgenic line *GFP_{1-10}* exhibited mild background fluorescence. However, upon several attempts to inoculate with *P. syringae* strain DC3000 expressing AvrPto-GFP_{11} or AvrPtoB-GFP_{11}, I was unable to see fluorescence in plant cells that would indicate effector delivery. Therefore, this approach was unsuccessful in general in my hands.

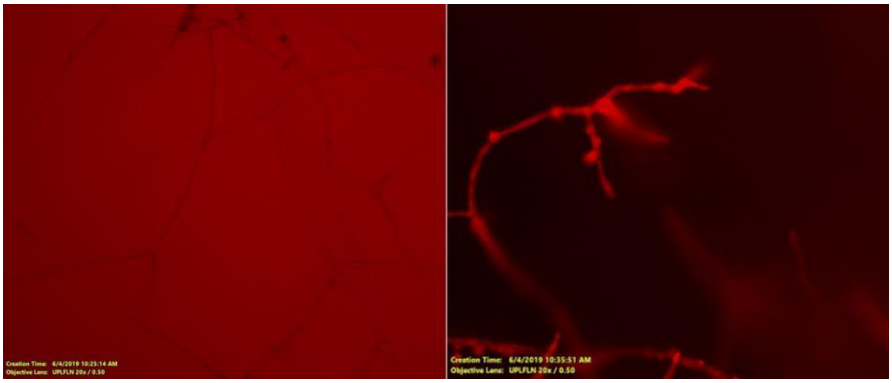

P. capsici PSR2-GFP$_{11}$

Transformation results

Red fluorescent colonies per G418 resistant colonies	***PSR2-GFP$_{11}$***	***ΔspPSR2-GFP$_{11}$***
Transformation 1	3/40	2/35
Transformation 2	2/80	2/80

Figure 1.6 *P. capsici* hyphae co-transformed with pTOR::*PSR2-GFP$_{11}$* and pTOR::*tdTomato*.

Microscopy images showing hyphae from wild-type *P. capsici* (left) and *P. capsici* transformed with plasmids carrying *PSR2-GFP$_{11}$* and tdTomato (right). Red fluorescence was observed from some transformed strains in their hyphae. Table below showing *P. capsici* transformation results.

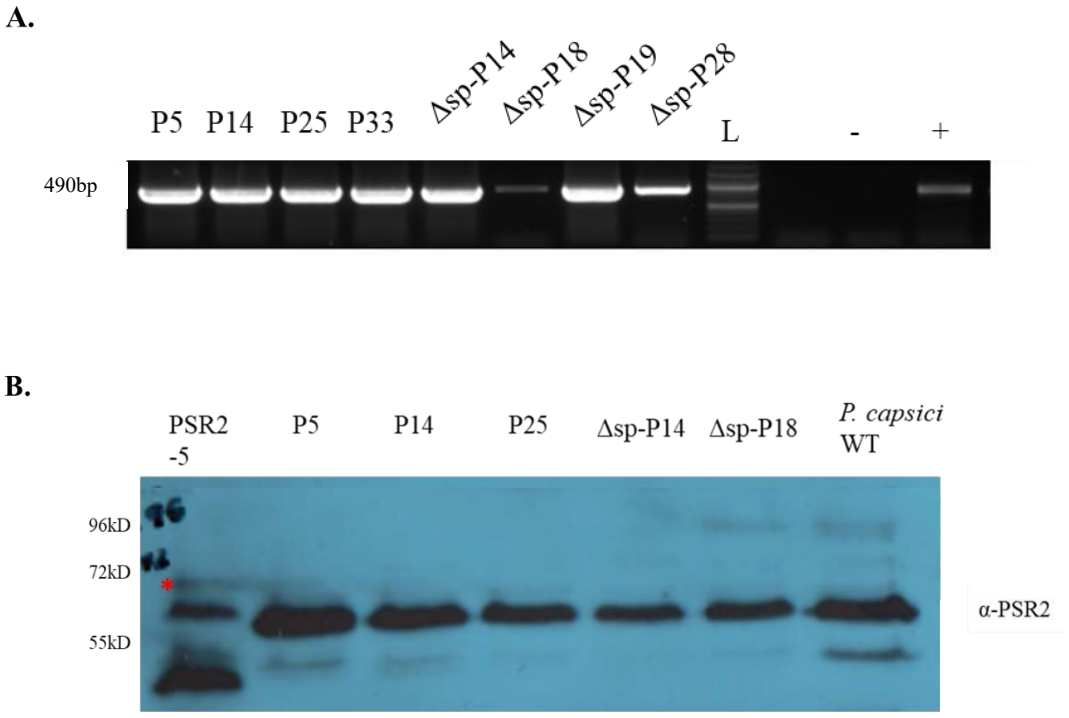

Figure 1.7 RT-PCR and western blot of *P. capsici* samples exhibiting red fluorescence.

A. RT-PCR gel showing PSR2 was expressed in all red fluorescent samples. Samples were *P. capsici* transformant cDNA. Full length PSR2 samples labelled "P", signal peptide truncates "Δsp". **B.** Westering blotting for the detection of PSR2-GFP_{11} from transformed *P. capsici*. Blot on the left shows bands resulting from PSR2 antibody. Positive control is PSR2-5 sample, which showed a 70 kDa band (red asterisk). *P. capsici* wild-type sample was used as a negative control. The anti-PSR2 antibody produced a non-specific band in *P. capsici*.

Mass Spectrometry reveals DRB4 phosphorylation sites

As PSR2 associates with both DRB4 and PP2A, one potential relationship of DRB4PP2A was hypothesized to be PP2A dephosphorylation of DRB4. One approach to investigate the dynamics of that relationship is to first identify if DRB4 may be phosphorylated. To identify phosphorylation sites, a previous PhD student, Dr. Yi Zhai, prepared samples for mass spectrometry of DRB4. Results showed 16 potential phosphorylation sites on the DRB4 protein from MS data. As Figure 1.8 is showing, the phosphorylated sites in red represent are those with a high ratio. This ratio shows fractional occupancy of a particular phosphorylation site. Interestingly, two phosphorylated sites are located within dsRBM2, while the rest are located in the C-terminal sequence with unknown function(s) (Figure 1.8).

Of the 16 potential phosphorylation sites in DRB4, all of them are on Serine or Threonine residues. DRB4-interacting proteins were also analyzed by Dr. Yi Zhai using IP-MS. Her results showed potential associations of DRB4 with multiple serine/threonine protein kinases. One of them is a Mitogen-activated protein kinase which was shown to phosphorylate HYL1 (DRB1), which is involved in processing miRNA precursors (Raghuram et al., 2015). This evidence further supported the hypothesis that DRB4 can be phosphorylated.

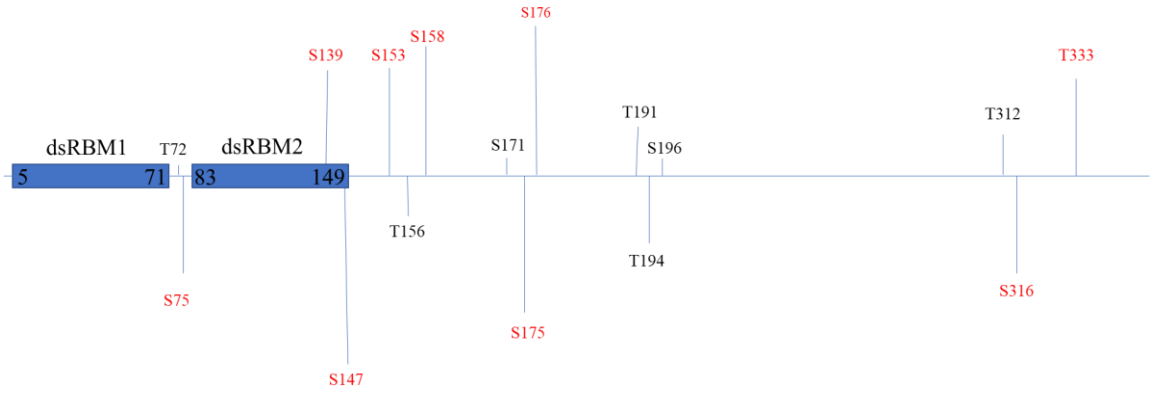

Figure 1.8 Phosphorylation sites of DRB4.

Phosphorylation site analysis using mass spectrometry reveals 16 potential serine or threonine phosphorylation sites in DRB4. Nine sites (in red) demonstrate a phosphorylated/unphosphorylated ratio of greater than 37/100. Two serine phosphorylation sites are located within dsRBM2. (Dr. Yi Zhai)

Detection of DRB4 phosphorylation

Because PSR2 interacts with both DRB4 and PP2A, I hypothesized that PSR2 may affect the phosphorylation status of DRB4 through the PP2A phosphatase activity and thus affecting its function. Phosphorylation of DRB4 on multiple sites has been identified by Dr. Yi Zhai using Mass Spectrometry analysis. Because phosphorylation of DRB4 has not been reported, I first confirmed it using the phosphate binding tag assay. DRB4-YFP was expressed under its native promoter in protoplasts of *A. thaliana*, which were co-transfected with plasmids carrying PSR2. Total proteins were extracted and DRB4 was detected by western blotting using an anti-GFP antibody (Figure 1.9a). Phosphatase treatment was included to distinguish phosphorylated and unphosphorylated forms of DRB4. Using this assay, I was able to show that DRB4 could indeed be phosphorylated. However, co-expression of PSR2 did not visibly change the phosphorylation band of DRB4 (Figure 1.9a). Since WY1 of PSR2 plays an important role in mediating the interaction with DRB4, an ΔWY1-PSR2 truncate was also expressed in Arabidopsis as a control. As expected, ΔWY1-PSR2 also did not visibly change the overall phosphorylation level of DRB4.

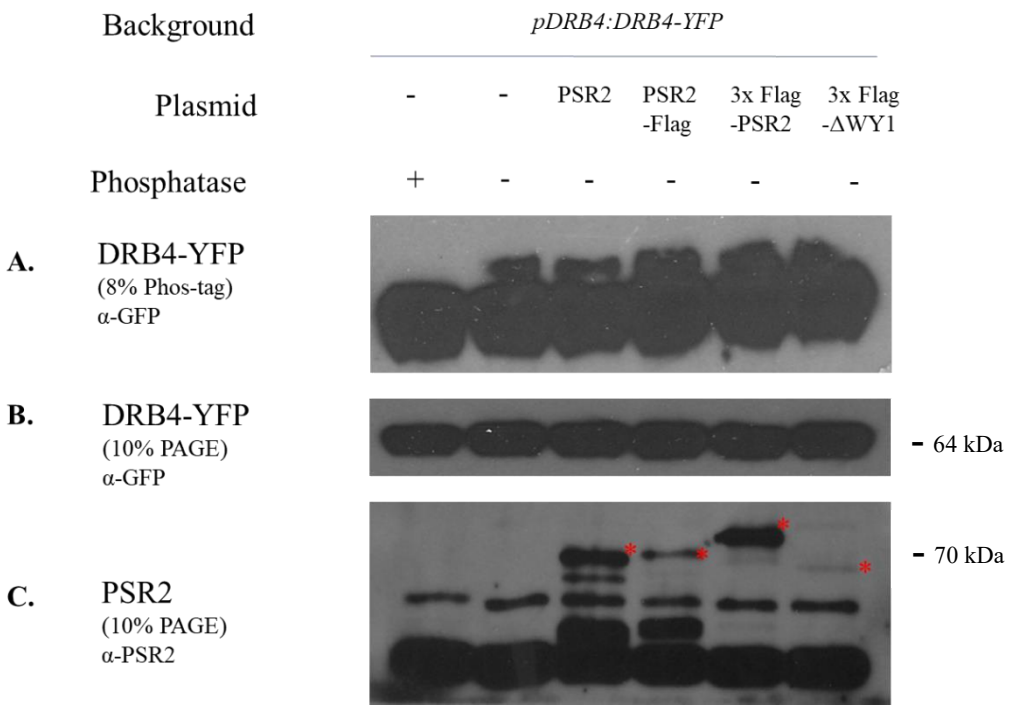

Figure 1.9 Detection of DRB4 phosphorylation in the presence of PSR2.

Arabidopsis protoplasts expressing DRB4-YFP were transfected with plasmids carrying various forms of PSR2. Total proteins were extracted and the phosphorylation levels of DRB4 were determined. **A.** Using 8% Phos-tag in the gel, western blotting detected two bands from DRB4 with the upper band representing the phosphorylated form, which disappeared after phosphatase treatment, and bottom band representing the unphosphorylated form. **B.** Western blotting detecting total DRB4 protein levels. **C.** Western blotting using an anti-PSR2 antibody to detect PSR2 expression in the protoplasts. Asterisks indicate PSR2 bands.

Next, I used Arabidopsis transgenic plants co-expressing PSR2 and DRB4 under its native promoter to examine the potential impact of PSR2 on DRB4 phosphorylation with the consideration that the protein expression levels are more consistent in the stable expression lines. Similar to what was observed in the protoplast assays, DRB4 was phosphorylated, but its phosphorylation band in the western blot was not clearly altered in transgenic plants co-expressing PSR2 (Figure 1.10). However, my results are not completely conclusive at this point without a careful quantification of band density. If further investigations can confirm DRB4 phosphorylation levels are unaltered, PSR2 may affect sRNA biogenesis through another mechanism.

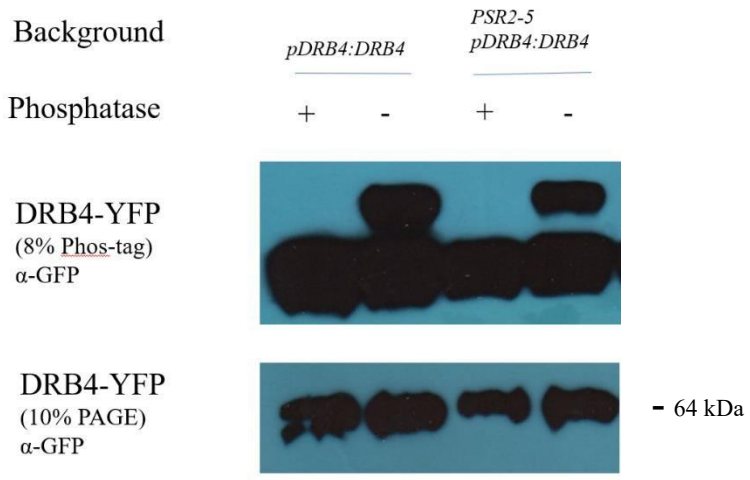

Figure 1.10 Detection of DRB4 phosphorylation in transgenic Arabidopsis plants expressing PSR2.

An anti-GFP antibody was used to detect DRB4 by western blotting in Phos-tag gel and SDS-PAGE.

PSR2 does not have significant interference with the interaction of DRB4 with DCL4

As mentioned in the introduction, dsRNAs are processed by DRB4 together with DCL4 (Figure 1.11a) to produce siRNAs (Fukudome et al., 2011) and DRB4 interacts with DCL4 in the nucleus (Pumplin et al., 2016). Meanwhile, our study found that PSR2 suppresses secondary siRNA biosynthesis and PSR2 interacts with DRB4 (Hou et. al 2019). Because the dsRNA-binding domains of DRB4 are involved in both interactions and DRB4PSR2 interaction also occurs in the nucleus, it is interesting to test whether PSR2 can interfere with DRB4-DCL4 interaction. This interference may lead to the suppression of secondary small RNA biosynthesis. To test this hypothesis, I first confirmed that DRB4DCL4 interact. As DCL4 is a long protein, I used the C-terminal version ($DCL4_{SC}$), which was shown to interact with DRB4 (Hiraguri et al., 2005). I then transiently expressed DRB4 and $DCL4_{SC}$ in *N. benthamiana* and performed a Co-IP assay (Figure 1.11b).

Next to examine for PSR2 interference in the DRB4-DCL4 interaction, I transiently expressed DRB4, DCL4 and PSR2 as different combinations in *N. benthamiana* using *A. tumefaciens* and performed Co-IP assays. $DCL4_{SC}$ and PSR2 were both tagged with Flag, and DRB4 was tagged with YFP. I used GFP-trap magnetic beads to pull-down DRB4 and an anti-Flag antibody was used to detect $DCL4_{SC}$ and PSR2. Co-immunoprecipitation among these proteins was examined in both the cytoplasmic and nuclear fractions.

My results show that DRB4 interacts with DCL4sc in the nucleus, but not in cytoplasm (Figure 1.12). In addition, co-precipitation of PSR2 with DRB4 could be detected in the nucleus (Figure 1.12b). However, the interaction between DRB4 with DCL4sc could still be observed when PSR2 was present (Figure 1.12b). These results suggest that PSR2

may not interfere with the interaction of DRB4 with DCL4, at least under the current experimental condition in a semi-quantitative manner.

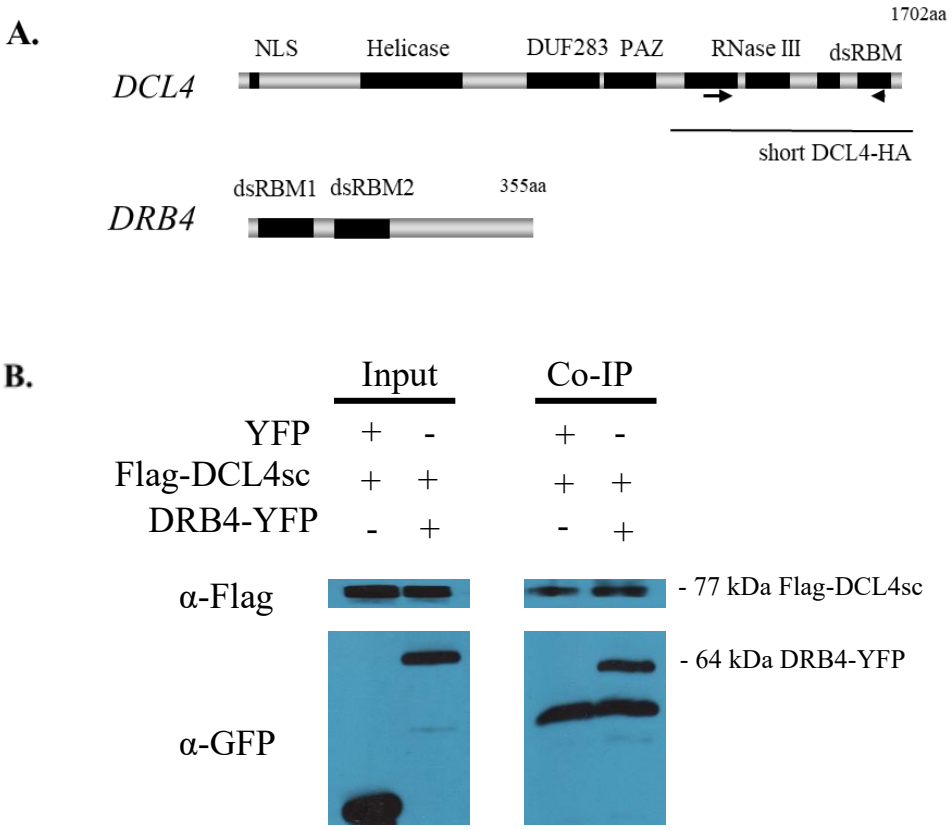

Figure 1.11 DRB4 and DCL4 interact.

A Co-IP assay was performed to confirm that DRB4 and $DCL4_{SC}$ can interact. **A.** Diagram of DCL4 (top) and DRB4 (bottom) genes and their motifs. **B.** Western blot analysis of Co-IP samples from *Agrobacterium* infiltrated *N. benthamiana*. Co-IP image using α-GFP antibody shows DRB4 and $DCL4_{SC}$ interaction.

A.

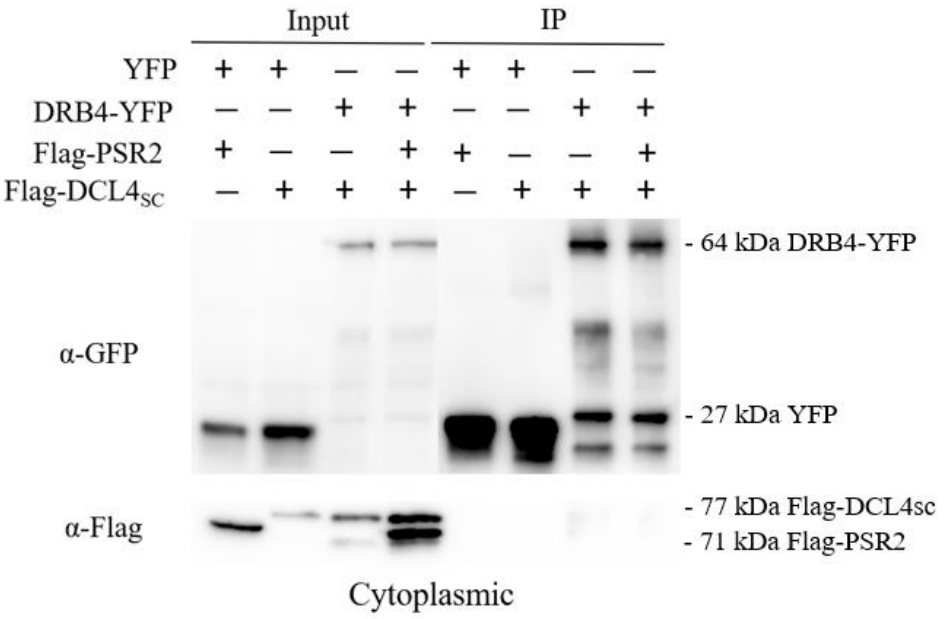
Input
IP
YFP + + — — + + — —
DRB4-YFP — — + + — — + +
Flag-PSR2 + — — + + — — +
Flag-DCL4sc — + + + — + + +
- 64 kDa DRB4-YFP
α-GFP
- 27 kDa YFP
α-Flag
- 77 kDa Flag-DCL4sc
- 71 kDa Flag-PSR2
Cytoplasmic

B.

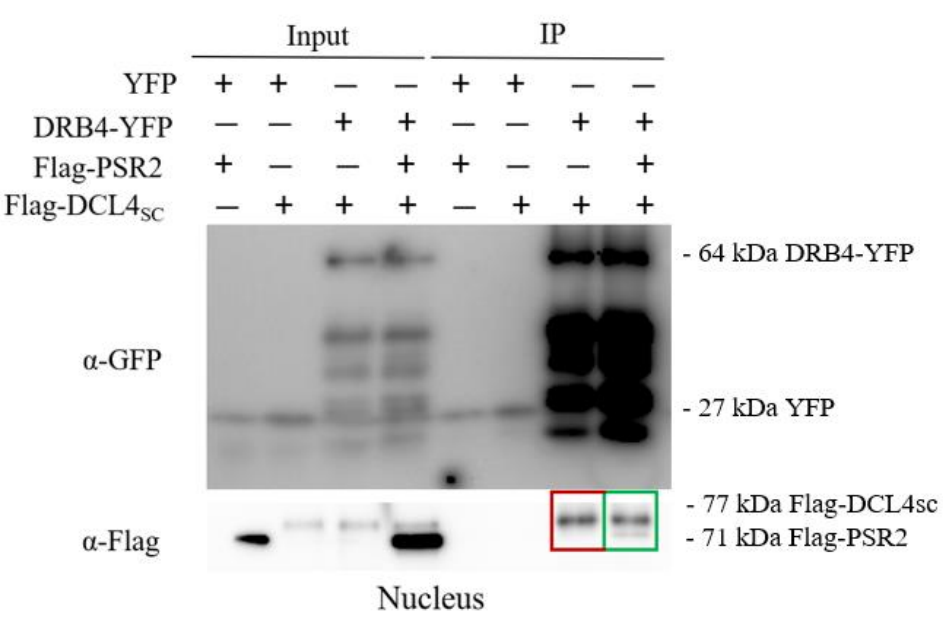
Input
IP
YFP + + — — + + — —
DRB4-YFP — — + + — — + +
Flag-PSR2 + — — + + — — +
Flag-DCL4sc — + + + — + + +
- 64 kDa DRB4-YFP
α-GFP
- 27 kDa YFP
α-Flag
- 77 kDa Flag-DCL4sc
- 71 kDa Flag-PSR2
Nucleus

Figure 1.12 PSR2 does not affect the interaction between DRB4 and DCL4.

Western blot analysis of cell fractionated Co-IP samples from *Agrobacterium* infiltrated *N. benthamiana*. As GFP beads were used to perform IP, when GFP tagged proteins were detected with GFP antibody, the same band results should be seen for both the Input and IP samples in the α-GFP gels. Lower bands are YFP, upper bands are DRB4-YFP. Upper band in α-Flag gel is DRB4, lower band is PSR2. **A.** Cytoplasmic fraction results do not show coprecipitation between DRB4 and PSR2 or DCL4. **B.** Co-IP shows DRB4-DCL4 interaction in the nucleus (red box). DRB4-DCL4 interaction was not affected by PSR2, which was also co-precipitated with DRB4 (green box).

MATERIALS AND METHODS

PSR2 construct generation

To clone PSR2 without a signal peptide, SignalP was used to predict the signal peptide cleavage position at a .98 likelihood between 17 and 18 (Figure 1.3a) (Teufel et al., 2022). To generate the *A. tumefaciens* strains, *PSR2* genes (full length and signal peptide truncate) were cloned from pTOR::Avh146 (PSR2) plasmid generated in the Wenbo Ma lab. A C-terminal fusion to GFP_{11} and linker strand with the *PSR2* fragments was made. To generate the construct *PSR2* and *ΔspPSR2* were separately inserted into TSK108 a pENTRY-D-topo based Gateway entry vector. The amplicon was subsequently introduced into pGWB411 destination vector for *A. tumefaciens* infiltration of *N. benthamiana*. To generate the *P. capsici* constructs, *PSR2*- GFP_{11} and *ΔspPSR2*- GFP_{11} were separately cloned into pTOR plasmid which has *Bremia lactucae* Ham34 promoter for expression within *Phytophthora* species.

Linker and GFP strand 11 amino acid sequence:

GDGGSGGGS RDHMVLHEYVNAAGIT

N. benthamiana Infiltration PSR2-GFP_{11} and DRB4

Fully developed leaves *of N. benthamiana* plants four-weeks old were infiltrated with *Agrobacterium* harboring necessary constructs. The *Agrobacterium* cells were then suspended in 10 mM $MgCl_2$ to OD600 = 1.0. The cells suspension that needs to be co-infiltrated were then mixed to reach OD600 = 0.5. Finally, the cells were activated using

10mM MES and 10mM Acetosyringone. After 3 hours of induction, the cell suspension was infiltrated into leaves using a needle-less 1mL syringe. Leaves were then harvested for experiments at 48 hours post infiltration (hpi).

Phytophthora capsici Protoplast Transformation

P. capsici LT263 was grown on 10% V8 (0.2% $CaCl_2$) agar plates under 25°C in dark conditions (Erwin and Ribeiro, 1996). Protoplast transformation protocol was modified from Fang et al. 2017. *Phytophthora* was grown on V8 media for three days. Fresh hyphae from the edge of the plate were inoculated onto NPB media plates and grown in the dark for 3-5 days until hyphal margin almost reached the edge of the plate. Cork borers were used to cut 6-10 hyphal plugs and transfer into flasks containing 75mL liquid NPB media. Flasks were kept in 25°C dark conditions for two days, shaken once per day to prevent surface hyphae from growing. Hyphae was filtered through two layers of cheesecloth and transferred into 35ml of 0.8M mannitol solution. The tube was inverted several times and hyphae filtered again through new cheesecloth. This time the hyphae was transferred into a tube with 40mL 0.8M mannitol and rotated at 60 rpm for ten minutes. During that time fresh lysing enzyme solution was prepared and filtered using a 0.40 µm PES filter (Fang et. Al 2017). The hyphae was once again filtered through cheesecloth and added to the lysing enzyme solution tube and rotated for 45-60 minutes depending on amount of hyphae. The lysed protoplasts were filtered through two layers of Miracloth into a cold beaker. All the following steps took place on ice and in a 4°C centrifuge, it is vital for protoplasts regeneration to keep a cold temperature. After checking the protoplasts with the microscope, they were transferred to a 50 mL tube and centrifuged at 500 *g* for 4 min at 4°C. The supernatant was then discarded,

and the protoplasts resuspended in 10 mL of pre-cooled W5 solution. The solutions total volume was then brought up to 35ml before being centrifuged again at 500 *g* for 4 min at 4°C. The protoplast concentration was check again. Following this, the supernatant was discarded once more, and the protoplasts were resuspended in 7ml of W5 solution before being incubated on ice for 30 min. The solution was centrifuged once again at 500 *g* for 4 min at 4°C. The supernatant was discarded again, and pre-cooled MMg solution was added to adjust the concentration to $2x10^6$/mL. The protoplasts were then kept on ice for 10 min. New 50ml tubes were put on ice, and equal mole of plasmids (pure and high concentration, >25 ug) at the tube bottom. 1 ml of protoplast solution was then added into each tube using a cut tip, and the tubes were kept on ice for 10 min. Three times 580 µL PEG buffer was then added along the tube wall, again using cut tips. The tubes were mixed, then kept on ice for another 20 min. 1/1000 amp was then added to PM solution and mixed. 2 mL of PM was then added to the protoplast tubes, inverted gently to mix, and incubated on ice for 2 minutes. Another 8 mL of PM was then added, mixed, and placed on ice for 2 more minutes. Then another 10 mL of PM was added, and the tubes were allowed to grow at 25°C overnight in the dark. The next day 5 µL cultures were then used to check recovered mycelium. The tubes were then centrifuged at 700 *g* for 5 min. The supernatant was removed, and 5ml of it was then re-introduced to resuspend. This was then added to 35 mL of PM agar (30 µg/mL G418), mixed and poured into 15 cm plates. The plates were allowed to dry then cultured at room temperature in the dark for 2 days. When small hyphae emerge from the PM agar, 50 mL of V8 agar (50 µg/mL G418) was added on top. After 2 days, colonies with the most mycelium were then selected, plugs were removed and placed onto new V8 plates (50 µg/mL G418). Recipes for NPB, PM media lysing enzyme solution from (Fang et al., 2017). The

resulting transformants were used for further analysis. The PSR2 samples were prepared for western blotting using a buffer consisting of 0.2 M Tris-HCl, 0.4 M DTT, 277 mM SDS (8.0%, w/v), 6 mM bromophenol blue, and 4.3 M glycerol, then boiled at 95°C for five minutes.

Phytophthora Transformant Screening

P. capsici colonies were screened for red fluorescence using Leica 5500 or SP5. *P. capsici* fluorescent transformants were grown in liquid 10% V8 media for three days. To extract RNA, 100 milligrams of hyphal tissue was ground to a fine powder in a mortar and pestle with liquid nitrogen. The ground tissue was transferred to a conical tube and mixed with 1mL of TRIzol Reagent (Life Technologies). 200µL of chloroform was added to the TRIzol mixture, vortexed, and incubated at room temperature for 5 minutes. The samples were centrifuged at 10,000 rpm (12,000 g) for 15 minutes at 4°C. The aqueous phase was transferred to a sterile conical tube and mixed with 500 µL isopropyl alcohol to precipitate the RNA. The samples were incubated at room temperature for 10 minutes and centrifuged at 10,000 rpm (12,000 *g*) for 10 minutes at 4°C. The RNA precipitate was washed with 2 mL of 75% ethanol and allowed to air dry for 5 to 10 minutes. RNA pellet was dissolved in diethylpyrocarbonate (DEPC)-treated water (autoclaved 0.1% DEPC water). RNA quality and concentration was determined by A260 measurement with the Nanodrop 1000 spectrophotometer (Thermo Scientific). PSR2 expression of transformed samples was detected using internal PSR2 primers, (PSR2 rtPCR F - ctcgccagtccacagttcaacac, PSR2 rtPCR R – gacgtattgcgcgcgaaaaacctg) using cDNA.

Arabidopsis Protoplast isolation

Well expanded leaves were harvested from 3-4 week old plants prior to flowering. 5-10 leaves were overlapped and 0.5-1mm leaf strips were cut using a fresh razor blade on top of white paper. Cut leaf strips were then transferred to a beaker where they were submerged in ~10 mL of enzyme solution. The beaker was then moved to the vacuum and vacuum infiltration was applied for 3 sessions of 10 minutes each, the beaker being agitated in between sessions. Digestion was then allowed to continue for 3 hours on a shaker set to 22°C and 50rpm, and a sterile pipette tip was used to disturb the mixture gently each hour. Following this, the protoplasts were then released by shaking for 1 minute at 80 rpm. The solution was then filtered through 35 – 75 nm mesh into a new 50 mL tube. The tube was then centrifugated at 100 *g* for 1-2 min at 500G and a pipette was used to gently remove the supernatant. 25 mL of W5 solution was added to the sidewall of the tube, which was then gently shaken and inverted to resuspend the protoplasts. The solution was once more centrifugated as above, before being washed with the W5 solution once more. Finally, an additional 20 mL of W5 solution was added to the tube, which was then placed on ice for 30 min in order to make the cells competent. Following this the supernatant was removed and 15 mL of MMg added to reach a concentration of $1x10^6$ protoplasts/mL) before being checked using the hemacytometer.

PEG Transfection

10–20 µL of DNA (10–20 µg of plasmid DNA of 5kb) (pEG100::3xFlag-PSR2, pEG100::Flag-PSR2, pEG100::PSR2, pEG100::ΔWY1-PSR2) was gently mixed with 200 µL of 1 X 10^6 protoplasts/ml protoplast solution. Following this, 210 – 220 µL of PEG/CA

2+ solution was also added to the tube and mixed. The sample was then allowed to incubate for 15 min at room temperature, before being further diluted with 0.8 mL of W5 solution. This mixture was centrifugated at speed 500rpm for 1 minute. The PEG was gently removed using a pipette, and the protoplasts were resuspended before having another 1 ml of W5 solution added and being washed again. Following this, the sample is centrifuged once more before being resuspended in 1ml of W5 solution before being allowed to sit overnight under indirect light for 16 hours. The solution was then centrifuged once more before being used for the following experiments.

Phosphatase Treatment

The total proteins of Arabidopsis protoplast expressed DRB4 were extracted with ice-cold protein extraction buffer (50 mM Tris-HCl, pH 7.5, 150 mM NaCl, 10 mM, 0.1 % NP-40, 1× EDTA-free complete protease inhibitor, 5 mM DTT). Then the samples were centrifuged at 12000 × g for 15 min and the supernatant was transferred into a new tube. For phosphatase treatment, the total proteins were resuspended in 5 μL of 10 X NEB Buffer for Protein MetalloPhosphatases (PMP), 1 μL of Lambda Protein Phosphatase and 5 μL of 10 mM MnCl2 to make a total reaction volume of 50 μL. Resuspended total proteins were incubated with or without lambda phosphatase for 30 min at 37°C. The treated total proteins was analyzed by normal SDS PAGE and Phos-tag SDS-PAGE. Phos-Tag™ was purchased from FUJIFILM Wako Pure Chemical Corporation and used according to the manufacturer's protocol. In brief, gels for Phos-tag SDS-PAGE consisted of a separating gel (8% (w/v) acrylamide, 50 μM Phos-tag acrylamide, 100 μM $MnCl_2$). Electrophoresis was performed at a constant current of 100 V with the SDS-PAGE running. For immunoblot analysis, gels

were washed in transfer buffer [25 mM Tris, 192 mM glycine, 0.1% (v/v) SDS, 20% methanol] with 10 mM EDTA for 10 min three times to remove metal ions, followed by two wash in transfer buffer for 10 min. Then, the proteins were electroblotted to the polyvinylidene difluoride (PVDF) membrane (ATTO Corporation).

Phosphorylation Detection

The gel casting system was prepared, and a resolving gel solution was prepared. The resolving gel solution was transferred between the glass plates, and butanol-saturated water/isopropanol was poured on top of the resolving gel solution. The solution was then allowed to polymerize for 30-60 minutes at room temperature. Following this, the "stacking gel" was prepared. Isopropanol was once more poured in between the glass, and any residual liquid was absorbed using a thin filter paper. The stacking gel solution was then poured on top of the resolving gel solution, and a comb was inserted. The gel solutions were then allowed to polymerize for another 15-30 minutes at room temperature.

Coimmunoprecipitation Assay & Nuclear-Cytoplasmic Fractionation

Three-week-old plants (0.5 g) were harvested and ground to a fine powder in liquid nitrogen and mixed with 2 mL/g of lysis buffer (20 mM Tris-HCl, pH 7.5, 20 mM KCl, 2 mM EDTA, 2.5 mM $MgCl_2$, 25% glycerol, 250 mM Suc, and 5 mM DTT) supplemented with protease inhibitor cocktail (Roche). The homogenate was filtered through a double layer of Miracloth. The flow-through was spun at 1500g for 10 min, and the supernatant, consisting of the cytoplasmic fraction, was centrifuged at 10,000 *g* for 10 min at 4°C and collected. The pellet was washed four times with 5 mL of nuclear resuspension buffer NRBT (20 mM Tris-HCl, pH 7.4, 25% glycerol, 2.5 mM $MgCl_2$, and 0.2% Triton X-100) and then resuspended with

500 µL of NRB2 (20 mM Tris-HCl, pH 7.5, 0.25 M Suc, 10 mM $MgCl_2$, 0.5% Triton X-100, and 5 mM β-mercaptoethanol) supplemented with protease inhibitor cocktail (Roche) and carefully overlaid on top of 500 µL NRB3 (20 mM Tris-HCl, pH 7.5, 1.7 M Suc, 10 mM $MgCl_2$, 0.5% Triton X-100, and 5 mM β-mercaptoethanol) supplemented with protease inhibitor cocktail (Roche). These were centrifuged at 16,000 *g* for 45 min at 4°C. The final nuclear pellet was resuspended in 400µL lysis buffer. To prepare the GFP magnetic beads, they were washed three times with Coimmuniprecipitation buffer. The buffer was removed using a magnetic stand. The beads were then resuspended in 1ml IP-B, and 20 µL of the bead slurry was aliquoted for each sample. Next the beads were incubated with samples with rotation for 2-3 h at 4°C. The end of the pipette tips were cut to allow easy handling of the beads. The beads were washed with IP-B three times using magnetic stand. Protein loading buffer was then added to the samples, and they were boiled for 5 minutes at 95°C to prepare for western blotting.

Electrophoresis and DRB4 Western Blotting

For the Western blots, proteins were prepared as described. The electrophoresis equipment was assembled, and the electrode chambers were filled with running buffer. The comb was gently removed from the stacking gel, and the wells were rinsed by pipetting before being loaded with samples. The gel was then run at constant current (30mA/gel) or constant voltage (120 – 130V) for 2 – 4 hours. The glass plates were then opened, and the gel was soaked in a general transfer buffer (1mM EDTA) for 10 minutes with gentle agitation. This washing was repeated two more times. The gel was then soaked in transfer buffer without EDTA for 10 minutes with gentle agitation. The gel was then transferred using a wet transfer method, in which the gel and methanol-activated PVDF membrane are “sandwiched” between a layer of

filter paper on each side. The gel was transferred at a constant current (100 mA) in a cold room, for one hour. The membrane was then blocked using 5% skim milk for 30 minutes, after which the primary antibody was added at a ratio of 1:1000 – 1:5000. This was then incubated with agitation for 1-2 hours at room temperature. The primary antibody was then collected, mixed with 0.02% Sodium Azide, and stored at 4C (α-Flag, α-GFP or α-PSR2 were used as written in the figures). The membrane was then rinsed with TBST three times for 10 minutes each. The membrane was then incubated with the secondary antibody in milk for 1 hour at room temperature. Following this the membrane was again rinsed with TBST 36 times for 10 minutes each. Finally, ECL substrate (BioRad) was applied to the membrane and allowed to incubate. Using a Gel Doc system, the western blot is imaged directly. The blue western blots were imaged using X-ray film.

DISCUSSION

Generation of PSR2-GFP$_{11}$

My hypothesis was that the structural architecture of PSR2 protein may promote effector delivery from the pathogen into host cells and/or mediate interactions with specific host factors. This hypothesis was tested first by investigating the delivery of PSR2 into plant cells. Our lab has discovered a linear structure of PSR2 consisting of multiple repeat units. A similar structure is predicted from a large number of *Phytophthora* effectors, leading to my hypothesis that it may facilitate delivery. I successfully applied the GFP strand method to PSR2 by expressing PSR2-GFP$_{11}$ through *Agrobacterium* infiltration together with GFP$_{1-10}$ in *N. benthamiana*. My results showed that the GFP$_{11}$ strand that is linked to PSR2 can form an intact fluorescence protein with GFP$_{1-10}$ expressed in plant cells; and PSR2 is mainly localized in the plant nucleus and membrane.

I intended to examine PSR2 delivery during natural infection using the GFP strand method; if successful, truncates of PSR2 could then be included to elucidate a role of the repeat units in effector delivery. I attempted to generate transgenic *P. capsici* that expresses PSR2-GFP$_{11}$. The transformants were planned to be used to infect transgenic Arabidopsis that expresses GFP$_{1-10}$. However, although I was able to introduce the PSR2 construct in *P. capsici*, I was unable to detect PSR2 proteins in the transformants. It is possible that the GFP$_{11}$-linker tag may have affected the protein accumulation of PSR2. Or PSR2 protein accumulation may have been regulated in *P. capsici*. Other lab members have observed posttranslational processing of PSR2 when expressed in plant cells. It is therefore also possible that PSR2-GFP$_{11}$ was processed in *P. capsici*, preventing its detection by western blotting. However, it is possible that the PSR2 protein was expressed but not imaged in the

western blot. A GFP polyclonal antibody to detect the presence of GFP_{11} may be an alternative for future experiments to detect the potential expression of PSR2-GFP_{11} proteins. Nonetheless, I was unable to detect AvrPto or AvrPtoB using the same method during *P. syringae* infection, which was reported by Henry et al., 2017. This could suggest, even if the *P. capsici* transformants were successfully generated and expressed PSR2 proteins, this visualization strategy may still be ineffective.

Future perspective: Optimizing PSR2 visualization

In order to address the GFP strand system delivery not expressing in *P. capsici* transformants, we could use the anti-PSR2 antibody available for immunofluorescence analysis as an alternative however this would not test direct effector translocation, only localization *in planta*. An optimization of the GFP strand method is to use tandem repeats of GFP_{11} fused to a protein of interest, this has been seen as successful for cellular protein labelling in mammalian cells (Kamiyama et al., 2016). Additionally, researchers have also used a tripartite split GFP interaction assay where the fluorescent intensity of the reconstructed GFP directly correlates with the strength of the interaction (Liu et al., 2018). However, until we know more about the effector translocation mechanisms, direct effector visualization from the pathogen into the host cell during a natural infection may be extremely difficult to undertake.

Characterizing PSR2 – DRB4 interaction

Studies have shown PSR2 association with DRB4 (Hou et al., 2019) and the protein phosphatase PP2A (Kuan, 2018). Unpublished data from a previous PhD student

Yi Zhai also suggested that DRB4 can be phosphorylated at various sites. Two phosphorylation sites are located between the dsRBMs, and an additional two on dsRBM2. In one study of human RNA-dependent protein kinase, five of 14 autophosphorylation sites were found located on the dsRBD and suggested that those sites may influence the RNA-binding properties of the enzyme (Jammi and Beal, 2001). Mass spectrometry interactome data revealed that multiple kinases were indeed identified to associate with DRB4. Several serine/threonine protein kinases were identified to associate as well as a Mitogen-activated protein kinase which provides supporting evidence that DRB4 may be phosphorylated. Therefore, I hypothesized that PSR2 may influence DRB4 phosphorylation. Additionally, PSR2 may interrupt the interaction of DRB4 with DCL4, thus affecting siRNA biogenesis. Using a protoplast expression system and stable expression plants, I observed for the first time that DRB4 could be phosphorylated.

However, in the presence of PSR2, DRB4's overall phosphorylation levels were not affected. This could suggest PSR2 may affect sRNA biogenesis through another mechanism underlying the potential manipulation of DRB4 by PSR2. Alternatively, it is also possible that PSR2 could specifically change one or more phosphorylation sites without significantly affecting the overall phosphorylation levels of DRB4. This could be explored quantitatively as the upper phosphorylated band in figures 1.9 and 1.10 show a slower migration in a Phos-tag gel based on the number of phosphorylation sites. Additionally, phosphorylation changes could be quantified by calculating a normalized intensity for the total and phosphorylated DRB4 using imaging software. Whether PSR2

could affect a phosphorylation site could also be examined by mass spectrometry-based analysis.

Enzymes involved in sRNA biogenesis are known to be regulated by posttranslational modifications. For example, Arabidopsis dsRNA-binding protein HYL1 has been shown to be regulated by phosphorylation (Chiliveri et al., 2017). Phosphorylation of HYL1 regulates its nuclear–cytosolic shuttling and protein stability (Achkar et al., 2018; Bhagat et al., 2022). Drosha, a human nuclease required for miRNA processing, can also be phosphorylated. This protein modification was shown to be important for the nuclear localization of Drosha (Tang et al., 2010). Another human RNA-binding protein Transactivation response element RNA-binding protein, TRBP, can also be phosphorylated (Paroo et al., 2009). This phosphorylation increases TRBP stability and subsequently the level of its associated Dicer. However, we currently do not know the effect phosphorylation has on DRB4. Although our current results did not indicate PSR2 affects the overall phosphorylation status of DRB4, further investigations are necessary to investigate and potentially quantify changes in specific phosphorylation site(s) of DRB4 using higher resolution approaches such as Mass Spectrometry. It would also be interesting to investigate whether mutants of these phosphorylation sites affect the function of DRB4.

The identification of the LWY tandem repeats in PSR2 structure offers exciting new opportunities to address different questions. These repeat modules enable the formation a stick-like overall shape of the effectors, which may promote effector delivery into the host cells, and their prevalence in Phytophthora effector repertoire indicates

functional significance. Future analysis of the LWY repeats on their role in effector delivery and virulence functions will advance our general understanding of pathogenesis.

REFERENCES

Achkar, N. P., Cho, S. K., Poulsen, C., Arce, A. L., Re, D. A., Giudicatti, A. J., Karayekov, E., Ryu, M. Y., Choi, S. W., Harholt, J., Casal, J. J., Yang, S. W., & Manavella, P. A. (2018). A Quick HYL1-Dependent Reactivation of MicroRNA Production Is Required for a Proper Developmental Response after Extended Periods of Light Deprivation. *Developmental Cell*, *46*(2), 236-247.e6. https://doi.org/10.1016/j.devcel.2018.06.014

Bhagat, P. K., Verma, D., Singh, K., Badmi, R., Sharma, D., & Sinha, A. K. (2022). Dynamic Phosphorylation of miRNA Biogenesis Factor HYL1 by MPK3 Involving Nuclear–Cytoplasmic Shuttling and Protein Stability in Arabidopsis. *International Journal of Molecular Sciences*, *23*(7), Article 7. https://doi.org/10.3390/ijms23073787

Chiliveri, S. C., Aute, R., Rai, U., & Deshmukh, M. V. (2017). DRB4 dsRBD1 drives dsRNA recognition in Arabidopsis thaliana tasi/siRNA pathway. *Nucleic Acids Research*, *45*(14), 8551–8563. https://doi.org/10.1093/nar/gkx481

Deslandes, L., Olivier, J., Peeters, N., Feng, D. X., Khounlotham, M., Boucher, C., Somssich, I., Genin, S., & Marco, Y. (2003). Physical interaction between RRS1-R, a protein conferring resistance to bacterial wilt, and PopP2, a type III effector targeted to the plant nucleus. *Proceedings of the National Academy of Sciences of the United States of America*, *100*(13), 8024–8029. https://doi.org/10.1073/pnas.1230660100

Dong, S., & Ma, W. (2021). How to win a tug-of-war: The adaptive evolution of Phytophthora effectors. *Current Opinion in Plant Biology*, *62*, 102027. https://doi.org/10.1016/j.pbi.2021.102027

Dunn, A. R., Fry, B. A., Lee, T. Y., Conley, K. D., Balaji, V., Fry, W. E., McLeod, A., & Smart, C. D. (2013). Transformation of Phytophthora capsici with genes for green and red fluorescent protein for use in visualizing plant-pathogen interactions. *Australasian Plant Pathology*, *42*(5), 583–593. https://doi.org/10.1007/s13313-013-0222-2

Fang, Y., Cui, L., Gu, B., Arredondo, F., & Tyler, B. M. (2017). Efficient Genome Editing in the Oomycete Phytophthora sojae Using CRISPR/Cas9. *Current Protocols in Microbiology*, *44*(1), 21A.1.1-21A.1.26. https://doi.org/10.1002/cpmc.25

Feng, B.-Z., Zhu, X.-P., Fu, L., Lv, R.-F., Storey, D., Tooley, P., & Zhang, X.-G. (2014). Characterization of necrosis-inducing NLP proteins in Phytophthora capsici. *BMC Plant Biology*, *14*(1), 126. https://doi.org/10.1186/1471-2229-14-126

Fukudome, A., Kanaya, A., Egami, M., Nakazawa, Y., Hiraguri, A., Moriyama, H., & Fukuhara, T. (2011). Specific requirement of DRB4, a dsRNA-binding protein, for the in vitro dsRNA-cleaving activity of Arabidopsis Dicer-like 4. *RNA (New York, N.Y.)*, *17*(4), 750–760. https://doi.org/10.1261/rna.2455411

Ghelis, T. (2011). Signal processing by protein tyrosine phosphorylation in plants. *Plant Signaling & Behavior*, *6*(7), 942–951. https://doi.org/10.4161/psb.6.7.15261

Ghosh, I., Hamilton, A. D., & Regan, L. (2000). Antiparallel Leucine Zipper-Directed Protein Reassembly: Application to the Green Fluorescent Protein. *Journal of the American Chemical Society*, *122*(23), 5658–5659. https://doi.org/10.1021/ja994421w

Haas, B. J., Kamoun, S., Zody, M. C., Jiang, R. H. Y., Handsaker, R. E., Cano, L. M., Grabherr, M., Kodira, C. D., Raffaele, S., Torto-Alalibo, T., Bozkurt, T. O., Ah-Fong, A. M. V., Alvarado, L., Anderson, V. L., Armstrong, M. R., Avrova, A., Baxter, L., Beynon, J., Boevink, P. C., … Nusbaum, C. (2009). Genome sequence and analysis of the Irish potato famine pathogen Phytophthora infestans. *Nature*, *461*(7262), Article 7262. https://doi.org/10.1038/nature08358

He, J., Ye, W., Choi, D. S., Wu, B., Zhai, Y., Guo, B., Duan, S., Wang, Y., Gan, J., Ma, W., & Ma, J. (2019). Structural analysis of Phytophthora suppressor of RNA silencing 2 (PSR2) reveals a conserved modular fold contributing to virulence. *Proceedings of the National Academy of Sciences of the United States of America*, *116*(16), 8054–8059. https://doi.org/10.1073/pnas.1819481116

Henry, E., Toruño, T. Y., Jauneau, A., Deslandes, L., & Coaker, G. (2017). Direct and Indirect Visualization of Bacterial Effector Delivery into Diverse Plant Cell Types during Infection. *The Plant Cell*, *29*(7), 1555–1570. https://doi.org/10.1105/tpc.17.00027

Hiraguri, A., Itoh, R., Kondo, N., Nomura, Y., Aizawa, D., Murai, Y., Koiwa, H., Seki, M., Shinozaki, K., & Fukuhara, T. (2005). Specific interactions between Dicer-like proteins and HYL1/DRB-family dsRNA-binding proteins in Arabidopsis thaliana. *Plant Molecular Biology*, *57*(2), 173–188. https://doi.org/10.1007/s11103-004-6853-5

Hou, Y., Zhai, Y., Feng, L., Karimi, H. Z., Rutter, B. D., Zeng, L., Choi, D. S., Zhang, B., Gu, W., Chen, X., Ye, W., Innes, R. W., Zhai, J., & Ma, W. (2019). A Phytophthora Effector Suppresses Trans-Kingdom RNAi to Promote Disease Susceptibility. *Cell Host & Microbe*, *25*(1), 153-165.e5. https://doi.org/10.1016/j.chom.2018.11.007

Hu, C.-D., & Kerppola, T. K. (2003). Simultaneous visualization of multiple protein interactions in living cells using multicolor fluorescence complementation analysis. *Nature Biotechnology*, *21*(5), 539–545. https://doi.org/10.1038/nbt816

Jiang, R. H. Y., Tripathy, S., Govers, F., & Tyler, B. M. (2008). RXLR effector reservoir in two Phytophthora species is dominated by a single rapidly evolving superfamily with more than 700 members. *Proceedings of the National Academy of Sciences*, *105*(12), 4874–4879. https://doi.org/10.1073/pnas.0709303105

Judelson, H. S., Tyler, B. M., & Michelmore, R. W. (1991). Transformation of the oomycete pathogen, Phytophthora infestans. *Mol. Plant-Microbe Interact*, 4, 602-607.

Kale, S. D., Gu, B., Capelluto, D. G. S., Dou, D., Feldman, E., Rumore, A., Arredondo, F. D., Hanlon, R., Fudal, I., Rouxel, T., Lawrence, C. B., Shan, W., & Tyler, B. M. (2010). External lipid PI3P mediates entry of eukaryotic pathogen effectors into plant and animal host cells. *Cell*, *142*(2), 284–295. https://doi.org/10.1016/j.cell.2010.06.008

Jammi, N. V., & Beal, P. A. (2001). Phosphorylation of the RNA-dependent protein kinase regulates its RNA-binding activity. *Nucleic Acids Research*, *29*(14), 3020–3029.

Kamiyama, D., Sekine, S., Barsi-Rhyne, B., Hu, J., Chen, B., Gilbert, L. A., Ishikawa, H., Leonetti, M. D., Marshall, W. F., Weissman, J. S., & Huang, B. (2016). Versatile protein tagging in cells with split fluorescent protein. *Nature Communications*, *7*(1), Article 1. https://doi.org/10.1038/ncomms11046

Khang, C. H., Berruyer, R., Giraldo, M. C., Kankanala, P., Park, S.-Y., Czymmek, K., Kang, S., & Valent, B. (2010). Translocation of Magnaporthe oryzae Effectors into Rice Cells and Their Subsequent Cell-to-Cell Movement. *The Plant Cell*, *22*(4), 1388–1403. https://doi.org/10.1105/tpc.109.069666

Kuan, T. (2018). *Molecular and Mechanistic Study of Phytophthora RxLR Effector PSR2 in Arabidopsis* [UC Riverside]. https://escholarship.org/uc/item/2d70k8c7

Lee, L.-Y., & Gelvin, S. B. (2014). Bimolecular fluorescence complementation for imaging protein interactions in plant hosts of microbial pathogens. *Methods in Molecular Biology (Clifton, N.J.)*, *1197*, 185–208. https://doi.org/10.1007/978-1-4939-1261-2_11

Liu, T.-Y., Chou, W.-C., Chen, W.-Y., Chu, C.-Y., Dai, C.-Y., & Wu, P.-Y. (2018). Detection of membrane protein-protein interaction in planta based on dual-intein-coupled tripartite split-GFP association. *The Plant Journal: For Cell and Molecular Biology*, *94*(3), 426–438. https://doi.org/10.1111/tpj.13874

Morgan, W., & Kamoun, S. (2007). RXLR effectors of plant pathogenic oomycetes. *Current Opinion in Microbiology*, *10*(4), 332–338. https://doi.org/10.1016/j.mib.2007.04.005

Nakazawa, Y., Hiraguri, A., Moriyama, H., & Fukuhara, T. (2007). The dsRNA-binding protein DRB4 interacts with the Dicer-like protein DCL4 in vivo and functions in the transacting siRNA pathway. *Plant Molecular Biology*, *63*(6), 777–785. https://doi.org/10.1007/s11103-006-9125-8

Paroo, Z., Ye, X., Chen, S., & Liu, Q. (2009). Phosphorylation of the Human Micro-RNA-Generating Complex Mediates MAPK/Erk Signaling. *Cell*, *139*(1), 112–122. https://doi.org/10.1016/j.cell.2009.06.044

Pumplin, N., Sarazin, A., Jullien, P. E., Bologna, N. G., Oberlin, S., & Voinnet, O. (2016). DNA Methylation Influences the Expression of DICER-LIKE4 Isoforms, Which Encode

Proteins of Alternative Localization and Function. *The Plant Cell*, *28*(11), 2786–2804. https://doi.org/10.1105/tpc.16.00554

Qiao, Y., Liu, L., Xiong, Q., Flores, C., Wong, J., Shi, J., Wang, X., Liu, X., Xiang, Q., Jiang, S., Zhang, F., Wang, Y., Judelson, H. S., Chen, X., & Ma, W. (2013). Oomycete pathogens encode RNA silencing suppressors. *Nature Genetics*, *45*(3), 330–333. https://doi.org/10.1038/ng.2525

Raghuram, B., Sheikh, A. H., Rustagi, Y., & Sinha, A. K. (2015). MicroRNA biogenesis factor DRB1 is a phosphorylation target of mitogen activated protein kinase MPK3 in both rice and Arabidopsis. *The FEBS Journal*, *282*(3), 521–536. https://doi.org/10.1111/febs.13159

Schornack, S., van Damme, M., Bozkurt, T. O., Cano, L. M., Smoker, M., Thines, M., Gaulin, E., Kamoun, S., & Huitema, E. (2010). Ancient class of translocated oomycete effectors targets the host nucleus. *Proceedings of the National Academy of Sciences of the United States of America*, *107*(40), 17421–17426. https://doi.org/10.1073/pnas.1008491107

Seshacharyulu, P., Pandey, P., Datta, K., & Batra, S. K. (2013). Phosphatase: PP2A structural importance, regulation and its aberrant expression in cancer. *Cancer Letters*, *335*(1), 9–18. https://doi.org/10.1016/j.canlet.2013.02.036

Snapp, E. (2005). Design and Use of Fluorescent Fusion Proteins in Cell Biology. *Current Protocols in Cell Biology / Editorial Board, Juan S. Bonifacino ... [et Al.]*, *CHAPTER*, Unit-21.4. https://doi.org/10.1002/0471143030.cb2104s27

Stam, R., Jupe, J., Howden, A. J. M., Morris, J. A., Boevink, P. C., Hedley, P. E., & Huitema, E. (2013). Identification and Characterisation CRN Effectors in Phytophthora capsici Shows Modularity and Functional Diversity. *PLOS ONE*, *8*(3), e59517. https://doi.org/10.1371/journal.pone.0059517

Tang, X., Zhang, Y., Tucker, L., & Ramratnam, B. (2010). Phosphorylation of the Rnase III enzyme Drosha at Serine300 or Serine302 is required for its nuclear localization. *Nucleic Acids Research*, *38*(19), 6610–6619. https://doi.org/10.1093/nar/gkq547

Teufel, F., Almagro Armenteros, J. J., Johansen, A. R., Gíslason, M. H., Pihl, S. I., Tsirigos, K. D., Winther, O., Brunak, S., von Heijne, G., & Nielsen, H. (2022). SignalP 6.0 predicts all five types of signal peptides using protein language models. *Nature Biotechnology*, *40*(7), Article 7. https://doi.org/10.1038/s41587-021-01156-3

Virshup, D. M., & Shenolikar, S. (2009). From Promiscuity to Precision: Protein Phosphatases Get a Makeover. *Molecular Cell*, *33*(5), 537–545. https://doi.org/10.1016/j.molcel.2009.02.015

Wawra, S., Trusch, F., Matena, A., Apostolakis, K., Linne, U., Zhukov, I., Stanek, J., Koźmiński, W., Davidson, I., Secombes, C. J., Bayer, P., & van West, P. (2017). The RxLR

Motif of the Host Targeting Effector AVR3a of Phytophthora infestans Is Cleaved before Secretion. *The Plant Cell*, *29*(6), 1184–1195. https://doi.org/10.1105/tpc.16.00552

Whisson, S. C., Boevink, P. C., Moleleki, L., Avrova, A. O., Morales, J. G., Gilroy, E. M., Armstrong, M. R., Grouffaud, S., van West, P., Chapman, S., Hein, I., Toth, I. K., Pritchard, L., & Birch, P. R. J. (2007). A translocation signal for delivery of oomycete effector proteins into host plant cells. *Nature*, *450*(7166), Article 7166. https://doi.org/10.1038/nature06203

Win, J., & Kamoun, S. (2008). Adaptive evolution has targeted the C-terminal domain of the RXLR effectors of plant pathogenic oomycetes. *Plant Signaling & Behavior*, *3*(4), 251–253. https://doi.org/10.4161/psb.3.4.5182

Win, J., Krasileva, K. V., Kamoun, S., Shirasu, K., Staskawicz, B. J., & Banfield, M. J. (2012). Sequence divergent RXLR effectors share a structural fold conserved across plant pathogenic oomycete species. *PloS Pathogens*, *8*(1), e1002400. https://doi.org/10.1371/journal.ppat.1002400

Yaeno, T., Li, H., Chaparro-Garcia, A., Schornack, S., Koshiba, S., Watanabe, S., Kigawa, T., Kamoun, S., & Shirasu, K. (2011). Phosphatidylinositol monophosphate-binding interface in the oomycete RXLR effector AVR3a is required for its stability in host cells to modulate plant immunity. *Proceedings of the National Academy of Sciences of the United States of America*, *108*(35), 14682–14687. https://doi.org/10.1073/pnas.1106002108

Zhai, Y. (2018). *Identification and Characterization of Phytophthora Effectors with RNA Silencing Suppression Activity* [UC Riverside]. https://escholarship.org/uc/item/93g4j3vb

Zhu, S., Jeong, R.-D., Lim, G.-H., Yu, K., Wang, C., Chandra-Shekara, A. C., Navarre, D., Klessig, D. F., Kachroo, A., & Kachroo, P. (2013). Double-Stranded RNA-Binding Protein 4 Is Required for Resistance Signaling against Viral and Bacterial Pathogens. *Cell Reports*, *4*(6), 1168–1184. https://doi.org/10.1016/j.celrep.2013.08.018

Chapter 2

Elucidating the role of secondary siRNAs in host-induced gene silencing

ABSTRACT

Plant secondary siRNAs contribute to resistance to *Phytophthora* putatively through host-induced gene silencing. Previous work in our lab identified *Phyca_554980* as a potential target of Arabidopsis *PPR*-siRNAs in *Phytophthora capsici*. In this chapter, I hypothesized that a *P. capsici* mutant with a modified siRNA target site in *Phyca_554980* would be resistant to *PPR*-siRNA-mediated resistance because, without a complementary gene sequence, the *PPR*-siRNA should not induce silencing of the mutated gene. Furthermore, over-expression of *Phyca_554980* may also confer tolerance of *P. capsici* to siRNA-mediated defense. This experiment could provide crucial evidence to support the contribution of HIGS mediated by *PPR*-siRNAs during *Phytophthora* infection. However, despite numerous attempts, I was unable to generate siRNA target mutants of *Phyca_554980* using CRISPR-Cas9 mediated gene editing. Additionally, this gene could not be overexpressed in *P. capsici*. Nonetheless, this attempt was important as it was one of the first to try and demonstrate a direct interaction of host sRNAs in HIGS by manipulating the target gene in the pathogen.

INTRODUCTION

Phytophthora capsici biology

Phytophthora capsici has a wide range of hosts, including many plants in the Solanaceae family, such as peppers, cucurbits, tomatoes (Satour & Butler, 1967; Erwin & Ribeiro, 1996; Hausbeck & Lamour, 2004). Depending on the plant host, *P. capsici* is capable of infecting most parts of the plant, including the roots, leaves, stems, as well as the fruits, causing wilting and rotting (Erwin & Ribeiro, 1996; Lamour et al., 2012). This pathogen causes in excess of $100 million in damages yearly (Bosland, 2008) and more in prevention and chemical management. Cultural practices, particularly irrigation management, are of vital importance as irrigation water and weather events can spread spores causing *P. capsici* to easily transmit from field to field and swiftly establish disease. Once established, *P. capsici* is difficult to eradicate (Lamour et al., 2012).

Very few sources of genetic resistance have been identified against *P. capsici*. Several QTLs that contribute to resistance in peppers have been identified (Quesada-Ocampo & Hausbeck, 2010; Thabuis et al., 2003). One accession of tomato exhibited resistance to four *P. capsici* isolates (Quesada-Ocampo & Hausbeck, 2010). Despite reports of partial resistance to *P. capsici* conferred by QTLs, no race-specific resistance genes have been identified (Xu et al., 2016). Understanding different methods of genetic resistance to *P. capsici* is vital in establishing resistance.

Despite cultural, chemical, and genetic-based pathogen management practices, *P. capsici* still poses a threat globally. Studying the interaction between this pathogen and plant hosts is complex due to its reproductive cycle that is characteristically comprised of both

sexual outcrossing and rapid asexual reproduction for propagation and survival (Lamour et al., 2012). *P. capsici* is heterothallic with isolates having A1 or A2 mating types. Both mating types are required in proximity for mating and formation of oospores to occur (Ko, 1988).

This is in contrast to other species, such as *P. sojae*, which are homothallic and can sexually cross and form oospores without another mating type present. Due to its diversity and broad host range, there is a need for research into methods of defense and resistance in plants.

The secondary siRNA pathway is important for Arabidopsis defense against *Phytophthora*

Two essential components of the secondary siRNA pathway are SGS3 and RDR6 (Adenot et al., 2006; Peragine et al., 2004). RDR6 converts single stranded RNA to dsRNA in tandem with SGS3 (Dalmay et al., 2000; Mourrain et al., 2000) which may stabilize the sRNA cleavage product for dsRNA synthesis (Yoshikawa et al., 2013). The dsRNAs are then processed by DCL4 together with DRB4 to produce siRNAs (Nakazawa et al., 2007). Our lab showed that disruption of this secondary siRNA pathway via knockout mutants of DRB4, SGS3 or RDR6 caused hypersusceptibility to *P. capsici* (Figure 2.1) (Hou et al., 2019). Importantly, the RxLR effector, *Phytophthora* Suppressor of RNA Silencing 2 (PSR2) specifically suppresses the secondary siRNA accumulation in Arabidopsis and also causes hypersusceptibility. These results support that the secondary siRNA pathway is required for defense against *Phytophthora*.

PSR2 inhibits the accumulation of specific 21nt secondary siRNAs

Arabidopsis transgenic plants expressing PSR2 shows no developmental defects, apart from developing slightly elongated, curled leaves, which are reminiscent to *drb4* mutants (Nakazawa et al., 2007). However, inoculation of PSR2-5 with *P. capsici* isolate LT263, which has no close homolog of *PSR2*, shows hypersusceptibility (Figure 2.1) (Xiong et al., 2014) (Hou et al., 2019). Small RNA profiling of PSR2-5 plants showed a reduction only in the 21-nucleotide sRNAs, leading to further investigations on the roles of this 21nucleotide sRNA population. Analysis of specific 21-nt sRNA classes revealed a small reduction in the abundance of miRNAs (5%) but a drastic reduction in that of secondary siRNAs generated from *TAS1*, *TAS2*, and some *PPR*-encoding gene loci. siRNAs produced from other loci remained unchanged. These results indicate that PSR2 may inhibit the accumulation of siRNAs produced from *PPR* and *TAS1*/2 transcripts, begging the question of what functions secondary siRNAs have in regards to plant immunity. The most severe decrease (90%) in PSR2-5 plants was from *PPR* derived secondary siRNAs. Most of these *PPR*-siRNAs are produced from fifteen *PPR* loci. Thirteen of the fifteen *PPR* loci that produce PSR2-inhibited siRNAs contain a target site of the microRNA161 (miR161) (Hou et al., 2019).

miR161 and *PPR*-siRNAs are induced as a defense response to *Phytophthora* infection

Upon *P. capsici* infection, qRT-PCR of pri-miRNA, a hairpin containing primary transcript, detected an increase of pri-miR161 abundance, whereas pri-miR173, a miRNA that could trigger tasiRNA production, stayed unaffected. Northern blotting of miR161 revealed that its accumulation increased during infection, particularly at 6 and 24 hours post

inoculation (hpi). Similarly, miR393, which was previously shown to contribute to basal plant defense (Navarro et al., 2006), was also induced. The induction of miR161 at 6 hpi suggests that *P. capsici* elicits an immune response during an early infection stage in *Arabidopsis* (Figure 2.2a). In *Arabidopsis*, the co-receptors somatic-embryogenesis receptor-like kinase 4 (SERK4) and brassinosteroid insensitive 1-associated kinase 1 (BAK1) are required to activate pattern-triggered immunity (Roux et al., 2011). *Bak1*-5 *serk4* mutant plants abolished the induction of both miR161 and miR393, suggesting that increased accumulation of miR161 could be a defense response prompted by *P. capsici* perception (Figure 2.2b). Since miR161 is a major trigger of *PPR*-siRNA production, increased levels could boost accumulation of these secondary siRNAs. During *P. capsici* infection, northern blotting demonstrated that, corresponding with miR161, the levels of two *PPR*-siRNA increased unlike the miR173-dependent tasiRNA, which did not increase during infection. To determine whether miR161 can contribute to plant defense, Hou et al., generated *MIR161* knockout (MIR161cri) and *MIR161* overexpression (MIR161OX) transgenic lines in Arabidopsis. During *P. capsici* infection, the MIR161cri plants showed hypersusceptibility while MIR161OX exhibited enhanced resistance (Figure 2.2c). Overexpression of miR173 did not influence *Arabidopsis* resistance to *P. capsici*, in support of the previous results that miR173 is not induced during infection and therefore may not contribute to plant defense in the same way.

***PPR*-siRNAs potentially silence *Phytophthora* genes and confer resistance**

249 *P. capsici* genes were predicted to be potential targets of 3,922 unique *PPR*siRNA sequences. Among them, *Phyca_554980* encodes a U2-associated splicing factor

and has been suggested to regulate *P. capsici* development and virulence (Hou et al., 2019). The *Phyca_554980* transcript has potential target sites of seven *PPR*-siRNAs including the relatively more abundant siR1310 and siR0513. In addition to the number of *PPR*-siRNAs predicted to target *Phyca_554980*, this gene was chosen for further analysis because: 1) it is constitutively expressed; and 2) it has homologous genes in other *Phytophthora* species.

To mimic what may happen during a natural infection, an siR1310 synthetic duplex was introduced directly into *P. capsici*. As a negative control, an siRNA designed to target the *GFP* gene (siRGFP) was also introduced. Introduction of siR1310 duplex, but not the siRGFP duplex nearly abolished *P. capsici's* ability to infect *Nicotiana benthamiana* (Figure 2.3), suggesting that this *PPR*-siRNA, if can enter the pathogen cells, can significantly affect virulence. It is important to note that secondary siRNA production through a miRNA-*PPR* circuit is conserved in dicots (Xia et al., 2013), suggesting that *PPR*-siRNAs might be a conserved component of plant immunity through HIGS.

The primary goal of my project was to demonstrate that plant secondary *PPR*siRNAs confer resistance through HIGS in *Phytophthora*. In this chapter, I attempted to generate a *P. capsici* mutant of *Phyca_554980* with the *PPR*-siRNA target site mutated in order to examine whether this mutant can tolerate *PPR*-siRNA-mediated resistance. This experiment aimed to provide key evidence to support the contribution of HIGS mediated by *PPR*-siRNAs during *P. capsici* infection.

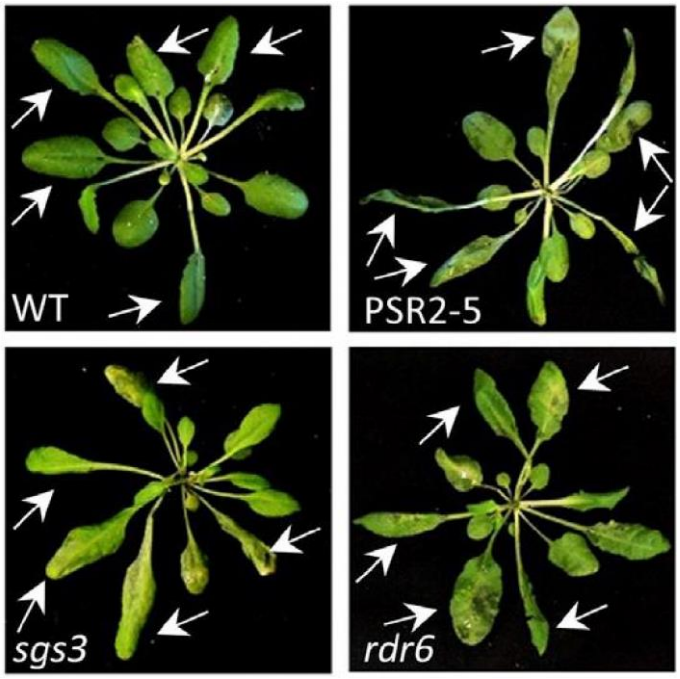

Figure 2.1 Arabidopsis mutants in the secondary siRNA pathway are hypersusceptible to *P. capsici.*

Arabidopsis plants were inoculated with *P. capsici* zoospores. Photos were taken three days post inoculation. WT = wild-type Arabidopsis accession Col-0 (Image from Hou et al., 2019).

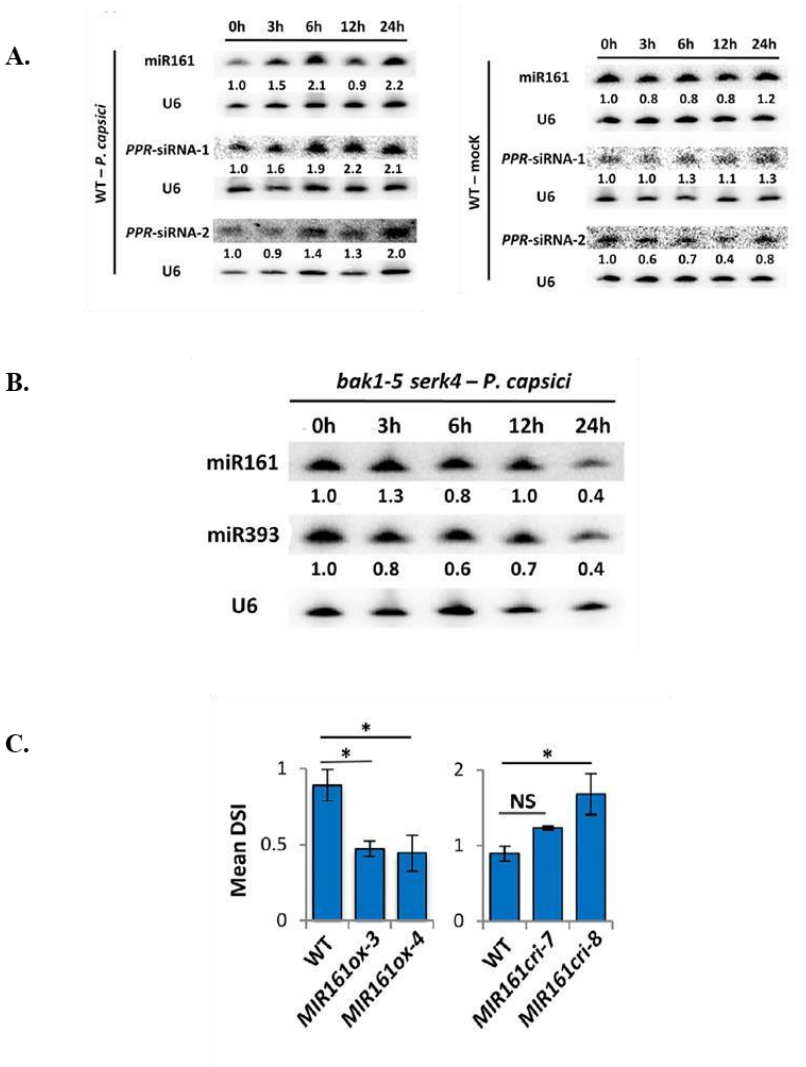

Figure 2.2 miR161 and *PPR*-siRNAs are induced during infection.

A. Northern blotting shows induced accumulation of miR161 and two *PPR*-siRNAs in WT Arabidopsis during *P. capsici* infection (left) or mock treatment (water, right). Numbers represent relative signal intensities in northern blots. **B.** Northern blotting of *Bak1*-5 *serk4* mutant plants shows the abolishment of the induction of miR161 or miR393. **C.** Arabidopsis MIR161cri plants showed hypersusceptibility while MIR161OX exhibited enhanced resistance during *P. capsici* infection (Image from Hou et., al 2019).

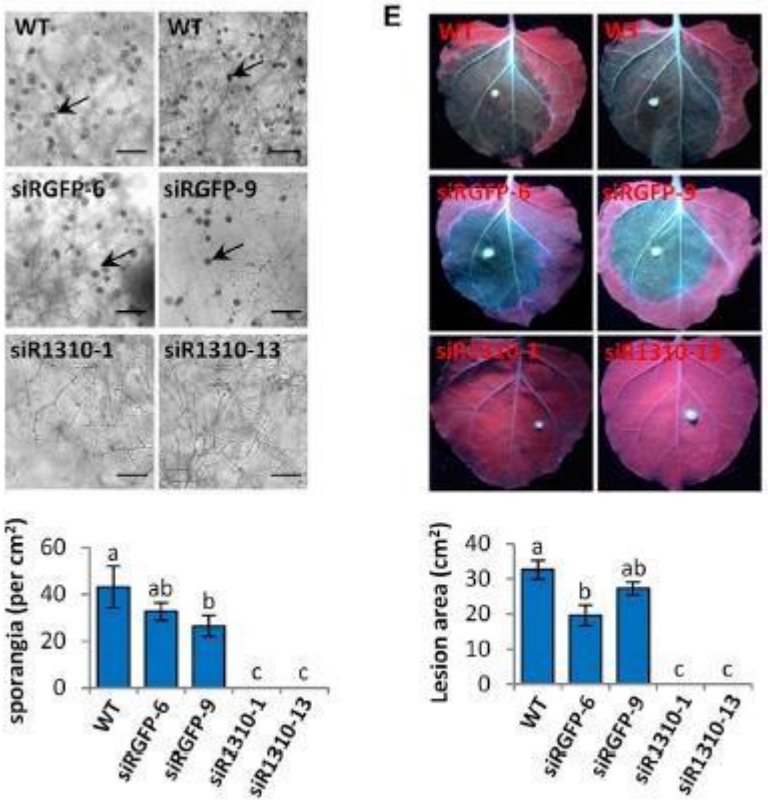

Figure 2.3 siRNA1310 confers resistance to *P. capsici*.

Numbers of sporangia is largely reduced in *P. capsici* transformants with siR1310 (left). *P. capsici* transformants with siRNA1310 lost the virulence activity in *N. benthamiana* (right). (Image from Hou et al., 2019). WT = wild-type *P. capsici*

RESULTS

Identification of *PPR*-siRNA target gene candidates in *P. capsici*

Previously, the *P. capsici* gene *Phyca_554980* was hypothesized to be targeted by *Arabidopsis PPR*-siRNAs (Hou et al., 2019). To determine whether these *PPR*-siRNAs were the executors of *Phyca_554980* gene silencing during natural infection, I attempted to make *P. capsici* mutants with *Phyca_554980* "camouflaged" through the introduction of mutations in the siRNA target site. To remove sequence complementarity with *PPR*-siRNAs whilst still maintaining the gene function, I designed a *Phyca_554980* synonymous mutant. I chose the sites to be synonymously mutated in *Phyca_554980* by analyzing 3922 unique *PPR*-siRNAs using a plant small RNA target analysis server (Dai & Zhao, 2011). Using a relaxed threshold (expectation score ≤ 5) this analysis revealed 47 *PPR*-siRNAs predicted to target *Phyca_554980* (Figure 2.4a). Applying a stringent threshold, (expectation score ≤ 3) (Dai and Xiao, 2011), six of the 47 sites were targeted for modification by introducing sequence changes in order to prevent targeting by *PPR*-siRNAs (Figure 2.4b). One of those predicted *PPR*-siRNAs is siRNA1310, which was characterized in detail previously (Hou et al., 2019). The mutated version did not change the amino acid sequence as to not disrupt its functions (Figure 2.5). I hypothesize that without a complementary gene sequence, the *PPR*-siRNA should not induce silencing of the mutated gene, and therefore the defense conferred by *PPR*siRNAs to *P. capsici* may be compromised.

A.

B.

siRNA Identifier	*P. capsici* gene	Expectation Score	siRNA Length	Target Site Start	Target Site End	Target Sequence
PPR-siRNA-5	*Phyca_554980*	1.5	21	1790	1810	AGAGGAUGUCAACCAGAUCUG
PPR-siRNA-644	*Phyca_554980*	1.5	21	1792	1812	AAAGAGGAUGUCAACCAGAUC
PPR-siRNA-321	*Phyca_554980*	2	21	1789	1809	GAGGAUGUCAACCAGAUCUGG
PPR-siRNA-64	*Phyca_554980*	2.5	21	1788	1808	AGGAUGUCAACCAGAUCUGGU
PPR-siRNA-1979	*Phyca_554980*	3	21	1790	1810	AGAGGCUGUCAACCAGAUCUG
PPR-siRNA-2162 (siR1310)	*Phyca_554980*	3	21	1792	1812	AAAGAGGCUGUCAACCAGAUC

Figure 2.4. *PPR*-siRNA target sites predicted in *Phyca_554980.*

A. *P. capsici* gene *Phyca_554980* contains sequences that are predicted to be targeted by multiple *PPR*-siRNAs. The pink box labels the position within *Phyca_554980* at which the *Arabidopsis PPR*-siRNAs are predicted to target. **B.** List of six *PPR*-siRNAs that potentially target *Phyca_554980* and their target sequences.

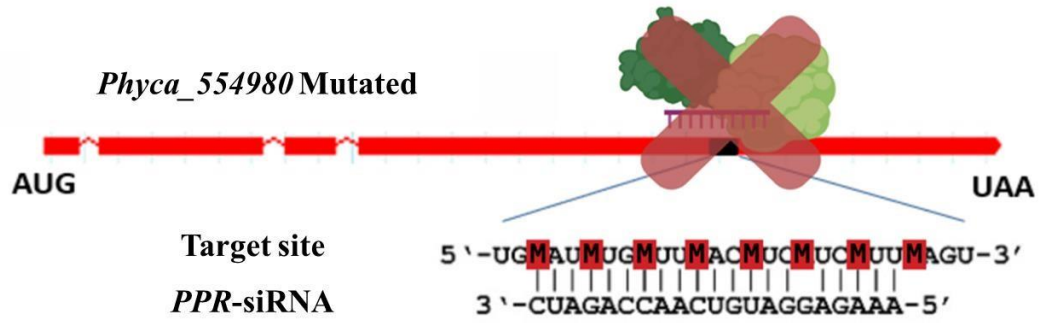

Figure 2.5. Schematic diagram of mutations introduced into the predicted *PPR*-siRNAs in *Phyca_554980*.

Mutations in *Phyca_554980* are shown in red. The protein complex, RISC (in green), is hypothesized to not induce gene silencing without the presence of a complementary gene sequence. (Adapted from Hou et. al 2019)

PPR-siRNA target gene editing strategies

I utilized two gene editing strategies to introduce a potentially *PPR*-siRNA resistant *Phyca_554980* gene: CRISPR-mediated gene editing (Figure 2.6a-b) and target gene overexpression (Figure 2.6c-d). CRISPR-mediated gene editing allows for targeted manipulation or replacement of a target gene. I hypothesized that by replacing the target gene with a synonymously mutated version of itself (Figure 2.6a), the *PPR*-siRNAs would not silence *Phyca_554980*. This could show a more direct interaction of *PPR*-siRNAs to *P. capsici* genes and elucidate the role of secondary siRNAs in HIGS. To completely replace *Phyca_554980*, I chose to generate a total target gene replacement construct using a *hygromycin* resistance gene as the replacement gene (Figure 2.6b). Lastly, constructs were generated to overexpress the wild type *Phyca_554980* (Figure 2.6c) as well as the *Phyca_554980* synonymously mutated form (Figure 2.6d). My hypothesis was that increased accumulation of *Phyca_554980* transcripts from both constructs would be able to tolerate the potential silencing by *Arabidopsis PPR*-siRNAs thereby providing evidence of their role in HIGS.

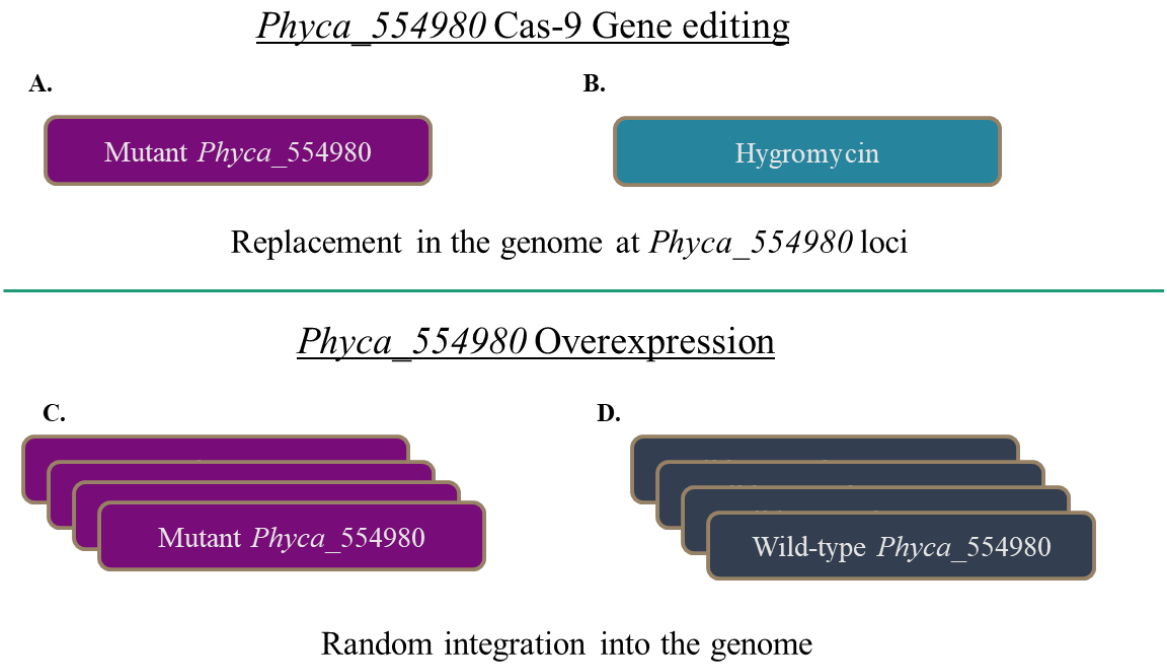

Figure 2.6 *PPR*-siRNA target site synonymous mutations strategies.

The CRISPR/Cas-9 gene editing strategy (top) to replace *Physa_554980* with either a synonymous mutant (**A**) or hygromycin resistance gene (**B**). A second strategy (bottom) is to overexpress *Physa_554980* as a synonymous mutant (**C**) or wild-type version (**D**).

Generation of *PPR*-siRNA resistant mutants of *P. capsici* by CRISPR/Cas9

I constructed plasmids for a CRISPR/Cas9-mediated targeted gene editing to be used for *P. capsici* transformation. I first designed single guide RNAs (sgRNAs) which guide the Cas9 enzyme to produce a targeted double-stranded nick in the gene chosen for editing (Ran et al., 2013). Using the sgRNA design protocol described in Fang et al., 2017 and a sgRNA design software, EuPaGDT (Peng & Tarleton, 2015), I identified multiple sgRNA pairs upstream of a protospacer adjacent motif which is required for targeting. It has been reported previously that sgRNAs whose total efficiency score from the sgRNA design program are above "0.5" generally do not show noticeable improvements from higher efficiency scores (Table 2.1) (Fang et al., 2017). Based on this observation, I prioritized candidates closer to the siRNA target site instead of higher efficiency scores. Additional requirements for a good sgRNA candidate include low off-target sites containing matches with two or less mismatched positions within the *P. capsici* genome (Wyvekens et al., 2015). While the EuPaGDT software incorporates an off-target analysis, I additionally tested for off-target sites using the alignment tool on FungiDB. Lastly, I analyzed the secondary DNA structure using the *RNA structure* program (Reuter & Mathews, 2010). All candidate sgRNAs had three or less nucleotides predicted to have strong self-complementarity (Figure 2.7), which potentially prevents binding to the target DNA. SgRNA 1 and sgRNA 2 were the two best choices at the time, without any off-targets sites or strong self-complementarity. They are both upstream of the *PPR*-siRNA target site (Figure 2.8).

	Single guide RNA	gRNA id	gRNA sequence (PAM "|NGG")	Total score	efficiency score based on Doench et al.2014	efficiency score based on CRISPRater	On-target hits in the genome	Off-target hits (perfect-match | nonperfect-match)	GC content	Potential problems during transcription
A.	SG1	Phyca554980_866 revcom	GCAGGTGCAGTAGTGCCCGG|**TGG**	0.39	0.48	0.88	0 | 0	0 | 0	0.7	No problem found
	SG2	Phyca554980_1179 revcom	CAACTCAGGCGGTATCCACA|**CGG**	0.37	0.61	0.78	0 | 0	0 | 0	0.55	gRNA does not start with "G" or "A", please manually add a leading "G" or "A"
B.	SG3	Phyca554980_1710	ATTGCTGGAGGAACTGACCC|**TGG**	0.6	0.61	0.74	1 | 0	0 | 0	0.55	No problem found
	SG4	Phyca554980_1972	ATTGCGCACAAAAATATTGT|**TGG**	0.59	0.45	0.75	1 | 0	0 | 0	0.3	No problem found

Table 2.1 Single guide RNA selection.

CRISPR/Cas9 sgRNAs selected from Eu-PaGDT (http://grna.ctegd.uga.edu/). Candidates whose efficiency score are above 0.5 are generally considered good based on a scoring matrix developed by (Doench et al., 2014). **A.** First pair of guide RNAs developed. **B.** Second pair of guide RNAs developed.

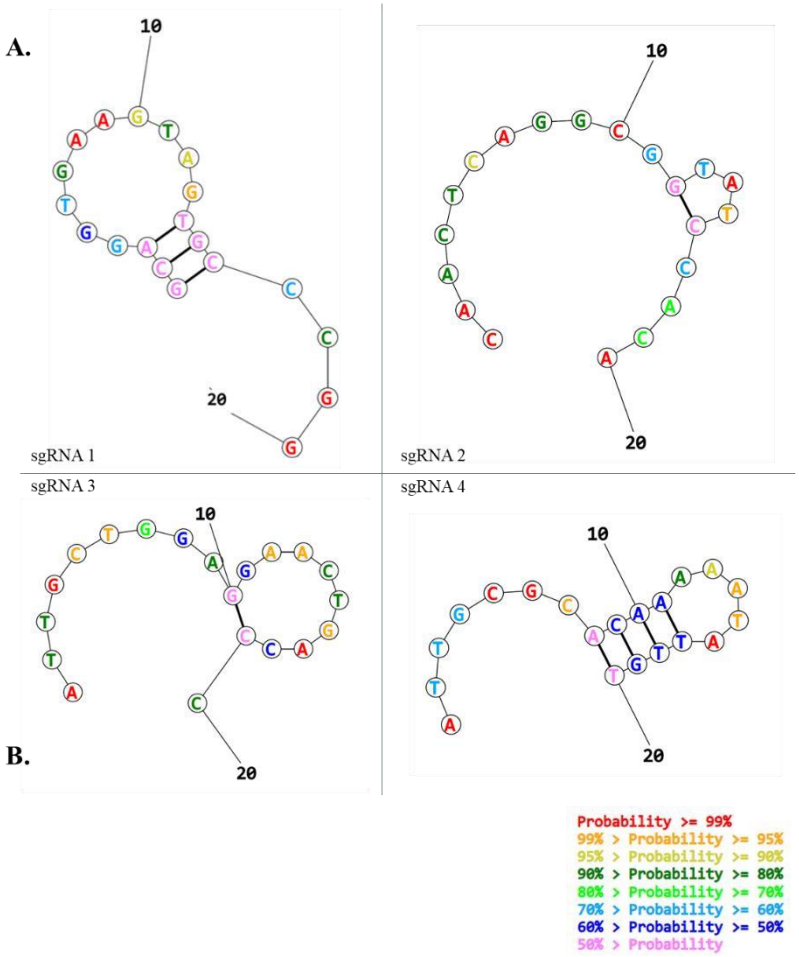

Figure 2.7 Secondary structures of sgRNAs designed to target *Phyca_554980*.

The structures were predicted using http://rna.urmc.rochester.edu/RNAstructureWeb. Based on Fang et. Al 2017 no more than three consecutive based pairs is acceptable. **A.** First pair of guide RNAs developed. **B.** Second pair of guide RNAs developed.

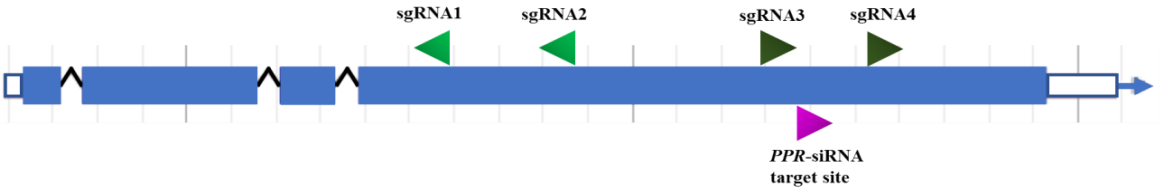

Figure 2.8 A gene map of *Physca_554980* illustrating the sgRNA target sites.

Four single guide RNAs were designed to target the *P. capsici* gene *Physca_554980*. The *PPR*-siRNA target site is shown as the pink box.

To prevent non-homologous end joining (NHEJ) after a Cas9 enzyme nick, a homologous donor gene is prepared with 1000 bp flanks on either end of the targeted gene (Figure 2.9) to encourage homologous recombination. In this replacement, a hygromycin resistance gene was used as the donor gene (Figure 2.9). To produce the *PPR*-siRNA resistant *Phyca_554980*, the *PPR*-siRNA target site was mutated. Additionally, to avoid homologous recombination from reoccurring in the gene, the sgRNA target sites were also synonymously mutated within the donor fragment. A full length *Phyca_554980* gene containing those mutations was synthesized (Figure 2.8).

Using a three-plasmid transformation system, the guide RNAs, CRISPR/Cas9 (Figure 2.10a), and the homologous donor, were transformed into *P. capsici* protoplasts by PEGmediated protoplast transformation. As a positive control, I used a pTOR::tdTomato plasmid which confers constitutive expression of red fluorescence in *P. capsici*. Transformation experiments were performed twice using plasmids carrying sgRNA1, sgRNA2, and the mutated *Phyca_554980* construct. After the second transformation attempt, I added an additional control of untransformed *P. capsici* protoplasts as a negative control to the G418 antibiotic. Though the growth of the untransformed *P. capsici* was initially inhibited by G418, 36-42 hours after recovery on V8, the hyphal colonies were a compatible size with that of the *P. capsici* hyphal colonies transformed with a plasmid carrying the G418 resistance gene. This suggests that there may be false positives. Therefore, I used the criterium that

"G418 resistant colonies" should grow more than 1cm after five days of subculturing after the transformation. This hyphal growth measurement was chosen because, in general, colonies that did not grow to that length would generally not grow again once re-subcultured

for transformant screening or DNA/RNA extraction. The guide RNA plasmids (Figure 2.10a – right) encode a GFP gene for transformant screening.

From the 97 *Phyca_554980mut* subcultures and 72 *Phyca_554980Hyg* subcultures screened for GFP fluorescence, 5% and 0% exhibited fluorescence stronger than background fluorescence, respectively (Figure 2.11). The positive control had a ~7% transformation rate which is an expected rate indicative of the protoplast transformation system successfully working. When examined for genomic integration using sequencing of the target site, none of the *Phyca_554980mut* colonies were gene edited.

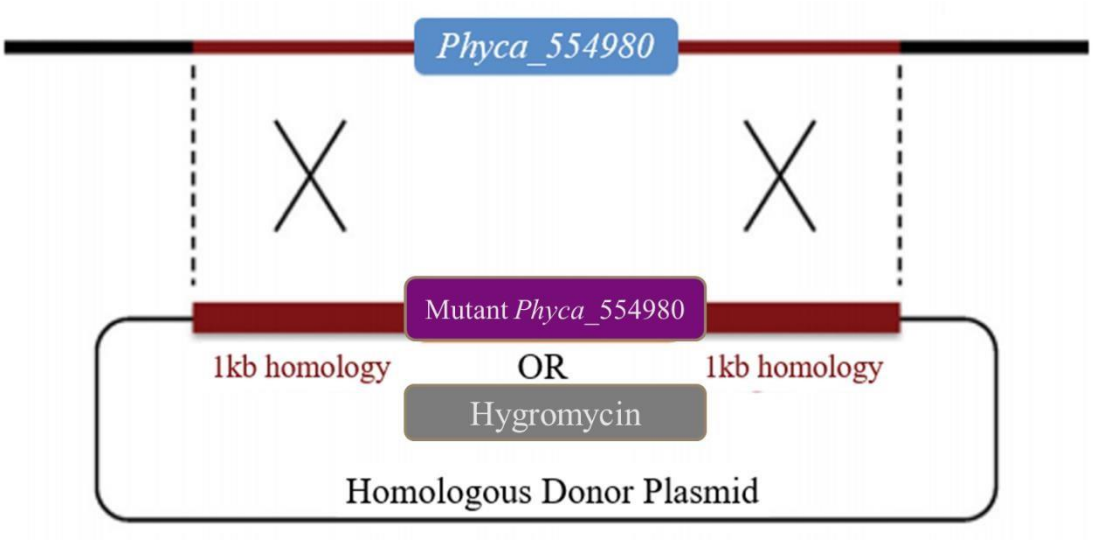

Figure 2.9 Experimental design of CRISPR/Cas9-mediated homologous donor gene replacement in *P. capsici*.

Homologous donor gene plasmid used to replace wild-type *Phyca_554980* with a synonymous mutant or a Hygromycin resistance gene. 1kb homologous sequences on both sides of the target gene (in red) were cloned to flank the homologous donor plasmid inserts in order to facilitate recombination (Figure adapted from Fang et. Al 2018).

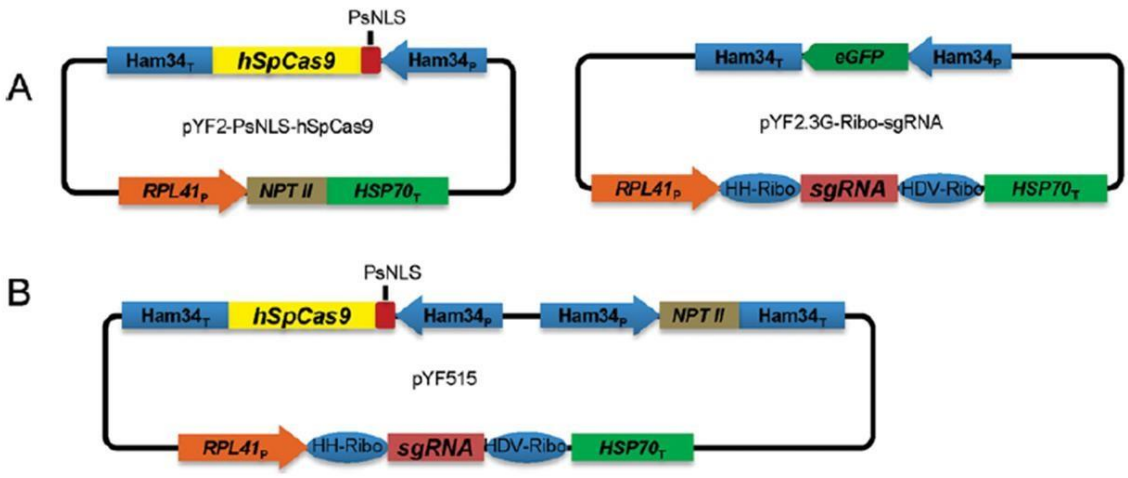

Figure 2.10 Maps of plasmids carrying Cas9 and the sgRNAs.

A. The Cas9 plasmids (left) carries Cas9 fused with a Nuclear Localization Signal sequence from *Phytophthora sojae* (PsNLS) under the *Bremia lactucae* promoter *Ham34* and the *NPTII* gene as resistance marker. The single guide RNA plasmid (right) carries the sgRNA sequence flanked by a hammerhead ribozyme sequence (HH-Ribo and HDV-Ribo) and promoter (RPL41) and terminator (HSP70), and GFP as a fluorescence marker. **B.** The pYF515 "All in one" plasmid carries *Cas9*, *NPTII* and sgRNA in one plasmid (Image from Fang et. al., 2018).

Hygromycin and *Phyca_554980-mut* Replacement (sgRNA 1-2)		
Fluorescent/G418 resistant colonies	Transformation 1	Transformation 2
Phyca_554980-mut	0/25	5/72
Hygromycin	0/32	0/40
tdTomato (control)	3/21	4/28

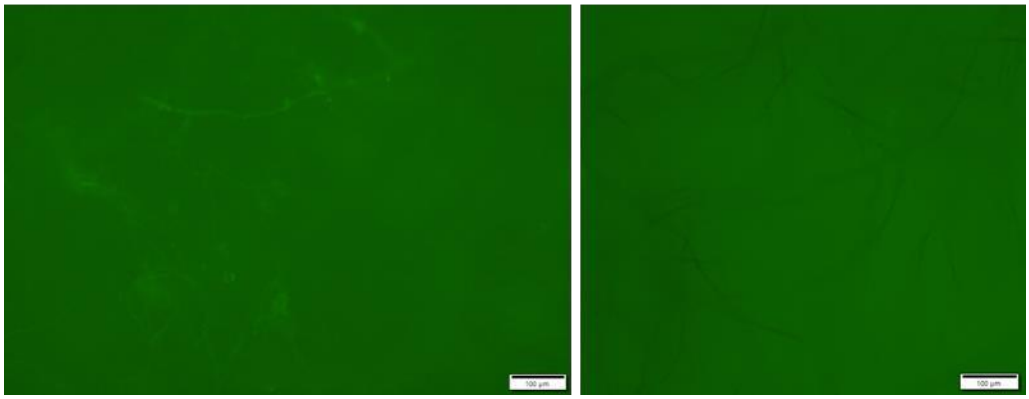

Figure 2.11 Summary of *P. capsici* transformations using two plasmids carrying Cas9 and sgRNA1-2 respectively.

Table shows *P. capsici* transformants with G418 resistance and GFP expression in different treatments. A representative image of a positive *P. capsici* transformant expressing GFP (left) and negative hyphae (right).

Further optimization of *P. capsici* transformation to generate *PPR*-siRNA resistant mutant

Because the initial transformations of CRISPR-Cas9 constructs were unsuccessful, I used an "all-in one" plasmid pYF515 (Figure 2.10b). This vector allows the introduction of both the *Cas9* gene and the sgRNA in one plasmid and presumably has a higher cotransformation rate as fewer plasmids are needed to enter the protoplast. GFP was no longer used as a selection marker, and only G418 resistance was used to screen for transformants. sgRNA1 and sgRNA2 were re-cloned into pYF515. For *P. capsici* transformations, I increased the amount of G418 from 50 µg/µL to 55 µg/µL to limit the growth of false positive colonies. Analysis of total DNA extracted from the colonies by plasmid specific primers for PCR indicated that the sgRNA-Cas9 plasmid was present in *P. capsici* transformants. However, sequencing using genomic specific primers outside of the upstream and downstream homologous donor gene flanks showed that none of them carried mutations in *Phyca_554980* (Table 2.2).

To enhance transformation efficiency (based on a personal correspondence with Dr. Yufeng Fang), a second pair of guide RNAs were designed and included in the experiments (Table 2.1b and Figure 2.7b). Compared to the sgRNA1-2, sgRNA3-4 are closer to the *PPR*siRNA target site in *Phyca_554980*. The homologous donor plasmid was also re-constructed so that the donor sequence included synonymous mutation at the new sgRNA sites (Figure 2.8). Unfortunately, I was unable to generate gene edited transformants after two transformation experiments (Table 2.3). To identify what the potential issue was, DNA was extracted from hundreds of colonies and analyzed, which confirmed that the homologous donor and Cas9-sgRNA plasmids were present in 80% of

the transformants (Figure 2.12a-b) that grew more than 1cm after four days. Using RT-PCR, I also confirmed that Cas9 gene was expressed in the transformants (Fig 2.12c). This suggests that, though the plasmids were successfully introduced into the protoplasts, they did not lead to a CRISPR-Cas9 mediated mutation in *Phyca_554980*.

Hygromycin and *Phyca_554980-mut* Replacement (Cas9 sgRNA 1-2)			
Transformants/ G418 resistant colonies	Transformation 1	Transformation 2	Transformation 3
Phyca_554980-mut	0/60	0/87	0/388
Phyca_554980 Hyg	0/30	0/78	0/120
tdTomato (control)	3/40	2/60	18/158

Table 2.2 Cas9 and sgRNA 1-2 "all-in one plasmid" pyF515 *P. capsici* transformants.

Three *P. capsici* transformations were performed using a sgRNA-Cas9 plasmid and their respective homologous donor plasmids. I was able to obtain transformants from the positive control plasmid which carries the tdTomato gene.

Physca_554980-mut
Transformation Results Summary

Construct type	Transformed/ G418 positive	tdTomato positive control
sgRNA 1-2 Cas9 separate	0/97	7/49
sgRNA 1-2-Cas9	0/535	23/258
sgRNA 1-4-Cas9	0/109	9/40

Table 2.3 Summary of *Physca_554980-mut* gene-edited transformants.

Using three construct types and multiple sgRNAs, *Physca_554980* loci was not gene edited.

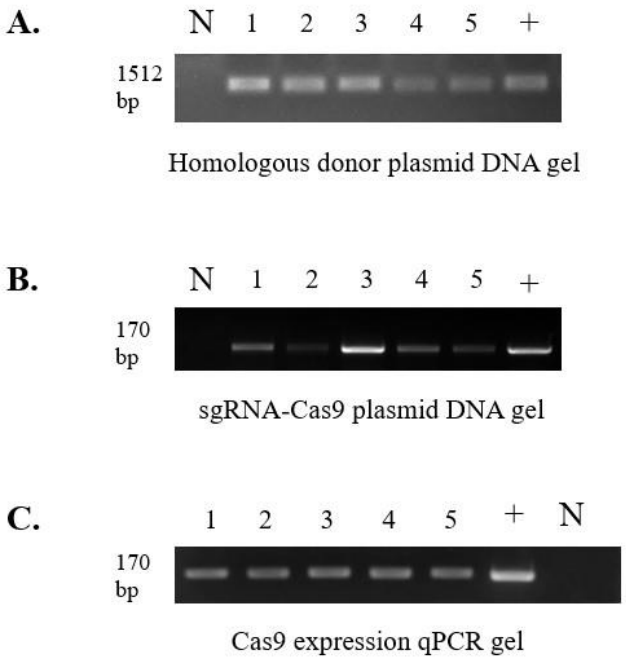

Figure 2.12 PCR and RT-PCR results from *P. capsici* transformants obtained from transformation using the "All-in one" pYF515 plasmid.

A. PCR results showing that the homologous donor plasmid was present in the *P. capsici* transformants. **B.** PCR results showing the CRISPR-Cas9 plasmid was present in the same *P. capsici* transformants as in **A**. **C.** RT-PCR results showing Cas9 expression in the *P. capsici* transformants. Positive (+) control used the Cas9 plasmid DNA. Negative (N) control used cDNA from WT *P. capsici.*

Generation of *P. capsici* strains overexpressing *Phyca_554980*

With the unsuccessful experiments using the CRISPR/Cas9 constructs, I opted for a different strategy in generating *P. capsici* strains that would overexpress the *PPR*-siRNA target gene *Phyca_554980*. I chose to overexpress the wild type *Phyca_554980* as well as the mutated form of *Phyca_554980* with the synonymous mutations at the *PPR*-siRNA target site. My hypothesis was that both would reduce the potential silencing by *Arabidopsis PPR*siRNAs, resulting in increased virulence as the HIGS defense mechanism would be compromised.

I cloned the wild-type *Phyca_554980* gene and the synonymously mutated form into the pTOR vector and N-terminally fused it with tdTomato so that the production of red fluorescence could be used for transformant screening. A pTOR::tdTomato plasmid was used as a positive control for the transformation (Figure 2.13a). From twelve *P. capsici* transformations, only two of nearly 1,220 colonies showed red fluorescence, both of which were from transformation using the wild-type *Phyca_554980* gene, *Phyca_554980wt-ox* (Table 2.4). In both transformants, red fluorescence was exclusively located in the nucleus in the hyphae, consistent with the role of Phyca_554980 as a splicing factor (Figure 2.14a). Conversely, 31 of 200 colonies transformed by pTOR::tdTomato showed red fluorescence. This drastic difference indicates that over-expression of *Phyca_554980* may affect the growth of *P. capsici*.

I next analyzed the fluorescent transformants for the expression levels of *Phyca_554980*. It was disappointing that, compared to a wild-type *P. capsici*, there was no increase in *Phyca_554980* expression in the transformants (Figure 2.14b). To eliminate the

possibility that the tdTomato tag may affect the expression of *Phyca_554980*, I cloned wildtype and mutated *Phyca_554980* gene into pTOR without a tag (Figure 2.13b). However, neither transformants exhibited increased expression of *Phyca_554980* in the transformants (Figure 2.15). Lastly, in order to confirm that the tdTomato fusion constructs can function, I transformed the soybean pathogen *P. sojae* with the recombinant plasmids. A high percentage of the transformants carrying either the wild-type (four of eight colonies) or the mutated (three of eight colonies) gene constructs exhibited fluorescence (Figure 2.16a) and expressed the *P. capsici Phyca_554980* gene (Figure 2.16b). Therefore, the lack of *P. capsici* transformants over-expressing *Phyca_554980* was not due to issues with the constructs.

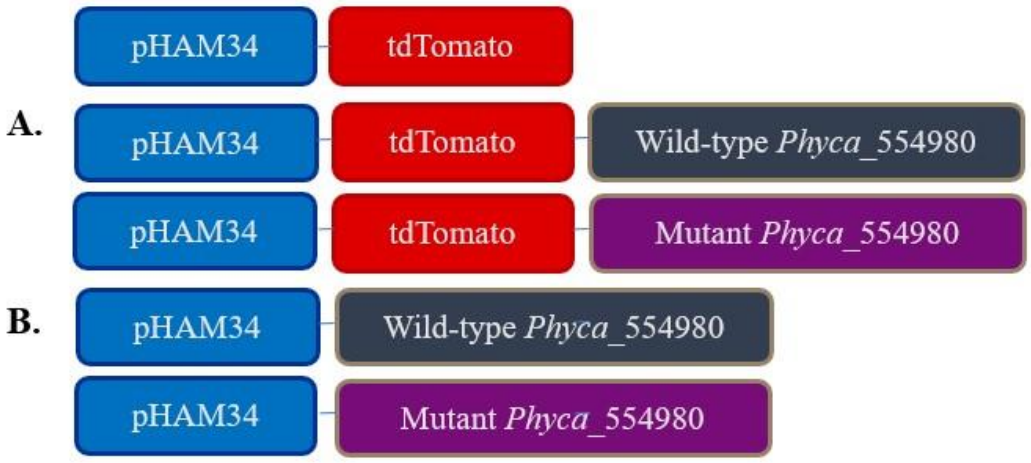

Figure 2.13 The constructs carrying wild-type and mutant *Phyca_554980* gene for overexpression in the vector pTOR.

A. tdTomato was used to tag wild-type or mutated *Phyca_554980* gene at the N-terminus. All the genes are under the controls of HAM34 promoter **B.** Constructs carrying tag-free wildtype and mutated *Phyca_554980* gene.

P. capsici Phyca_554980 Overexpression transformant results	
Constructs transformed	Fluorescent transformants/G418 positive
WT-OX tdTomato	2/620
Mut-OX tdTomato	0/600
tdTomato only control	31/200

Table 2.4 Results of *P. capsici* transformation using pTOR carrying tdTomato-tagged *Phyca_554980*.

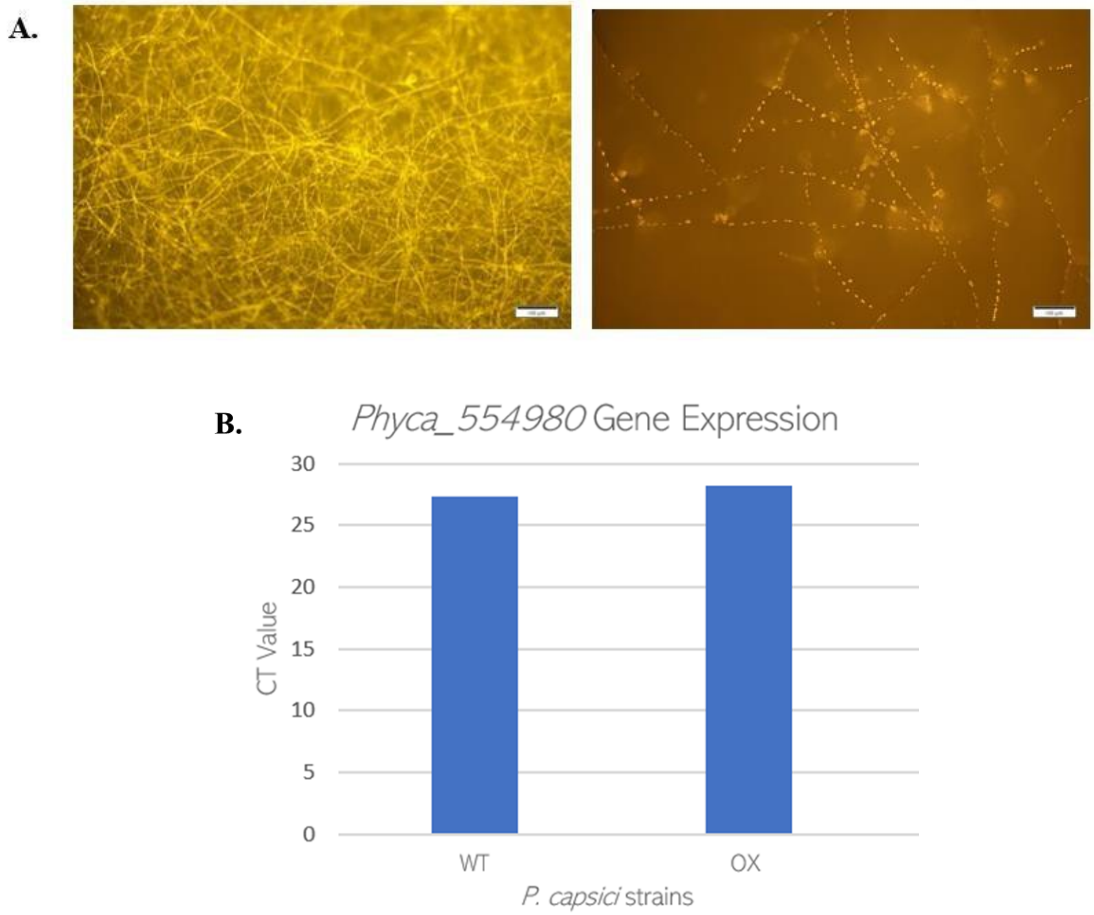

Figure 2.14 *P. capsici* transformants transformed by pTOR::*tdTomatoPhyca_554980* exhibited red fluorescence in the nucleus.

A. Confocal images of hyphae from a *P. capsici* transformant carrying pTOR::*tdTomato-Phyca_554980*. **B.** qRT-PCR results showing the transcript levels of *Phyca_554980* in the *P. capsici* transformant carrying pTOR::*tdTomato-Phyca_554980* compared to wild-type *P. capsici*. A housekeeping gene Pc76 was used as the internal control.

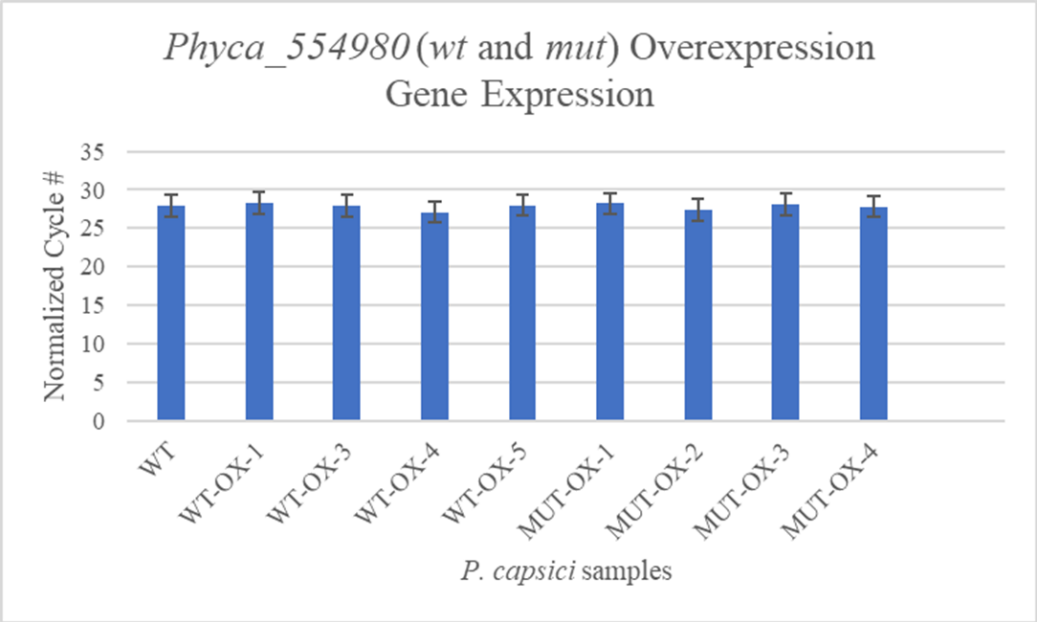

Figure 2.15 qRT-PCR results of *P. capsici* transformants carrying the tag-free *Phyca_554980* construct.

qRT-PCR results showing the transcript levels of *Phyca_554980* in the *P. capsici* transformants carrying tag-free pTOR::*Phyca_554980wt* or pTOR::*Phyca_554980ox* compared to wild-type *P. capsici*. A housekeeping gene Pc76 was used as the internal control.

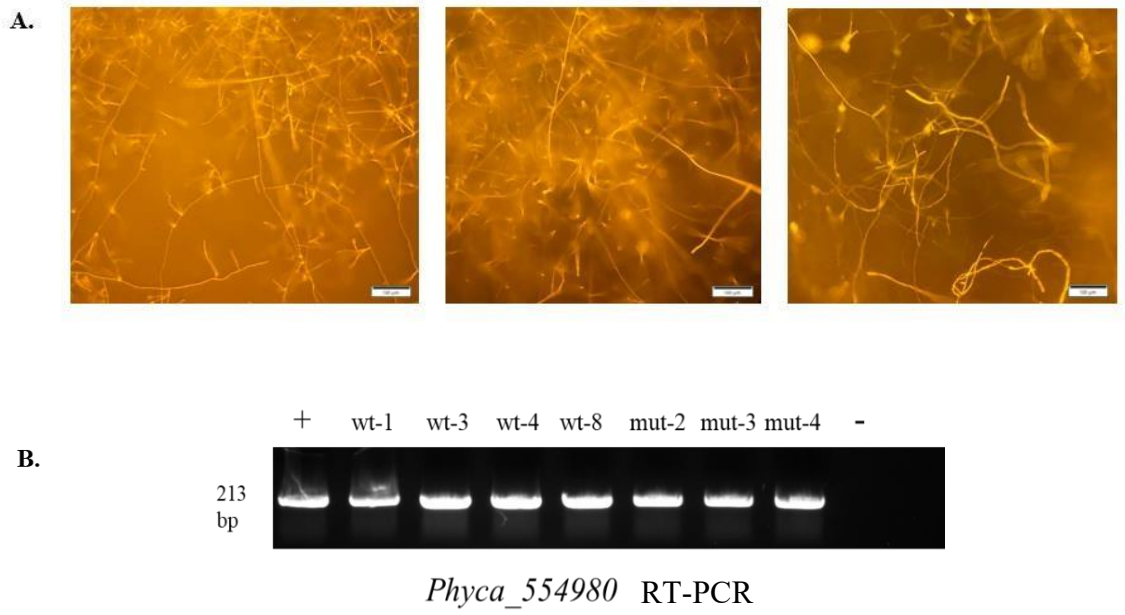

Figure 2.16 *Phyca_554980* expression in *P. sojae* transformants.

A. Confocal images of *P. sojae* hyphae from transformants transformed with pTOR::*tdTomato* or pTOR::*tdTomato-Phyca_554980*. (Left) *P. sojae* transformed with pTOR::*tdTomato* as a transformation positive control. (Middle) *P. sojae* hyphae transformed with the wild-type *Phyca_554980* gene fused to tdTomato. (Right) *P. sojae* transformed with the mutated *Phyca_554980* gene fused to tdTomato. **B.** RT-PCR results showing the expression of *Phyca_554980* in *P. sojae*. Positive control (+) is a synthesized *Phyca_554980* fragment and negative control (-) from wild-type *P. sojae*.

PPR-siRNA target prediction in *P. capsici*

In addition to *Phyca_554980,* I aimed to identify additional *P. capsici* genes as potential targets of *PPR*-siRNAs. For this purpose, I used the list of unique Arabidopsis *PPR*siRNAs from Hou et al., 2019 and predicted 211 *P. capsici* genes as potential targets of 40 or more unique *PPR*-siRNAs. The majority of these *P. capsici* genes were annotated as encoding hypothetical proteins. They were further analyzed for potential functions using BLAST for homologues in other organisms or PFAM and InterPro for domain analysis. From the top 13 hits however, 8 were predicted to be dynein heavy chain/sporangia induced dynein heavy chain proteins, which make up the components necessary for flagella beating (Lindemann & Lesich, 2010). A homologous gene is not present in *A. thaliana* (King, 2002; Wickstead & Gull, 2007). Therefore, it could be another important target of PPR-siRNAs in *Phytophthora* to reduce virulence.

Gene Name	Total predicted *PPR*-siRNAs	Gene Type
Phyca_529822	135	Dynein heavy chain
Phyca_531377	124	Sporangia induced dynein heavy chain
Phyca_10392	122	DNA breaking-rejoining enzyme
Phyca_528395	122	U3 small nucleolar RNA-associated protein
Phyca_103654	117	Dynein heavy chain
Phyca_10826	116	Dynein heavy chain
Phyca_8294	115	Dynein heavy chain
Phyca_530037	113	Dynein heavy chain
Phyca_104354	106	no domain
Phyca_525221	103	Sporangia induced dynein heavy chain
Phyca_537721	103	Fatty acid synthase
Phyca_121416	100	Dynein heavy chain
Phyca_97558	100	no domain

Table 2.5 List of *PPR*-siRNAs predicted to target *P. capsici* genes.

Thirteen *P. capsici* genes were predicted to be targeted by 100 or more unique *PPR*-siRNA sequences.

MATERIAL AND METHODS

PPR-siRNA Target gene candidate analysis

I chose the sites to be synonymously mutated in *Phyca_554980* by predicting from a list of 3922 unique secondary *PPR*-siRNAs (Hou et al., 2019) on a plant small RNA target analysis server: PsRNATarget (http://plantgrn.noble.org/psRNATarget) (Dai & Zhao, 2011). The submitted small RNA sequences were scored against *Phyca_554980* with at an expectation threshold of 4.5. The *PPR*-siRNAs most highly (expectation threshold ≤3) predicted to target *Phyca_554980* mRNA at the sequence location "1789-1815 nt" CAGUGGAUCUGGUUGACAUCAUCUUUGAG. The mutated version: GTGGACCTAGTGGATATTATATTCGAA, did not change the original amino acid sequence: VDLVDIIFE. Additional *PPR*-siRNA targets were predicted the same list of 3922 unique secondary *PPR*-siRNAs, but against the whole *P. capsici* v.11.0 (https://mycocosm.jgi.doe.gov/Phyca11/Phyca11.home.html) (Lamour et al., 2012). Gene functions were identified using InterPro protein family and domain database (Blum et al., 2021) as well as FungiDB (https://fungidb.org/fungidb/app) to identify functions of homologous *Phytophthora* genes. *Phytophthora* Growth Conditions

Phytophthora capsici LT263 was grown on 10% V8 (0.2% $CaCl_2$) agar plates under 25°C in dark conditions (Erwin and Ribeiro, 1996).

CRISPR-Cas9 Mediated Transformation Plasmid Design and Cloning

Single guide RNA Design based on (Fang et al., 2017). Sense and antisense oligos were annealed using T4 DNA ligase buffer and PNK ligase. To generate the homologous donor construct, 1 kb flanks were PCR amplified from the *Phyca_554980* loci from genomic DNA into a pBluescript SK II + vector using InFusion cloning. Hygromycin resistant gene or synthesized *Phyca_554980mut* gene were cloned into the pBluescript vector with 1kb flanks. CRISPR-Cas9 mediated transformation cloning was done as in Fang et al. 2018 with some changes.

Overexpression Construct Cloning

To over express the wild-type and synonymously mutated target gene *Phyca_554980*, the gene was amplified from *P. capsici* LT263 cDNA and synthesized, respectively. Both genes were cloned into pTOR with red fluorescence tdTomatoM marker fused on the C-terminal using InFusion cloning. Both genes were also cloned into pTOR empty vector using InFusion cloning.

Phytophthora capsici Protoplast Transformation and Screening

Protoplast transformation was performed as described in Chapter 1. The CRISPR-Cas9 mediated gene editing was completed as described in (Fang et al., 2017). In general, around 20 hyphal colonies were subcultured per tube of transformants ($2x10^6$ protoplasts) which were then recovered using 30 µg/mL G418-supplemented media. From those colonies then re-subcultured onto V8 plates containing 50 µg/mL G418. Colonies that grew more than 1cm

over one week, enough to collect hyphae for DNA and RNA extraction, where subcultured once more onto V8 supplemented with 50 µg/mL G418.

Fluorescence microscopy was used to screen for CRISPR-Cas9 mediated gene editing transformants that used the three-plasmid system (pYF2.3sgRNA and pYF5.1Cas9). GFP was screened to identify the presence of sgRNA plasmids in the transformants. Red fluorescence was screened in transformants transformed with pTOR::*tdTomato* or pTOR::*tdTomato-Phyca_559480*.

DNA Extraction

DNA was extracted from samples using a CTAB based protocol, as follows. Samples were transferred to safety tubes containing metal beads, then submerged in liquid nitrogen. The tubes were then shaken twice and were submerged in liquid nitrogen between shakings. Then, 200-400 µL of 2% CTAB solution (1.4 M NaCl, 2% CTAB, 20 mM EDTA, 100 mM Tris-HCl (pH 8)) was added depending on sample size, and vortexed well. Tubes were then incubated at 65°C for 10 minutes in a water bath. Samples were then removed from the water bath and allowed to cool before being transferred to new tubes. Then, 200 µL of chloroform was added to each tube and vortexed well. Tubes were then centrifuged at room temperature for 10 minutes at 13,000 rpm. The supernatant was then removed, and the pellet re-suspended in 300 µL of 70% ethanol. The tubes were then centrifuged again at room temperature for 2 minutes at 13,000 rpm. The supernatant was removed again, and the pellet re-suspended in 300 µL of 70% ethanol, before being centrifuged at room temperature for 2 minutes at 13,000 rpm. The ethanol was then removed, and the tubes allowed to dry in the laminar flow

hood for 20-30 minutes or until dry. Finally, the pellets were resuspended in 30-40 µL of sterile water and incubated in a water bath at 65°C for 10 minutes.

RNA Extraction

P. capsici and *P. sojae* transformants were grown in liquid 10% V8 media for three days. Total RNAs were extracted 100 milligrams of hyphal tissue was ground to a fine powder with a mortar and pestle in liquid nitrogen. The ground tissue was transferred to a conical tube and mixed with 1mL of TRIzol Reagent (Life Technologies). 200 µL of chloroform was added to the TRIzol mixture, vortexed, and incubated at room temperature for 5 minutes. The samples were centrifuged at 10,000 rpm for 15 minutes at 4°C. The aqueous phase was transferred to a new tube and mixed with 500 µL isopropyl alcohol to precipitate the RNA. The samples were incubated at room temperature for 10 minutes and centrifuged at 12,000G for 10 minutes at 4°C. The RNA precipitate was washed with 2 mL of 70% ethanol and allowed to air dry for 5 to 10 minutes. RNA pellet was dissolved in diethyl-pyrocarbonate (DEPC)-treated water. To produce cDNA 1µg of total RNA was DNase-treated and reverse transcribed by RevertAid Reverse Transcriptase with RiboLock RNase Inhibitor at 42°C for one hour using oligo-dT as a primer (Kit from Thermo Scientific, Waltham, MA).

Primers used for qPCR or RT-PCR

Pc76RTF	ATGGCCTATGTGACGCAGAT
Pc76RTR	TATTGGTCGATTCGCTTGGC
phyca-554980-qRT-F	AGGTTGGTAGCACGACTTCA
phyca-554980-qRT-R	CTACACCATCAGCCTCCACA
HsPCas9 qRT F	CCATCAACGCCAGCGG
HsPCas9 qRT F	CGAAGTTGCTCTTGAGG

Construct for Cloning

Construct Name	Use	Contains
pYF2.3sgRNA	CRISPR-Cas9 transformation	Single guide RNAs
pYF5.1Cas9	CRISPR-Cas9 transformation	CAS9 enzyme
pBSK II+	CRISPR-Cas9 transformation	Homologous donor
pYF515 “All in one”	CRISPR-Cas9 transformation	Single guide RNAs and Cas9 enzyme
pTOR-tdTomato	Overexpression construct	Red fluorescence

DISCUSSION

Previous studies found a correlation between introducing synthesized *PPR*-siRNA duplexes in *P. capsici* and silencing in target gene transcripts, as well as a decrease in virulence (Hou et al., 2019). This led to the hypothesis that *PPR*-siRNAs produced by Arabidopsis can silence target gene(s) in invading pathogens through host-induced gene silencing. However, we still need to gather definitive evidence that *PPR*-siRNAs can act as mobile defense molecules by translocating into *P. capsici* and silencing a gene vital to its virulence or development. I endeavored to directly manipulate a gene of *P. capsici* (*Phyca_554980*) that was previously shown to be targeted by *PPR*-siRNAs, in order to eradicate its interaction with the host siRNAs. However, despite several years of *P. capsici* transformations and optimization to the protocols to increase transformation efficiency, I was unable to manipulate *Phyca_554980* through synonymous mutations, homologous replacement, or overexpression.

As multiple *PPR*-siRNAs were predicted to target *Phyca_554980*, I aimed to eliminate the sequence complementarity with *PPR*-siRNAs by first generating a CRISPRCas9 mediated synonymous mutant and a complete replacement of the target gene with a siRNA-resistant version. It was previously reported that transformation rate of CRISPR/Cas9 in *P. sojae* could be as high as 80% (Fang et. al 2017), so it was anticipated that at least some transformants would have the desired gene edit. Indeed, there have been several successful examples of gene manipulation in *P. capsici* using CRISPR/Cas9. CRISPR/Cas9 was used to confirm two point mutations in *P. capsici* isolates which rendered them resistant to the fungicide oxathiapiprolin (Miao et al., 2018). A targeted gene

replacement of the effector *PcAvh1* also resulted in impaired virulence in *P. capsici* (Chen et al., 2019).

However, of the hundreds of *Phyca_554980mut-crispr* hyphal colonies screened, five were shown to be positive for the sgRNA marker GFP, but none had homologous recombination with the donor that carried the mutated target site. To improve the transformation process, I added more sgRNAs and designed them closer to the target site. Doing so could increase the recombination efficiency as it induces more double-stranded breaks (Yarrington et al., 2018). Despite this, there were no gene edited *P. capsici* transformants.

Multiple hypotheses could explain why the CRISPR/Cas9 system may not be efficient in *P. capsici*. The secondary structures of sgRNA1 and sgRNA4 were predicted to have some weak self-hybridization which could diminish the efficiency. Furthermore, sgRNA3-4 were designed two years after sgRNA1-2 which resulted in the "efficiency score" of sgRNA1-2 being lower than the necessary score of 0.5, which may be due to new updated models in the newer prediction program. Another key factor to consider in gene manipulation is that *Phyca_554980* could have been a more difficult target for homologous recombination. Genomic DNA in eukaryotes is assembled into chromatin where some DNA sequences are present in varying chromatin contexts (Yarrington et al., 2018). Experiments using purified Cas9 have revealed that the nuclease is inhibited from cleaving some targets that have been assembled into nucleosomes. Therefore, Cas9 cleavage is very weak when nucleosomes are present but enhanced when nucleosomes are diminished (Yarrington et al., 2018). A recent study observed that DNA methylation can also indirectly impair Cas9 activity, possibly due to changes in chromatin structure (Přibylová et al., 2022). Experiments in mammalian and

plant cells show correlations between the cleavage efficiency of Cas9 and the accessibility of chromatin (Horlbeck et al., 2016). It is possible that one or more of these mechanisms could have prevented CRISPR-Cas9 mediated gene editing for *Phyca_554980*.

A decrease in *Phyca_554980* expression through the introduction of artificial siRNA1310 has been shown to prevent sporangia formation and abolish infection (Hou et al., 2019). While the function of this gene has not been directly confirmed, Pfam domains include U2 snrnp-associated surp motif-containing protein, RNA binding and processing. The two positive transformants for the *Phyca_554980-ox-wt* strains exhibited localization in the nucleus. The nuclear localization is to be expected since the spliceosome is primarily found within the nucleus (Will & Lührmann, 2001). However, based on qPCR analysis, neither transformant showed increased expression of *Phyca_559480*. To assess if there was an issue with the overexpression constructs, I transformed them using a different *Phytophthora* species, *P. sojae*. The genus *Phytophthora* is split into 11 clades, where *P. capsici* belongs to Clade 2, while its distant relative *P. sojae* belongs to Clade 7 (Yang et al., 2017). Though fewer hyphal colonies grew, 80% showed fluorescence, indicating that there was no issue with the overexpression constructs themselves. It may suggest instead that the expression of this gene is strictly regulated in *P. capsici* but not in *P. sojae* which has its own homologue. Alternatively, transformation rate of these constructs in *P. capsici* is 0.16% compared to 80% in *P. sojae* suggesting that *P. capsici* is a more difficult host to be genetically manipulated.

If *Phyca_554980* is tightly regulated, an inducible promoter would have been used to overexpress the target genes however, such expression system is not available for *Phytophthora spp*. In general, when subculturing the transformed hyphae, I only chose those that grew more than 1cm within a week. Analyzing colonies that did not continue to grow on

G418 media may mean they were potentially false positives of G418 resistance. Low transcript levels of *Phyca_554980* correlate to decreased sporangia formation and virulence (Hou et al., 2019). One hypothesis is that full deletion of *Phyca_554980* may cause growth deficiency or even be lethal. In such cases, true transformants would then be lost because colonies that did not grow well/fast were not pursued. Efforts to knockout a homologous gene of *Phyca_554980* in *P. sojae* were also unsuccessful (Min Qiu, Wenbo Ma, unpublished data), which is consistent with this possibility. The lack of increase expression in *Phyca_554980mut-ox* or *Phyca_554980wt-ox* could potentially be due to a tight regulation mechanism to control this essential gene.

Had a manipulation to the *Phyca_554980* in *P. capsici* been generated, I would have followed up with an *in vivo* evaluation of the *PPR*-siRNA resistant *P. capsici.* I planned to classify phenotypic changes such as growth speed, sporangia formation and sporulation compared to wild-type *P. capsici* to substantiate that the *in vivo* and *in planta* experimental data was a consequence of the target site mutation and not an unexpected result of CRISPR/Cas9 transformation or gene overexpression. I had planned to verify that the mutated *Phyca_554980* gene was resistant to the specific *PPR*-siRNAs, evaluating its transcript abundance during infection compared to *P. capsici* carrying the wild-type gene. Lastly, I intended to quantify the strains' virulence by measuring biomass and lesion size and posited an increase in both that corresponds to higher virulence in *P. capsici*. I hypothesized that this result would have been caused by removing the sequence complementary to the *PPR*-siRNAs and therefore the *P. capsici* gene vital for virulence, sporangia formation, and growth, would not be targeted by the plant host.

Following a confirmation of *PPR*-siRNA resistance/increased virulence, I had planned an *in planta* evaluation of *PPR*-siRNA resistant *P. capsici*. I planned to inoculate the siRNA-resistant *P. capsici* strains on Arabidopsis plants with variable levels of *PPR*-siRNAs to distinguish whether there are corresponding changes of *Phyca_554980* expression against different siRNA quantities. These Arabidopsis plant lines included *MIR161ox* plants which have high levels of *PPR*-siRNAs, wild-type, and *rdr6/sgs3* mutant which do not produce *PPR*-siRNAs. Compared to inoculation with a wild-type *P. capsici*, I would have anticipated the *PPR*-siRNA resistant strain to have increased biomass and lesion size in wild-type or potentially *MIR161ox* Arabidopsis, since the mutated target gene, *Phyca_554980*, would not be susceptible to HIGS. When inoculated with wild-type or resistant *P. capsici*, *rdr6/sgs3* plants would be expected to have the same biomass and lesion size since a siRNA-resistant strain would have no effect when HIGS is absent. I would also have anticipated transcript levels of *Phyca_554980* and its siRNA-resistant mutants would change in these Arabidopsis plants corresponding to their siRNA levels. These results could have provided important insight into the roles of secondary siRNAs in HIGS during natural infection.

Despite being unable to generate a *P. capsici* mutant that carries *PPR*-siRNA resistant *Phyca_554980*, there are other opportunities to evaluate the hypothesis that secondary siRNAs may be the executors of HIGS. One method is to reexamine the list of the *P. capsici PPR*-siRNA targets as there were 211 predicted to be targeted by over 40 siRNAs. The majority of these were hypothetical proteins making them less desirable candidates to study. However, eight of the topmost targeted *P. capsici* genes encoded dynein heavy chain proteins. This could be an interesting target for silencing by the plant hosts because all flowering plants have dispensed with dyneins (King, 2002; Wickstead & Gull, 2007).

Dyneins are cytoskeletal motor proteins which contain one to three dynein heavy chains (Asai & Wilkes, 2004). They are involved in transporting intracellular cargo along microtubules (Schroer et al., 1989). Additionally, dynein motor proteins have a role in powering the beating of flagella (Lindemann & Lesich, 2010), which is vital for *Phytophthora* zoospore motility. It would be exciting to suggest that *PPR*-siRNAs can simultaneously target multiple pathogen genes, which would be interesting to investigate in the future.

Along with this, several questions concerning secondary siRNAs still need to be elucidated: what is the mechanism of regulation of miRNA-siRNA pathway? Are specific secondary siRNAs expressed during different pathogen infection? What is the delivery mechanism? Although I was unable to confirm the interaction between a pathogen target gene and the host sRNA through "camouflaging" the target site due to technical difficulties, this is a necessary step to support direct gene silencing by specific host sRNAs in pathogens during infection. Future studies also include the identification of plant secondary siRNAs in the *P. capsici* RISC. This may be accomplished using Argonaut-RNA Immunoprecipitation sequencing (RIP-seq) (Petri & Jakobsson, 2018). In summary, there is still a lack of mechanistic understanding in HIGS that remains to be explored.

REFERENCES

Adenot, X., Elmayan, T., Lauressergues, D., Boutet, S., Bouché, N., Gasciolli, V., & Vaucheret, H. (2006). DRB4-Dependent TAS3 trans-Acting siRNAs Control Leaf Morphology through AGO7. *Current Biology*, *16*(9), 927–932. https://doi.org/10.1016/j.cub.2006.03.035

Asai, D. J., & Wilkes, D. E. (2004). The Dynein Heavy Chain Family1. *Journal of Eukaryotic Microbiology*, *51*(1), 23–29. https://doi.org/10.1111/j.1550-7408.2004.tb00157.x

Blum, M., Chang, H.-Y., Chuguransky, S., Grego, T., Kandasaamy, S., Mitchell, A., Nuka, G., Paysan-Lafosse, T., Qureshi, M., Raj, S., Richardson, L., Salazar, G. A., Williams, L., Bork, P., Bridge, A., Gough, J., Haft, D. H., Letunic, I., Marchler-Bauer, A., … Finn, R. D. (2021). The InterPro protein families and domains database: 20 years on. *Nucleic Acids Research*, *49*(D1), D344–D354. https://doi.org/10.1093/nar/gkaa977

Bosland, P. W. (2008). Think global, breed local: specificity and complexity of Phytophthora capsici. In 19th Int. Pepper Conf. Atlantic City, NJ.

Chen, X.-R., Zhang, Y., Li, H.-Y., Zhang, Z.-H., Sheng, G.-L., Li, Y.-P., Xing, Y.-P., Huang, S.-X., Tao, H., Kuan, T., Zhai, Y., & Ma, W. (2019). The RXLR Effector PcAvh1 Is Required for Full Virulence of Phytophthora capsici. *Molecular Plant-Microbe Interactions®*, *32*(8), 986–1000. https://doi.org/10.1094/MPMI-09-18-0251-R

Dai, X., & Zhao, P. X. (2011). psRNATarget: A plant small RNA target analysis server. *Nucleic Acids Research*, *39*(Web Server issue), W155–W159. https://doi.org/10.1093/nar/gkr319

Dalmay, T., Hamilton, A., Rudd, S., Angell, S., & Baulcombe, D. C. (2000). An RNA-Dependent RNA Polymerase Gene in Arabidopsis Is Required for Posttranscriptional Gene Silencing Mediated by a Transgene but Not by a Virus. *Cell*, *101*(5), 543–553. https://doi.org/10.1016/S0092-8674(00)80864-8

Doench, J. G., Hartenian, E., Graham, D. B., Tothova, Z., Hegde, M., Smith, I., Sullender, M., Ebert, B. L., Xavier, R. J., & Root, D. E. (2014). Rational design of highly active sgRNAs for CRISPR-Cas9–mediated gene inactivation. *Nature Biotechnology*, *32*(12), Article 12. https://doi.org/10.1038/nbt.3026

Erwin, D. C., & Ribeiro, O. K. (1996). Phytophthora diseases worldwide. *Phytophthora Diseases Worldwide*. https://www.cabdirect.org/cabdirect/abstract/19971001256

Fang, Y., Cui, L., Gu, B., Arredondo, F., & Tyler, B. M. (2017). Efficient Genome Editing in the Oomycete Phytophthora sojae Using CRISPR/Cas9. *Current Protocols in Microbiology*, *44*(1), 21A.1.1-21A.1.26. https://doi.org/10.1002/cpmc.25

Hausbeck, M. K., & Lamour, K. H. (2004). Phytophthora capsici on Vegetable Crops: Research Progress and Management Challenges. *Plant Disease*, *88*(12), 1292–1303. https://doi.org/10.1094/PDIS.2004.88.12.1292

Horlbeck, M. A., Witkowsky, L. B., Guglielmi, B., Replogle, J. M., Gilbert, L. A., Villalta, J. E., Torigoe, S. E., Tjian, R., & Weissman, J. S. (2016). Nucleosomes impede Cas9 access to DNA in vivo and in vitro. *ELife*, *5*, e12677. https://doi.org/10.7554/eLife.12677

Hou, Y., Zhai, Y., Feng, L., Karimi, H. Z., Rutter, B. D., Zeng, L., Choi, D. S., Zhang, B., Gu, W., Chen, X., Ye, W., Innes, R. W., Zhai, J., & Ma, W. (2019). A Phytophthora Effector Suppresses Trans-Kingdom RNAi to Promote Disease Susceptibility. *Cell Host & Microbe*, *25*(1), 153-165.e5. https://doi.org/10.1016/j.chom.2018.11.007

Isaac, R. S., Jiang, F., Doudna, J. A., Lim, W. A., Narlikar, G. J., & Almeida, R. (n.d.). Nucleosome breathing and remodeling constrain CRISPR-Cas9 function. *ELife*, *5*, e13450. https://doi.org/10.7554/eLife.13450

King, S. M. (2002). Dyneins motor on in plants. *Traffic (Copenhagen, Denmark)*, *3*(12), 930–931. https://doi.org/10.1034/j.1600-0854.2002.31208.x

Ko, W. (1988). Hormonal Heterothallism and Homothallism in Phytophthora. *Annual Review of Phytopathology*, *26*(1), 57–73. https://doi.org/10.1146/annurev.py.26.090188.000421

Lamour, K. H., Stam, R., Jupe, J., & Huitema, E. (2012). The oomycete broad-host-range pathogen Phytophthora capsici. *Molecular Plant Pathology*, *13*(4), 329–337. https://doi.org/10.1111/j.1364-3703.2011.00754.x

Lindemann, C. B., & Lesich, K. A. (2010). Flagellar and ciliary beating: The proven and the possible. *Journal of Cell Science*, *123*(4), 519–528. https://doi.org/10.1242/jcs.051326

Miao, J., Chi, Y., Lin, D., Tyler, B. M., & Liu, X. (2018). Mutations in ORP1 Conferring Oxathiapiprolin Resistance Confirmed by Genome Editing using CRISPR/Cas9 in Phytophthora capsici and P. sojae. *Phytopathology®*, *108*(12), 1412–1419. https://doi.org/10.1094/PHYTO-01-18-0010-R

Mourrain, P., Béclin, C., Elmayan, T., Feuerbach, F., Godon, C., Morel, J.-B., Jouette, D., Lacombe, A.-M., Nikic, S., Picault, N., Rémoué, K., Sanial, M., Vo, T.-A., & Vaucheret, H. (2000). Arabidopsis SGS2 and SGS3 Genes Are Required for Posttranscriptional Gene Silencing and Natural Virus Resistance. *Cell*, *101*(5), 533–542. https://doi.org/10.1016/S0092-8674(00)80863-6

Nakazawa, Y., Hiraguri, A., Moriyama, H., & Fukuhara, T. (2007). The dsRNA-binding protein DRB4 interacts with the Dicer-like protein DCL4 in vivo and functions in the transacting siRNA pathway. *Plant Molecular Biology*, *63*(6), 777–785. https://doi.org/10.1007/s11103-006-9125-8

Navarro, L., Dunoyer, P., Jay, F., Arnold, B., Dharmasiri, N., Estelle, M., Voinnet, O., & Jones, J. D. G. (2006). A plant miRNA contributes to antibacterial resistance by repressing auxin signaling. *Science (New York, N.Y.)*, *312*(5772), 436–439. https://doi.org/10.1126/science.1126088

Peng, D., & Tarleton, R. (2015). EuPaGDT: A web tool tailored to design CRISPR guide RNAs for eukaryotic pathogens. *Microbial Genomics*, *1*(4), e000033. https://doi.org/10.1099/mgen.0.000033

Peragine, A., Yoshikawa, M., Wu, G., Albrecht, H. L., & Poethig, R. S. (2004). SGS3 and SGS2/SDE1/RDR6 are required for juvenile development and the production of trans-acting siRNAs in Arabidopsis. *Genes & Development*, *18*(19), 2368–2379. https://doi.org/10.1101/gad.1231804

Petri, R., & Jakobsson, J. (2018). Identifying miRNA Targets Using AGO-RIPseq. *Methods in Molecular Biology (Clifton, N.J.)*, *1720*, 131–140. https://doi.org/10.1007/978-1-49397540-2_9

Přibylová, A., Fischer, L., Pyott, D. E., Bassett, A., & Molnar, A. (2022). DNA methylation can alter CRISPR/Cas9 editing frequency and DNA repair outcome in a target-specific manner. *New Phytologist*, *235*(6), 2285–2299. https://doi.org/10.1111/nph.18212

Quesada-Ocampo, L. M., & Hausbeck, M. K. (2010). Resistance in Tomato and Wild Relatives to Crown and Root Rot Caused by Phytophthora capsici. *Phytopathology®*, *100*(6), 619–627. https://doi.org/10.1094/PHYTO-100-6-0619

Ran, F. A., Hsu, P. D., Wright, J., Agarwala, V., Scott, D. A., & Zhang, F. (2013). Genome engineering using the CRISPR-Cas9 system. *Nature Protocols*, *8*(11), Article 11. https://doi.org/10.1038/nprot.2013.143

Reuter, J. S., & Mathews, D. H. (2010). RNAstructure: Software for RNA secondary structure prediction and analysis. *BMC Bioinformatics*, *11*(1), 129. https://doi.org/10.1186/1471-2105-11-129

Satour, M. M., & Butler, E. E. (1967). A ROOT AND CROWN ROT OF TOMATO CAUSED BY PHYTOPHTHORA CAPSICI AND P PARASITICA. Phytopathology, 57(5), 510.

Schroer, T. A., Steuer, E. R., & Sheetz, M. P. (1989). Cytoplasmic dynein is a minus enddirected motor for membranous organelles. *Cell*, *56*(6), 937–946. https://doi.org/10.1016/0092-8674(89)90627-2

Thabuis, A., Palloix, A., Pflieger, S., Daubèze, A.-M., Caranta, C., & Lefebvre, V. (2003). Comparative mapping of Phytophthora resistance loci in pepper germplasm: Evidence for conserved resistance loci across Solanaceae and for a large genetic diversity. *Theoretical and Applied Genetics*, *106*(8), 1473–1485. https://doi.org/10.1007/s00122-003-1206-3

Wickstead, B., & Gull, K. (2007). Dyneins Across Eukaryotes: A Comparative Genomic Analysis. *Traffic (Copenhagen, Denmark)*, *8*(12), 1708–1721. https://doi.org/10.1111/j.16000854.2007.00646.x

Will, C. L., & Lührmann, R. (2001). Spliceosomal UsnRNP biogenesis, structure and function. *Current Opinion in Cell Biology*, *13*(3), 290–301. https://doi.org/10.1016/s09550674(00)00211-8

Wyvekens, N., Topkar, V. V., Khayter, C., Joung, J. K., & Tsai, S. Q. (2015). Dimeric CRISPR RNA-Guided FokI-dCas9 Nucleases Directed by Truncated gRNAs for Highly Specific Genome Editing. *Human Gene Therapy*, *26*(7), 425–431. https://doi.org/10.1089/hum.2015.084

Xia, R., Meyers, B. C., Liu, Z., Beers, E. P., Ye, S., & Liu, Z. (2013). MicroRNA Superfamilies Descended from miR390 and Their Roles in Secondary Small Interfering RNA Biogenesis in Eudicots. *The Plant Cell*, *25*(5), 1555–1572. https://doi.org/10.1105/tpc.113.110957

Xiong, Q., Ye, W., Choi, D., Wong, J., Qiao, Y., Tao, K., Wang, Y., & Ma, W. (2014). Phytophthora Suppressor of RNA Silencing 2 Is a Conserved RxLR Effector that Promotes Infection in Soybean and Arabidopsis thaliana. *Molecular Plant-Microbe Interactions®*, *27*(12), 1379–1389. https://doi.org/10.1094/MPMI-06-14-0190-R

Xu, X., Chao, J., Cheng, X., Wang, R., Sun, B., Wang, H., Luo, S., Xu, X., Wu, T., & Li, Y. (2016). Mapping of a Novel Race Specific Resistance Gene to Phytophthora Root Rot of Pepper (Capsicum annuum) Using Bulked Segregant Analysis Combined with Specific Length Amplified Fragment Sequencing Strategy. *PLOS ONE*, *11*(3), e0151401. https://doi.org/10.1371/journal.pone.0151401

Yang, X., Tyler, B. M., & Hong, C. (2017). An expanded phylogeny for the genus Phytophthora. *IMA Fungus*, *8*(2), 355–384. https://doi.org/10.5598/imafungus.2017.08.02.09

Yarrington, R. M., Verma, S., Schwartz, S., Trautman, J. K., & Carroll, D. (2018). Nucleosomes inhibit target cleavage by CRISPR-Cas9 in vivo. *Proceedings of the National Academy of Sciences*, *115*(38), 9351–9358. https://doi.org/10.1073/pnas.1810062115

Yoshikawa, M., Iki, T., Tsutsui, Y., Miyashita, K., Poethig, R. S., Habu, Y., & Ishikawa, M. (2013). 3′ fragment of miR173-programmed RISC-cleaved RNA is protected from degradation in a complex with RISC and SGS3. *Proceedings of the National Academy of Sciences*, *110*(10), 4117–4122. https://doi.org/10.1073/pnas.1217050110

Chapter 3

Engineering host-induced gene silencing in soybeans

ABSTRACT

Soybeans are a staple crop worldwide. However, global soybean production is damaged by a multitude of diseases. Recently, host-induced gene silencing (HIGS) has surfaced as a powerful tool to enhance disease resistance in plants. A new HIGS strategy has been suggested wherein a secondary siRNA-generating loci can be engineered to produce a pool of siRNAs that can silence target genes in one or more pathogens. In this chapter I discuss my attempts to engineer a siRNA-producing cassette in soybean with the aim to accumulate antimicrobial siRNAs that can execute HIGS. Both an endogenous and heterologous siRNA-producing cassette were designed and transformed into soybeans using *Agrobacterium rhizogenes*-mediated hairy root system. Whilst both cassettes produced their respective miRNA trigger, I did not detect the accumulation of secondary siRNAs. Additionally, artificial siRNA duplexes were directly introduced into *P. sojae* in order to identify siRNA candidates that may successfully silence specific pathogen genes. These experiments represent a first attempt to heterologously express siRNA-producing construct for HIGS in crops. With further investigations, this approach may lead to the development of a robust broad spectrum defense strategy.

INTRODUCTION

Soybean biology and diseases

Soybeans are the most important legume grown worldwide and provide food for humans, feed for livestock, and biofuels. More than 217.6 million tons of soybeans are produced each year worldwide, and they are a major crop in many countries around the world including China, India, Russia, the US, and South America (Food and Agriculture Organization of the United Nations; Masuda & Goldsmith, 2009). Soybean is believed to have been domesticated from wild varieties in east Asia 6000-9000 years ago (Sedivy et al., 2017). Soybeans are an important part of various cropping systems due to their ability to fix nitrogen, which improves the soil quality for other crops in rotation (Hartman & Hill, 2010). Because soybeans are such a valuable crop worldwide, losses caused by disease can be extremely costly. In 2003, the estimated worldwide loss of soybeans due to diseases was 23% (Hartman & Hill, 2010). There are a wide variety of diseases capable of infecting soybeans, these include: fungal diseases such as Phomopsis seed decay, Rhizoctonia root rot, and charcoal rot caused by Macrophomina; viruses such as soybean mosaic virus; and the soybean cyst nematode *Heterodera glycines* (Hartman & Hill, 2010).

One of the most damaging pathogens of soybeans is *Phytophthora sojae*, an oomycete pathogen capable of infecting soybeans at any growing stage but with a particular affinity for emerging seedlings and the roots of young plants. Worldwide, *P. sojae* is responsible for 1-2 billion dollars in damage annually (Tyler, 2007). If susceptible cultivars are planted in fields with poor drainage and *P. sojae* present, yield losses can reach 100% (Dorrance, 2018). Symptoms of infection include seed/seedling damping off and brown, water-soaked lesions, much like many other oomycete pathogens (Hartman & Hill, 2010). *P.*

sojae is homothallic and capable of producing oospores in the environment, which act as survival structures in sub-optimal environments. In damp conditions, *P. sojae* develops sporangia that releases motile zoospores. When released, the zoospores encyst upon soybean roots, which they locate via chemotaxis. Upon germination, mycelia develop from the zoospore and penetrate the root tissue where oospores may develop. These oospores can persist in the soil long after the host has died, providing sources of inoculum against future generations of soybean (Dorrance, 2018).

Proper management of *P. sojae* can reduce or eliminate yield loss in affected areas. A multi-faceted approach is often implemented, including cultural practices, planting of resistant cultivars, and chemical applications. As like most other oomycete plant pathogens, *P. sojae* requires an ample amount of water in order to thrive, and cultural practices like irrigation management can be very effective at reducing the impact of *P. sojae* on soybean fields (Dorrance, 2018). Because of the host specificity of *P. sojae* (only infects soybean) and its long history of co-evolution with soybean, several host *R* genes have been found in the soybean genome that contribute to defense against *P. sojae* (Wang et al., 2021). This feature of the disease system has been used to our advantage, and many R-gene mediated resistant cultivars of soybeans have been developed, further lessening the impact of *P. sojae* on soybean yields. Quantitative resistance in which many R-genes contribute to defense can be particularly beneficial when R-gene mediated resistance has been overcome by *P. sojae* (Dorrance, 2018; Hartman & Hill, 2010). Finally, the last line of defense for growers is the application of fungicide compounds, especially in the form of seed treatments (Dorrance, 2018).

Engineering HIGS in plants to confer disease resistance

Recent research efforts focused on small RNAs have provided new prospects to engineer additional disease resistance in crops. There are several strategies to introduce pathogen-targeting sRNAs in transgenic plants. A common approach is to use a hairpin-structured RNA construct targeting a specific pathogen gene. These constructs are transformed into the host plant where they may serve as a precursor to produce sRNAs. If the sRNAs can enter the pathogen cells during infection, they may degrade the targeted transcripts and enhance disease resistance (Hou & Ma, 2020; Sang & Kim, 2020). For example, transgenic wheat lines expressing hairpin constructs targeting the rust fungal pathogen *Puccinia triticina* genes encoding a MAP kinase (*Pt*MAPK1) and cyclophilin (*Pt*CYC1) showed enhanced resistance to *P. triticina*. The genes were selected for this HIGS approach as they are essential in both regulating physiological processes and pathogenicity in the fungus (Panwar et al., 2018). Additionally, transgenic maize plants expressing a hairpin construct targeting the transcription factor aflR of the fungal pathogen *Aspergillus flavus* resulted in highly reduced levels of aflatoxin (Masanga et al., 2015). Another HIGS strategy utilizes transgenic plants that produce artificial miRNAs (amiRNAs) from the backbone of a *MIR* gene. Despite some success using these strategies, variations in the efficiency of HIGS have been often observed (Koch & Wassenegger, 2021). The underlying mechanism contributing to the variation of HIGS is not known.

Strengthening a natural siRNA-based defense could be a useful strategy to enhance disease resistance through HIGS. It has been recently shown that secondary siRNAs in Arabidopsis contribute to plant defense (Hou et al., 2019). The secondary siRNAs may act in a “shotgun” manner, where siRNA-producing loci generate a pool of secondary siRNAs that

target multiple pathogens. In Arabidopsis, *Pentatricopeptide repeat*-siRNAs represent a pool of ~4,000 sequences and are predicted to target multiple *P. capsici* genes (Hou et al., 2019). Further, these siRNAs have the potential to confer immunity against multiple pathogens (Hou and Ma, 2020). This "shot-gun" defense mechanism is expected to be more sustainable during the host-pathogen arms race.

The generation of secondary siRNAs is prevalent in dicots through a conserved miRNA-*PPR*-siRNA circuit (Xia et al., 2013). In soybean, *Glycine max* (*Gma*) *PPR*-siRNA generation is triggered by miR1509 (Xia et al., 2013). It has been suggested that endogenous secondary siRNA generating *PPR* genes can be engineered to modify sequences in the *PPR*-siRNA population. The siRNA sequences could be designed to specifically target important genes in one of more pathogens of concern to improve the efficiency of HIGS (Figure 3.1). The secondary siRNA sequence replacement strategy has been accomplished successfully in Arabidopsis for silencing its *FAD2* gene (de la Luz Gutiérrez-Nava et al., 2008); however, it has not yet been applied to HIGS.

In this chapter, I generated siRNA-producing cassettes and expressed them in soybean. I hypothesized that co-expression of the miRNA trigger and the siRNA-producing *PPR* transcript would lead to the accumulation of secondary *PPR*-siRNAs in soybean, thereby conferring resistance to *P. sojae* through HIGS.

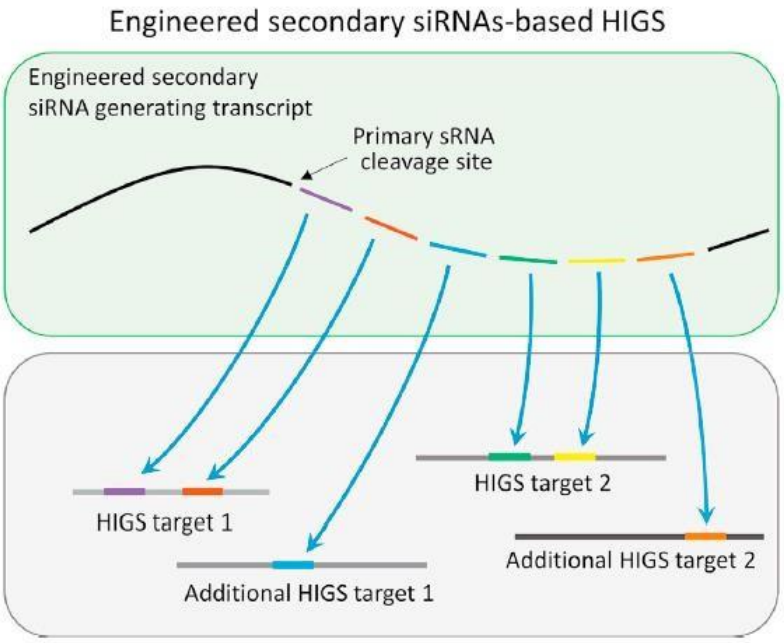

Figure 3.1 Engineered secondary siRNA-based HIGS approach could be used to increase HIGS efficiency.

The siRNA-generating region of a gene can be replaced to produce siRNAs engineered to specifically target and silence potentially multiple pathogen genes. (Image from Hou and Ma, 2020)

RESULTS

Construction of vectors carrying *MIR-PPR* cassettes for soybean transformation

A general plasmid cassette was generated for *Agrobacterium*-mediated hairy root induction. The cassette was built for expression of both the miRNA trigger and the primary target transcript which are necessary for secondary siRNA production (Figure 3.2a). DNA fragments encoding the *MIR* genes were amplified from cDNA of Arabidopsis or soybean by PCR using gene specific primers. The PCR products were inserted into a modified binary vector, which contains a *GFP* gene under the mannopine synthase promoter. Since not all soybean hairy roots uptake T-DNA, GFP expression was used as a reporter for transgenic roots. The *MIR-PPR* cassettes were cloned after the constitutive CaMV 35S promoter and the soybean polyubiquitin promoter *Gmubi* (Figure 3.2b).

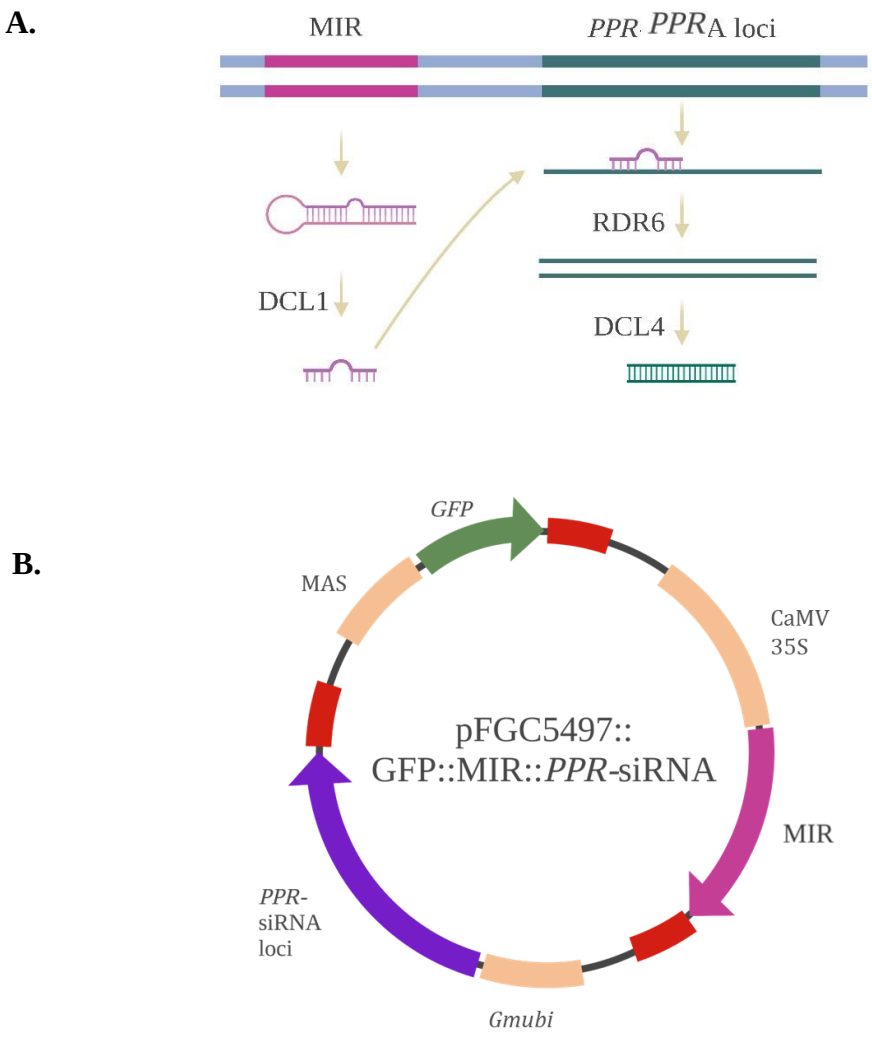

Figure 3.2 Diagram showing the plasmid carrying a miRNA-*PPR* cassette.

A. The *MIR-PPR* gene cassette includes a *MIR* which will be transcribed into pri-miRNA. The mature miRNA produced from pri-miRNA will trigger cleavage at the target site of the *PPR* transcript, which will then be processed into secondary *PPR*-siRNAs. **B.** Physical map of the plasmid pFGC5497 carrying a miRNA-*PPR*-siRNA cassette for soybean hairy root induction.

A bioinformatic pipeline to identify miRNA-PPR circuit candidates

A soybean sRNA-seq dataset (Lunardon et al., 2020) was used to identify miRNA-siRNA circuits that produce *PPR*-siRNAs in soybean. From that dataset, I identified the gene loci of 2,229 siRNAs using a genome viewer from Plant Small RNA Genes (Lunardon et al., 2020). Then, siRNA-generating loci were then analyzed to identify their miRNA triggers. The list of siRNAs was further narrowed down to those that had relatively high abundance (Figure 3.3). Using this pipeline selecting for PPR genes, a miR1508-Glyma16g28020 circuit was chosen. The production of secondary siRNAs from this circuit was also reported previously (Wong et al., 2014).

Two sets of *MIR-PPR* cassette were cloned for this experiment (Table 3.1). One set was adapted from previous studies in Arabidopsis *PPR*-siRNAs (Hou et al., 2019) which are produced from the miR161-*At1G62914* circuit. *PPR*-siRNAs produced from this circuit target a *P. capsici* gene *Phyca_554980* which has a homologue in *P. sojae*. Therefore, I introduced an Arabidopsis *MIR161-PPR* cassette into soybeans but changed the sequence of the *PPR* gene *At1G62914* (*At1g62914mut*) so that the resulting siRNAs would better target the *P. sojae* homolog of *Phyca_554980*. One of such *Phyca_554980* homolog-targeting *PPR*siRNA is At-siR1310. The *At1g62914mut* transcript is expected to produce At-siR1310mut. The second cassette was based on the miR1508-Glyma16g28020 circuit identified from my bioinformatic pipeline. The *PPR* gene (*Glyma16g28020*) has a target site of miR1508 and was predicted to generate siRNA-799 (GmsiR799) which was present in high abundance in the sRNA-seq dataset. The corresponding *MIR* genes of the miRNAs and their target *PPR* genes were cloned as two *MIR-PPR* cassettes into the plasmid pGFC5497 (Figure 3.2).

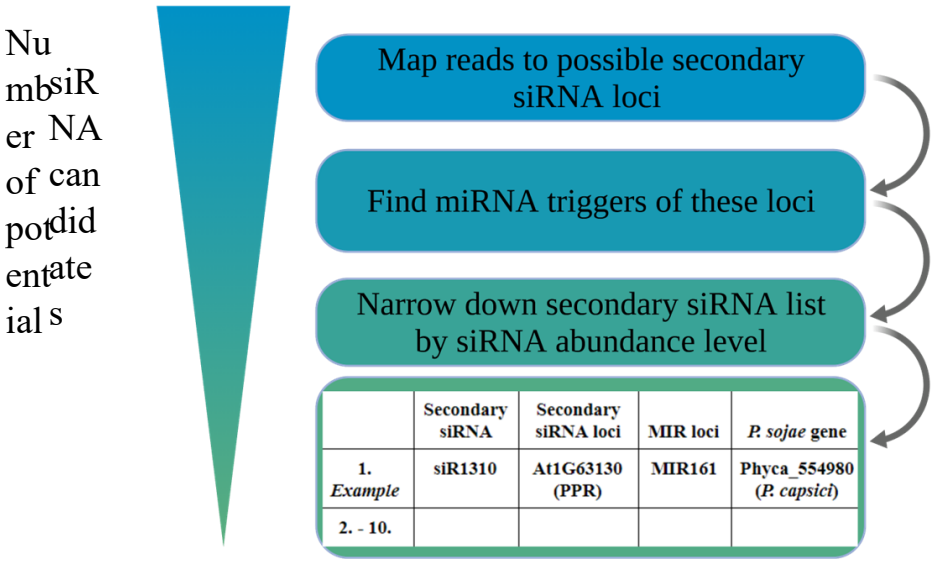

miRNA	siRNA	siRNA sequence	*PPR* gene	abundance
gmamiR1508b	799	AAAGAAAAGGACAUUUGGCCC	glyma.16g28020.1	34087
gmamiR1508b	796	AUUAACUGACUGGCAAGGCAA	glyma.16g16190.3	23248
gmamiR1508b	803	UAUGAGUAUACAUCUGGCUGA	glyma.16g19590.1	21538
gmamiR4413b	2087	AAGCCAUAGAUUAGAGUACUG	glyma.16g16310.1	19059
gmamiR4413a	805	UUUCAUUUCAUUCGUCAAGGA	glyma.16g19570.2	5224
gmamiR4413b	810	UAGGUGACAACAUCCGGGGAA	glyma.16g19500.1	2780

Figure 3.3 A bioinformatic pipeline for identifying miRNA-PPR circuits.

The table includes the top six miRNA-siRNA circuits predicted using the pipeline illustrated above.

miRNAs	Secondary siRNA *PPR* transcript	*PPR*-siRNA
*At*miR161	*At1G62914mut*	*At*siR1310mut
*Gm*miR1508	*Glyma16g28020*	*Gm*siR799

Table 3.1 miRNA-siRNA circuit constructs used for soybean transformation.

The miRNA-siRNA circuits may produce the specific *PPR*-siRNAs from the table. The *PPR*-siRNA column shows the siRNAs designed to be accumulated in the transformed soybean expressing the specific *MIR-PPR* cassette.

Agrobacterium-mediated hairy root induction in soybean

To generate transgenic material, soybean cotyledons were inoculated with *Agrobacterium rhizogenes* strain K599 that harbors the recombinant plasmids. Williams and Williams 82 cultivars were used as the former is susceptible and the latter shows quantitative resistance due to the R gene *Rps*1k (Dorrance et al., 2004; Gao et al., 2005). Using a protocol described in Kereszt et al., 2007, sterilized seeds were inoculated with a bacterial suspension at cotyledonary node and the hypocotyl, then kept under high humidity (Figure 3.4a). After 9-12 days hairy roots started to sprout from the inoculation site. Once roots were over 1cm in length (Figure 3.4b) I removed the original stem and replanted the transgenic roots (Figure 3.4c). The transformed hairy roots were indicated by GFP expression.

Hairy root growth was initially inconsistent. Hairy roots would sprout generally anywhere between one to twelve roots, and some would not continue to grow past 2 cm in length. Therefore, I optimized the protocol using an *A. rhizogenes* strain carrying the empty pFGC5497 vector. Inoculating with a bacterial paste resulted in many more roots expanding and showed more GFP expression over using a bacterial suspension (Figure 3.4d). Additionally, sterilizing seeds in a bleach solution, despite fewer seeds sprouting, led to both stronger fluorescence in the transformed roots and less fungal/bacterial contamination. I also tested a chlorine gas sterilization, which resulted in slightly fewer GFP expressing hairy roots (Figure 3.4d). After optimizing the transformation protocol, I was able to consistently generate GFP expressing hairy roots in soybean using bacterial paste inoculation and bleach sterilization.

A. **B.** **C.**

D.

Soybean hairy root transformation through *A. rhizogenes* infiltration

Bact. inoculation type	Seed Sterilization Type			
	Chlorine Gas		**Bleach - Triton**	
	GFP Roots	Total	GFP Roots	Total
Paste	15	**36**	30	**40**
Suspension	NA	NA	3	**36**

Figure 3.4 Soybean hairy root induction through *A. rhizogenes* inoculation.

A. Injection of a five-day old soybean hypocotyl with *A. rhizogenes* cell suspension using a needle. **B**. After 9-12 days hairy roots will have grown; the stem of the seedlings with roots 1cm in length would be cut and replanted. **C**. After two weeks the long roots can be used for assays. **D**. A summary of soybean hairy root transformation efficiency using different sterilization and bacterial inoculation methods.

miRNA accumulation through *MIR* expression in soybean hairy roots

Initial soybean transformations were performed with *A. rhizogenes* strains harboring constructs cloned only with the *MIR* genes, *AtMIR161* and *GmMIR1508*, to determine whether expression of the *MIR* genes would lead to accumulation of the corresponding miRNA. In all trials the *A. rhizogenes* strain carrying the empty pFGC5497 vector induced hairy roots from 90% of the inoculated seedlings. Additionally, 62% of those roots were positive for GFP expression. *A. rhizogenes* strain carrying pFGC5497::*AtMIR161* and pFGC5497::*GmMIR1508* both could induce hairy roots (Figure 3.5a). On average, *A. rhizogenes* strain carrying pFGC5497::*AtMIR161* induced roots from approximately 70% of the seedlings and 30% of these roots expressed GFP. However, *A. rhizogenes* strain carrying pFGC5497::*GmMIR1508* only induced hairy roots from 25% of the soybean seedlings after two weeks. Of these roots, only 16% expressed GFP (Figure 3.5b). Moreover, soybeans inoculated with *A. rhizogenes* strain carrying pFGC5497::*GmMIR1508* grew inconsistently and the roots would sometimes be induced at much later times after three weeks. Additionally, some roots would stop growing after reaching 0.5-1 cm in length. These observations indicate that over-expression of *GmMIR1508* may lead to growth inhibition in soybean roots.

Roots expressing GFP were further tested for the accumulation of *At*miR161 and *Gm*miR1508 using stem loop PCR. The results confirmed that *At*miR16*1* and *Gm*miR1508 were present in the transformed roots (Figure 3.5c). However, the expression of *Gm*miR1508 did not increase compared to untransformed roots (Figure 3.5d).

A.

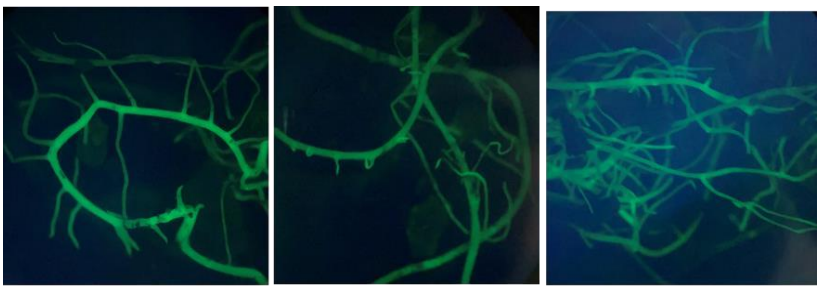

miR161 miR1508 EV

B.

	*At*MIR161	*Gm*MIR1508	EV
GFP positive soybeans	21/72	16/64	54/60
% of GFP positive roots	30%	16%	62%
miRNA accumulation	100%	100%	NA

C.

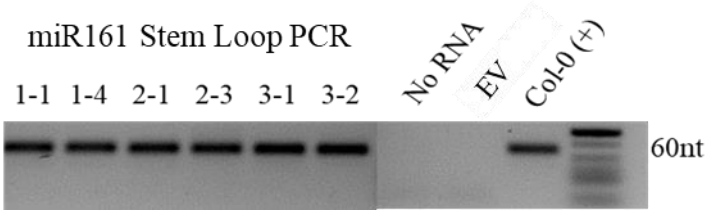

D.

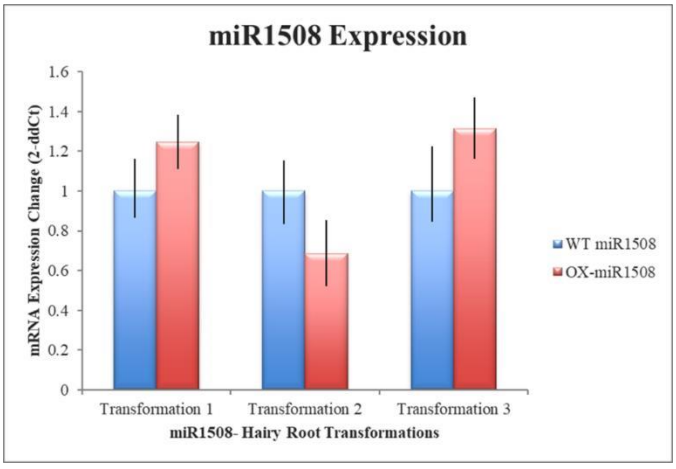

Figure 3.5 Soybean hairy roots expressing *MIR* genes accumulated corresponding miRNAs.

A. GFP expression detected from 4-week old soybean hairy root transformed by the empty vector (EV) pFGC5497 or pFGC5497 carrying *AtMIR161* or *GmMIR1508*. Scale bar, 5mm. **B.** A summary of hairy root transformation efficiency by the different plasmids. **C**. Stem loop PCR results showing miR161 accumulation in the transformed soybean roots. **D**. Stem loop qRT-PCR results showing the abundance of miR1508 expression in transformed soybean hairy roots. Each experiment used four root samples and the graph shows the average Ct values. The values were normalized using samples inoculated with *A. rhizogenes* carrying EV which should express endogenous miR1508. There was no significant difference between the samples.

Soybean roots transformed by the *MIR-PPR* cassettes did not accumulate *PPR*-siRNAs

After the *MIR* gene only expression, I introduced *A. rhizogenes* strains harboring constructs containing the entire *MIR-PPR* cassette. My hypothesis was that this construct would lead to an accumulation of secondary siRNAs spawned from the *PPR* transcript. Though a higher expression level of miR1508 was not confirmed, stem loop PCR revealed a natural expression. Therefore, a potential over-expression of the siRNA-generating gene *Glyma16g28020* may still lead to an increased *PPR*-siRNA production.

Inoculation by *A. rhizogenes* carrying pFGC5497::*AtMIR161-At1G62914mut* or pFGC5497::*GmMIR1508-Glyma16g28020* produced GFP-expressing roots in soybean seedlings (Figure 3.6a). Similar to the transformation efficiency difference observed in the previous experiments, the number of plants with roots expressing GFP was lower in seedlings inoculated with *A. rhizogenes* carrying the *MIR-PPR* cassette, specifically in *A. rhizogenes* carrying pFGC5497::*GmMIR1508-Glyma16g28020* (Figure 3.6b). However, stem loop PCR showed that *At*siR1310mut was undetectable in the roots transformed by pFGC5497::*AtMIR161-At1G62914mut* (Figure 3.6c) and *Gm*siR799 was not overexpressed (Figure 3.6d). RT-PCR showed that *At1g62914mut* was expressed in some but not all of the transformed roots (Figure 3.7). Since a mature miR161 is produced but not *At*siR1310mut, there may be some processing incapability within the soybean.

A.

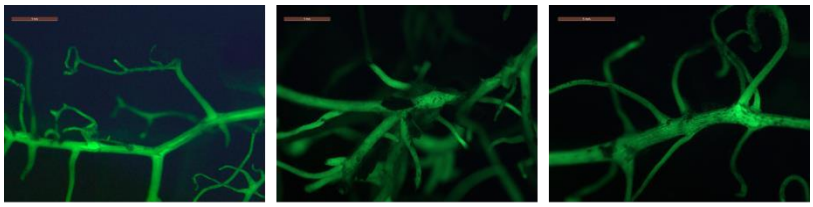

miR161-*At*1g62914mut | miR1508-*Glyma*16g28020 | EV

B.

	miR161-*PPR*	miR1508-*PPR*	EV
GFP positive soybeans	31/99	13/92	69/80
% of GFP positive roots	28%	10%	58%
siRNA accumulation	0	NA	NA

C.

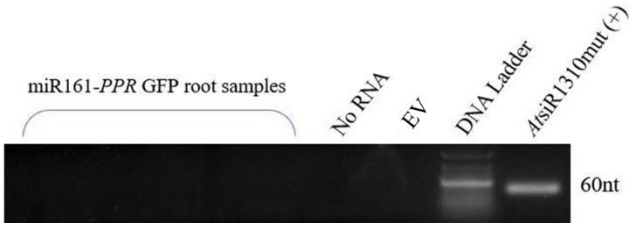

D.

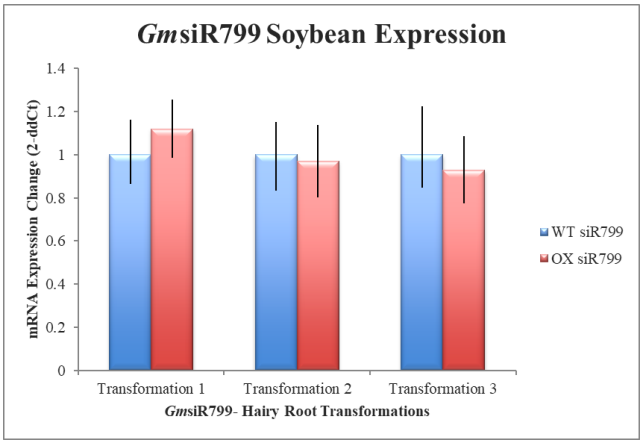

Figure 3.6 miRNA-PPR transformed hairy root results.

A. GFP expression detected from 3-week old soybean hairy root transformed by the empty vector (EV) pFGC5497 or pFGC5497 carrying *AtMIR161-At1G62914mut* or *GmMIR1508-Glyma16G28020*. Scale bar, 5mm. **B**. A summary of hairy root transformation efficiency by the different plasmids. **C**. Results of stem loop PCR detecting *At*siR1310mut from roots induced by *A. rhizogenes* carrying *AtMIR161-At1G62914mut*. **D**. Results of qRT-PCR determining the abundance of *Gm*siR799 hairy roots induced by *A. rhizogenes* carrying *GmMIR1508-Glyma16G28020*. This was normalized using roots induced by *A. rhizogenes* carrying EV which should express endogenous *Gm*siR799. There was no difference between the samples.

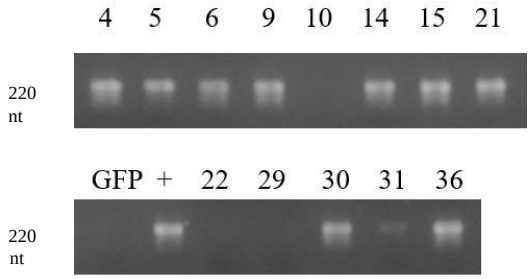

Figure 3.7 RT-PCR results showing the accumulation of *At1g62914mut* transcripts in some but not all the GFP-expressing roots transformed by *A. rhizogenes* carrying *AtMIR161-At1G62914mut*.

Samples are from the third transformation where 13 out of a total 42 soybean roots expressed GFP. Positive control (+) used cDNA from *A. thaliana* with primers designed from non-mutated sites of *At1g62914*. Negative control (GFP) used cDNA from soybean hairy roots inoculated with EV-GFP.

Target gene expression in *P. sojae* did not change in the presence of artificial *PPR*-siRNAs

The mechanism for translocation of plant siRNAs out of the plant and into *Phytophthora* is currently unknown. Previously, a synthesized *A. thaliana* PPR-siRNA siR1310 was introduced into *P. capsici* protoplasts to mimic what may happen during an infection. This resulted in a specific silencing effect of its target gene, *Phyca_554980*, and led to greatly reduced virulence activities (Hou et al., 2019). I designed a similar direct siRNA introduction method to study the potential silencing effect of candidate siRNAs on *P. sojae* targets genes. This assay could bypass the unknowns of whether the constructs would accumulate secondary siRNAs or translocation activity/mechanisms. The sense strand was designed with TT' overhangs to increase thermodynamic stability based on the design in Hou et al., 2019. However, no other modifications on the 5' or 3' ends were added. These siRNAs were introduced in *P. sojae* protoplasts along with a plasmid that confers G418 resistance and red fluorescence, pTOR::tdTomato. Transformants with G418 resistance may also uptake siRNAs and express red fluorescence allowing for easier screening.

The *At*siR1310mut duplex was synthesized to silence *P. sojae* gene *Physodraft_528320*, the homologous gene of *Phyca_554980* of *P. capsici*, which is targeted by *At*siR1310. Additionally, I also synthesized the endogenous soybean *PPR*-siRNA *Gm*siR799, predicted to target *Physodraft_468888* that encodes a hypothetical protein that contains FYVE domains. As a negative control, a siRNA duplex designed to target a *GFP* gene (siRGFP) from Hou et al., 2019 was also synthesized. Each artificial duplex (8 µg) were used to transform $2x10^4$ protoplasts together with the pTOR::tdTomato plasmid DNA. As a negative control to the protoplast transformation, one set of protoplasts were "transformed"

without either siRNA duplexes or the plasmid. No colonies recovered from the negative "no plasmid" *P. sojae* transformations on G418 selective media until six to nine days later. This contrasts with past "no plasmid" *P. capsici* colonies which surprisingly could recover in G418-containing media 36-42 hours after transformation (Chapter 2). As a positive control of the transformation, pTOR::tdTomato without artificial siRNA duplexes was also transformed.

Recovered colonies were grown for three days on selective media and screened for red fluorescence. RNA was extracted from the fluorescent colonies and used for stem loop PCR to detect the siRNAs. The results showed the presence of their respective siRNA in every sample (Figure 3.8). However, qRT-PCR of the target *P. sojae* genes *Physodraft_528320* and *Physodraft_468888* did not show changed abundance of their transcripts (Figure 3.9). One trial of transformants were inoculated onto soybeans on the same day as screening for fluorescence: two siRGFP, five siR1310 and five siR799. This was completed before confirmation of siRNA presence or target gene expression to reduce loss of artificial siRNAs as they are transient and may degrade. There was no clear reduction in lesion size consistent with no reduction in target gene expression (Figure 3.10). During one transformation, I increased the artificial duplex concentration of *At*siR1310mut by three times, 24 ug. All five transformants exhibited red fluorescence, however qRT-PCR results showed no significant decrease in *Physodraft_528320* expression. This could suggest that the artificial siRNA duplexes are inefficient in silencing the predicted target genes, potentially due to the lack of 5' modification (phosphorylation). Further optimization of the siRNA design is necessary to improve this experiment.

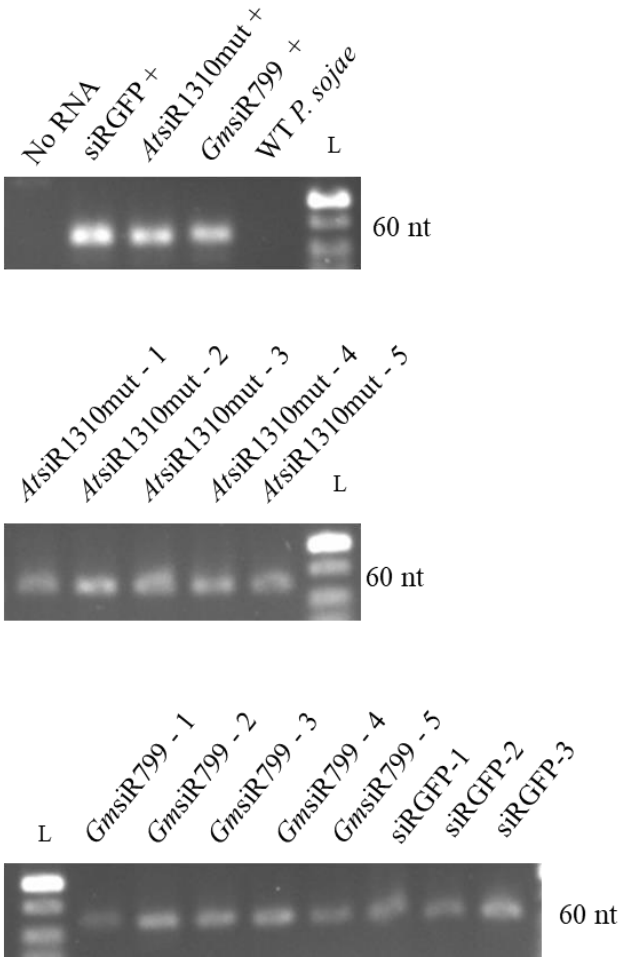

Figure 3.8 Detection of the artificial siRNA duplexes in transformed *P. sojae* by stem loop PCR.

The artificial siRNA duplexes were used as a positive control, and no RNA and WT *P. sojae* was used as a negative control (top gel). Band size for stem loop PCR product is 60 nt.

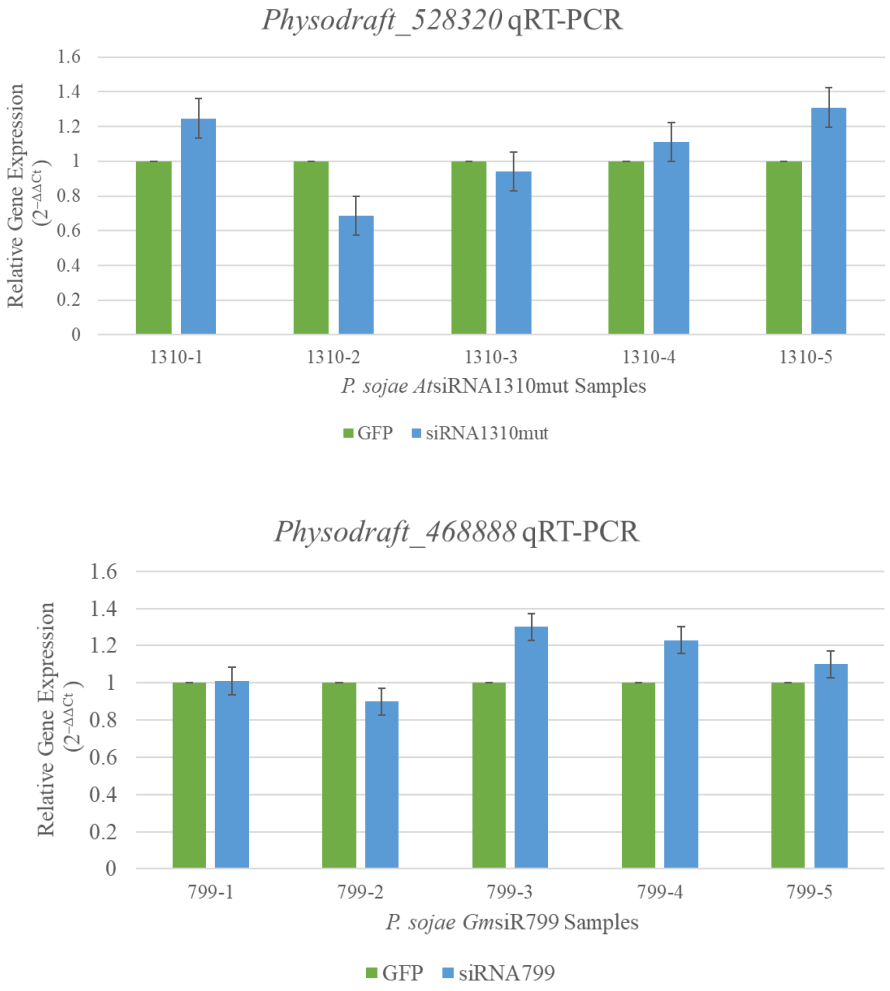

Figure 3.9 qRT-PCR results showing the transcript abundance of predicted target gene in *P. sojae* by artificial siRNAs.

P. sojae Actin gene was used as the internal control. None of the relative gene expression changes were significant.

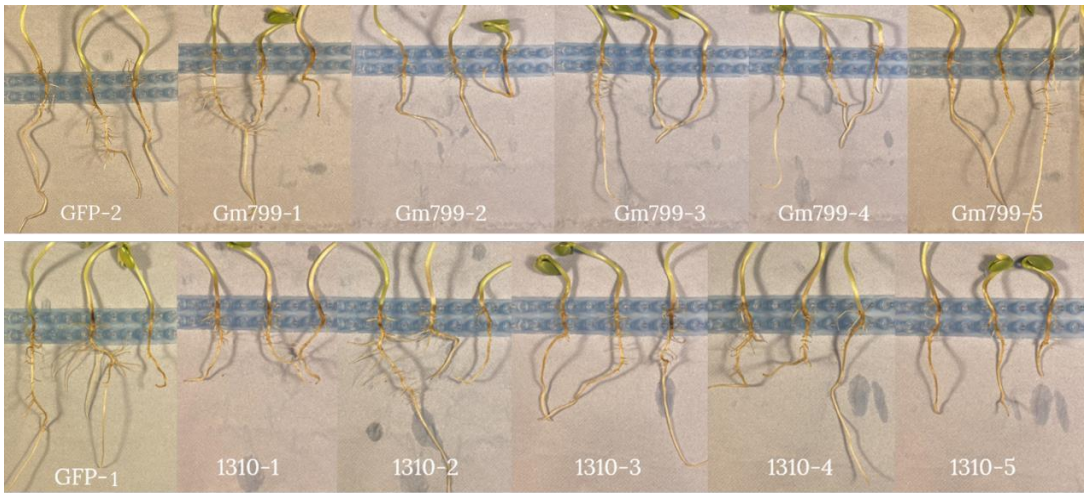

Figure 3.10 Artificial siRNA-transformed *P. sojae* did not show a change in virulence when inoculated on soybeans.

This assay was completed using a three-day hyphal plug inoculation on five-day old soybeans.

Specific artificial siRNA duplexes did not silence tdTomato expression in *P. sojae*

The two artificial siRNA duplexes tested in the previous session did not silence their predicted target genes in *P. sojae*. Therefore, I attempted to establish a system to function as a positive control of gene silencing for the artificial siRNA duplex assay. I designed siRNAs to target *tdTomato* gene in a red fluorescence expressing *P. sojae*. From the *tdTomato* gene sequence I produced a list of 682 21-nt sRNAs, siRtdTomato. To narrow down the list of candidates, sRNAs predicted to target *P. sojae* genes were removed. However, all siRtdTomato candidates were predicted to target *P. sojae* genes to some degree. Therefore, those with the lowest prediction score and number of hits to different *P. sojae* genes were chosen. One design chosen began with uridine siRtdTomato-202, the other with adenosine, siRtdTomato-209 (Figure 3.11a). In Arabidopsis, some AGO proteins preferentially load sRNAs with a 5′ terminal adenosine or 5′ uridine (Mi et al., 2008). Therefore, I decided to choose an artificial siRNA duplex with one of each. The duplexes were transformed into a wild-type *P. sojae* along with pTOR plasmid which confers G418 resistance. After screening 26 colonies including 12 transformed by siRtdTomato-202 and 14 transformed by siRtdTomato-209, none had visibly lost red fluorescence when compared to wild-type tdTomato expressing *P. sojae* (Figure 3.11b).

A.

682 tdTomato siRNAs → 27,013 matches → 6,570 matches → Top 4 final matches

```
>1
ATGGTGAGCAAGGGCGAGGAG
>2
TGGTGAGCAAGGGCGAGGAGG
>3
GGTGAGCAAGGGCGAGGAGGT
>4
GTGAGCAAGGGCGAGGAGGTC
>5
TGAGCAAGGGCGAGGAGGTCA
>6
GAGCAAGGGCGAGGAGGTCAT
>7
AGCAAGGGCGAGGAGGTCATC
>8
GCAAGGGCGAGGAGGTCATCA
```

Predicted siRNA matches to the *P. sojae* genome

With a low off-target prediction score. Sequences that begin with U' or A'

Fewest off-target predictions	
# of predicted targets	siRNA
10	200
3	202
6	209
9	577

B

Figure 3.11 Silencing *P. sojae* red fluorescent strain using artificial siRNA duplexes. **A.** Pipeline used to design siRNAs for silencing *tdTomato* in *P. sojae*. Candidates with the fewest predicted off-target hits were chosen. **B.** Representative images of *P. sojae* hyphae expressing *tdTomato* after transformed with synthesized siRtdTom. *P. sojae* transformed with siRGFP was used as a negative control.

MATERIALS AND METHODS

MiRNA-siRNA circuit prediction pipeline

Using a list of 73,171 *Glycine max* (soybean) sRNAs loci from Plant small RNA genes online repository, (https://plantsmallrnagenes.science.psu.edu/genomes.php?id=9) (Lunardon et al., 2020), I identified the loci of 2,219 siRNAs. This was done by removing known miRNAs using miRBase (https://www.mirbase.org/) (Griffiths-Jones et al., 2008; Kozomara et al., 2019), and only keeping siRNAs whose major reads were 21nt in size. Then the siRNAs were matched to their siRNA-generating loci. Those miRNA triggers for those siRNAgenerating loci were predicted using a plant small RNA target analysis server: PsRNATarget (http://plantgrn.noble.org/psRNATarget) (Dai & Zhao, 2011). The submitted siRNAgenerating loci sequences were scored against all *Glycine max* miRNAs with at an expectation threshold of 3.0. The remaining potential secondary siRNAs were ranked based on abundance and PHAS score from the Plant small RNA genes online tool. List of 682 tdTomato "siRNA" were produced by writing a short Python program to produce a recursive list of 21nt long sequences.

MiRNA-siRNA circuit plasmid construction

The original binary vector pFGC5491 expressed GFP under the Mannopine synthase promoter and MAS terminator. *MIR* genes are inserted between CaMV promoter and *A. thaliana* heat shock protein terminator. The siRNA-generating loci are cloned between the Glycine max polyubiquitin promoter (Gmubi) and Octopine synthase terminator. The miRNA-siRNA cassette plasmid was generated by inserting a set of synthesized promoter and terminator fragments using InFusion cloning by linearizing the plasmid at the Nco1AvrII

restriction site. This construct allows for any miRNA to be easily inserted by linearizing the plasmid at the Asc1 and Kpn1 site. For the siRNA loci, they can be inserted by linearizing AvrII, XbaI, PacI or SpeI restriction enzyme sites.

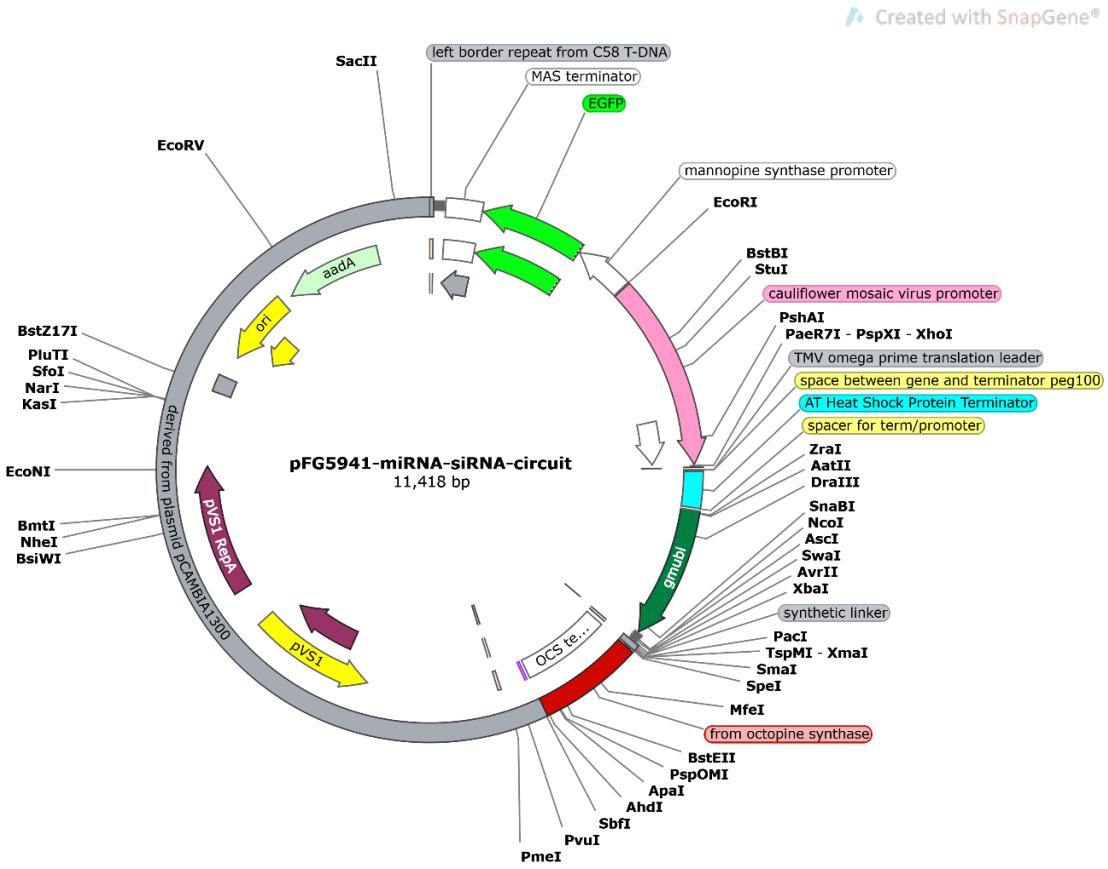

Figure 3.12 Plasmid map of pFGC5941-miRNA-siRNA for *A. rhizogenes*-mediated hairy root transformation.

The plasmid contains three promoter-terminator pairs. GFP is inserted between the Mannopine synthase promoter and terminator and used to screen for transformed roots. *MIR* genes are inserted between CaMV promoter and *A. thaliana* heat shock protein terminator. The siRNA-generating loci are cloned between the Glycine max polyubiquitin promoter (Gmubi) and Octopine synthase terminator.

Soybean growth

Seeds are surface sterilized with bleach solution (30% commercial bleach + 0.02% Triton X100) for 15 min, washed 3 times with sterile water. Seeds are then planted 1cm inside autoclaved vermiculite and set on a 12-hour light cycle at 26°. Soybeans were watered with B&D solution every three days (1000 µM$CaCl_2{-}2H_2O$, 500 µM KH_2PO_4, 10 µM Fe-Citrate, 250 µM $MgSO_4{-}7H_2O$, 1500 µM K_2SO_4, 1 µM $MnSO_4{-}H_2O$, 2 µM H_3BO_4, 0.5 µM $ZnSO_4{-}7H_2O$, 0.2 µM, $CuSO_4{-}5H_2O$, 0.1 µM $CoSO_4{-}7H_2O$, 0.1 µM $Na_2MoO_4{-}2H_2O$).

Soybean hairy roots induction

Soybean hairy roots were induced by *Agrobacterium rhizogenes* strain K599.
A. rhizogenes was grown and maintained with Luria-Bertani medium and supplemented with antibiotics for plasmid maintenance. Using a protocol described in Kereszt et al., 2007 sterilized seeds were inoculated at cotyledonary node and the hypocotyl, then kept under high humidity. After 9-12 days hairy roots sprouted from the inoculation site. Once roots were over 1cm in length the stem was cut 1cm below the hairy root growth and replanted. Hairy roots development was monitored during a period of four weeks and the roots that exhibited GFP fluorescence under a fluorescent microscope (Leica DM5500 or Leica SP5) were used for stem loop PCR and *P. sojae* infection.

P. sojae transformation

PEG-mediated protoplast transformation protocol is the same as Chapter 1 with some minor changes. 25µg of pTOR::tdTomato was co-transformed with 8µg of their respective artificial siRNA duplex per 20,000 protoplasts. This is a significantly lower number of protoplasts than in regular *Phytophthora* transformation. One assay uses three times the concentration of

siRNA, 24 µg. Duplex was annealed from sense and antisense single strand oligonucleotides by first dissolving each oligonucleotide in annealing buffer (10 mM Tris, pH 7.5 - 8.0, 50 mM NaCl, 1 mM EDTA). Equal volumes are heated to 95 °C for 2 min. Then cooled to 25°C over 45 min.

Artificial siRNA duplex oligonucleotides used in this chapter:

siRNA1310mut sense	UAGAAUAACGUUGACGAGAUC
siRNA1310mut antisense	UCUCGUCAACGUUAUUCUATT
GM799-siRNA-sense	AAAGAAAAGGACAUUUGGCCC
GM799-siRNA-sense	TTGGGCCAAAUGUCCUUUUCU
AcGFP-siRNA-sense	GCAUCAAGGUGAACUUCAATT
AcGFP-siRNA-antisense	UUGAAGUUCACCUUGAUGCCA
tdTomato siRNA202sense	UACGGCUCCAAGGCGUACGUG
tdTomato siRNA202antisense	CGUACGCCUUGGAGCCGUATT
tdTomato siRNA209sense	AAGGCGUACGUGGAUGAUCCG
tdTomato siRNA209antisense	CGGCUACUACGUACGCCUUTT

Quantitative PCR (qPCR) for *P. sojae* genes.

The RNA was extracted as described in Chapter 1. RNA from two-day-old *P. sojae* hyphae used to make cDNA. 1µg of total RNA was DNase-treated and reverse transcribed by RevertAid Reverse Transcriptase with RiboLock RNase Inhibitor at 42°C for one hour using oligo-dT as a primer. 30X diluted cDNA was then used for qPCR analysis using SYBR Green Supermix and Bio-Rad CFX96 thermocycler. For the qPCR reaction primers were used at a final concentration of 5µM. Cycle conditions were an initial denaturation at 95°C for 2min followed by 42 cycles of 95°C for 15s, 56°C for 30s, and 72°C for 30s and a melt curve cycle at 65°C for 5s and 95°C for 5s. Relative expression levels calculated using *P. sojae* actin as the internal control and calculated using 2^{-DDCt}.

qPCR primers used:

PsACT qRT R	CCACCACCTTGATCTTCATG
PsACT qRT F	ACTGCACCTTCCAGACCATC
qPHYSODRAFT_528320 1F	TAGTTGGGCTGCTGTACGTG
qPHYSODRAFT_528320 1R	ACATACGACCGACGATGCTC
qPhysoDRAFT_468888 1F	CGACTTCGTGTGGACTGTGA
qPhysoDRAFT_468888 1R	GCGCGTTCACGACTTTTCTT

Stem loop PCR

RNA was extracted in *P. sojae* hyphae and hairy root transformants for the stem loop PCR as described in Chapter 1. However, *P. sojae* hyphae was grown for only two days post transformation on V8 media plates before collection for RNA extraction. Half of the V8 plate where the hyphae grew was submerged in liquid nitrogen and then the hyphae was scraped off for RNA extraction. The other half of the V8 plate with hyphae growing was used to inoculate soybeans. Stem loop PCR protocol was adapted from (Varkonyi-Gasic et al., 2007). When testing many RNA samples for one miRNA, a "no RNA" RT master mix (per sample: 0.5 µL 10 mM dNTP mix, 11.15 µL nuclease-free water, 1 µL of appropriate stem-loop RT primer (1 µM)) was added to a nuclease-free microcentrifuge tube proportional to the number of reactions being prepared. When testing many different miRNAs in one sample, a "no RT primer" RT master mix (per sample: 0.5 µL 10 mM dNTP mix, 11.15 µL nuclease-free water, 1 µL of appropriate RNA template) was added to a nuclease-free microcentrifuge tube proportional to the number of reactions being prepared. Following the preparation of the RT master mix, the tube was then heated to 65°C for five minutes, then incubated on ice for 2 minutes. The tube was then briefly centrifuged to consolidate the solution at the bottom, and

the following reagents were added to the tube (again proportional to the number of reactions being performed): 4 µL 5x First-Strand buffer, 2 µL 0.1 M DTT, 0.1 µL RNaseOUT (40 units/µL), and 0.25 µL SuperScript III RT (200 units/µL). This solution was mixed gently, then centrifuged to bring the solution to the bottom of the tube. The RT reactions were then assembled, and the following were added to each reaction tube: 19 µL of master mix, 1 µL RNA template for "no RNA" master mix. Negative RT controls were prepared by omitting reverse transcriptase, and water controls were prepared by adding nuclease-free water in place of RNA. Samples were loaded into the thermal cycler, and incubated for 30 min at 16°C, followed by pulsed RT of 60 cycles at 30°C for 30 seconds, 42°C for 30 seconds, and 50°C for 1 second. Then the samples were incubated at 85°C for 5 minutes to inactivate the reverse transcriptase. A PCR master mix (15.4 µL nuclease-free water, 2 µL 10x PCR buffer, 0.4 µL 10 mM dNTP mix, 0.4 µL forward primer (10 µM), 0.4 µL reverse primer (10 µM), 0.4 µL Advantage 2 Polymerase mix) The reactions were prepared by aliquoting 19 µL of PCR master mix and 1µL RT product into PCR tubes. Water controls were prepared by adding nuclease-free water in place of the RT product. Reactions were placed into a 94°C preheated thermal cycler, and incubated at 94°C for 2 minutes, followed by 20-40 cycles of 94°C for 15 seconds and 60°C for 1 minute. Reaction products were then analyzed by electrophoresis on a 4% agarose gel in 1x TAE. Invitrogen™ Ultra Low Range DNA Ladder was used as ladder for the gel.

To examine the expression of miR1508 or GmsiR799, a 5x SYBR Green I master mix was prepared according to manufacturer's instructions. Then, a PCR master mix (12 µL nuclease-free water, 4 µL SYBR Green I master mix, 1 µL forward primer (10 µM), 1 µL reverse primer (10 µM)) Final mix of 18 µL of master mix was added into each tube, followed by 2

µL of RT product. The samples were then incubated at 95°C for 5 minutes, followed by 3545 cycles of 95°C for 5 seconds, 60°C for 10 seconds, and 72°C for 1 second. Fluorescence signals were collected at 530 nm wavelength continuously from 65°C to 95°C at 0.2°C per second.

DISCUSSION

As new methods of disease resistance need to be uncovered, strategies based on HIGS-mediated by secondary siRNA hold promise. A pool of secondary siRNAs can potentially target multiple genes in one pathogen, or even target various eukaryotic pathogenic organisms. Importantly, this "shot-gun" approach is presumably more sustainable in the host-pathogen arms race. Some studies using sRNA profiling of apoplasts and extracellular vesicles suggest that while many miRNAs are relatively enriched in the plant cytoplasm, secondary siRNAs are enriched in the apoplast (Baldrich et al., 2019). This indicates that miRNAs have a lower tendency to be secreted into extracellular spaces Therefore, though amiRNA constructs have been used in HIGS, utilizing a cassette that produce siRNAs instead of a miRNA could improve silencing efficiency. Furthermore, engineering of siRNA production using *MIR-PPR* cassette would modify the *PPR*-siRNA population in a plant and may strengthen the gene silencing efficiency in invading pathogens.

As promoter read-through and promoter recombination can occur, I constructed a plasmid using three separate promoter and terminators. However, since *At1g62914mut* did not consistently express *in planta* it may be one factor to consider as to whether the inconsistent expression may have contributed to the lack of AtsiR1310mut production. It's possible that the *MIR* genes did not trigger the production of the secondary siRNAs. To investigate this issue, miRNA cleavage of the target mRNA could be examined by RLM-RACE (Wang & Fang, 2015). Expression of *AtMIR161* and *GmMIR1508* led to reduced hairy root induction. This is particularly significant for *GmMIR1508*. It is possible that these miRNAs may inhibit root development, which somehow affect the production of secondary siRNAs. Furthermore, only one secondary siRNA from each cassette was examined. There

could be other siRNAs produced in these roots. Small RNA-seq could be used to investigate whether this is the case.

If secondary siRNAs are indeed produced from the roots expressing *MIR-PPR* cassettes, the roots would have been examined for their susceptibility to *P. sojae*. The predicted *P. sojae* target genes would have been monitored for their transcript levels in the infected roots. The sequencing information could also have been used to predict potential natural HIGS targets in *P. sojae*. Had promising results been seen, stable transformants would have been generated. The transformed soybeans would then be inoculated with *P. sojae* and tested to confirm siRNA production. I would also have tested their resistance to *P. sojae* by determining biomass and disease index. I would have anticipated increased resistance in the stably transformed soybeans towards *P. sojae*. Though soybeans that can accumulate specific anti-pathogenic secondary siRNAs were unable to be generated, these constructs can still be valuable in optimizing this secondary siRNA production strategy. Through this, we can continue studying HIGS and eventually use this mechanism as an additional layer of protection against pathogens in soybean and other crops.

Using the secondary siRNA replacement strategy relies on three unknown elements; whether the miRNA-siRNA circuits will produce the intended siRNAs, if the siRNAs are produced will they translocate into the pathogen from the host plants, and lastly, once translocated, will the candidate siRNA actually silence the target pathogen gene. Therefore to identify good candidates to target in *P. sojae* and remove the first two unknown elements in this strategy, I directly introduced artificial siRNA duplexes into *P. sojae* protoplasts. Using a sRNA prediction program, I identified that *Gm*siR799 may target *Physodraft_468888* which is predicted to encode a FYVE-type domain-containing protein. This gene has been

associated with endosome function (Leevers et al., 1999). Additionally in *P. sojae,* a FYVE-domain-containing protein, PsFP1, is involved with functions such as vegetative growth and virulence (Zhang et al., 2021). This target prediction made *Gm*siR799 an interesting siRNA candidate to examine its silencing effects on *P. sojae*. Moreover, the target of *At*siR1310mut, *Physodraft_528320,* is the homologue of *P. capsici* gene, *Phyca_554980,* encoding a U2 associated spliceosome factor. The *P. capsici* gene decreased in its expression and saw decreased virulence in the presence of *At*siR1310. Therefore, both siRNAs' target gene in *P. sojae* were hypothesized to exhibit some phenotypic changes correlating with expression change. However, none of the transformants for either siRNA resulted in decreased expression in their respective target *P. sojae* genes. It is unlikely that this is due to the artificial siRNA duplexes completely degrading as stem loop PCR results indicate their presence in the hyphae. RNA was extracted from hyphal samples two days after recovery, the soonest possible time for sufficient hyphal regeneration for simultaneous extraction and soybean inoculation to prevent siRNA degradation. The siRNA sense and antisense strands were designed to exactly match the artificial siRNA strands used for *P. capsici* gene targets in Hou et al., 2019 which successfully correlated to decreased expression when introduced into protoplasts. These results could suggest that there may be another mechanism that can prevent silencing in these target genes or that the design of the artificial siRNAs need optimization. Natural siRNAs are generated with a 5'-phosphate and 3'hydroxyl groups (Elbashir et al., 2001; Lau et al., 2001). The 5'-phosphate is required during RISC assembly. Specifically, the 5' phosphorylation of a duplex siRNA in human cells was a determinants of strand incorporation into RISC (Chen et al., 2008). In plants, further methylation at the 3' end is also important for sRNA stability and loading. However, the artificial siRNAs were not

designed with any end modifications apart from a leading strand TT'. Modifying the artificial siRNA may lead to greatly increased silencing efficiency. A traditional knock-down in soybean using amiRNA could have been an alternative to direct siRNA duplex introduction for identifying good candidates of silencing to examine the effect on pathogen virulence and fitness. However, it was not chosen as it did not represent the siRNA duplex that would be produced from the construct. Co-immunoprecipitation assays in *P. infestans* revealed that the *P. infestans* AGO1 (*Pi*Ago1) largely associates with 20-22-nt sRNAs, with a preference for 5′ C (Bollmann et al., 2018). However, a recent study found that *Pi*Ago1 changes 5′ nucleotide preference from C to U during infection (Hu et al., 2022). Therefore, siRNAs with 5′ C could have been more suitable candidates. In my experiments, only two from the potential list of 682 siRNAs were used for protoplast transformation. One method to identify a suitable siRNA candidate would be to methodically screen by using a larger subset of artificial siRNA duplexes. Performing a large-scale screening could potentially give information concerning whether siRNAs with certain 5′ nucleotides are more suitable for silencing genes in *P. sojae*.

The secondary siRNA replacement strategy of soybean and Arabidopsis genes represents a first attempt to apply this new approach in HIGS and test it in an economically important crop. In addition to *P. sojae*, the transgenic soybean generated using this strategy could potentially target genes in, and thus confer resistance to, other pathogens such as soybean cyst nematodes, *Pythium*, or *Fusarium oxysporum*. I still hypothesize that this system can be utilized to produce customized siRNAs by modifying the sequence of *PPR* genes in order to target specific genes in specific pathogens. A similar approach could

potentially be applied to other pathosystems. In summary, this first effort has given some insight into has the promise to confer broad-spectrum resistance to soil-borne pathogens.

REFERENCES

Arikit, S., Xia, R., Kakrana, A., Huang, K., Zhai, J., Yan, Z., Valdés-López, O., Prince, S., Musket, T. A., Nguyen, H. T., Stacey, G., & Meyers, B. C. (2014). An Atlas of Soybean Small RNAs Identifies Phased siRNAs from Hundreds of Coding Genes. *The Plant Cell*, *26*(12), 4584–4601. https://doi.org/10.1105/tpc.114.131847

Baldrich, P., Rutter, B. D., Karimi, H. Z., Podicheti, R., Meyers, B. C., & Innes, R. W. (2019). Plant Extracellular Vesicles Contain Diverse Small RNA Species and Are Enriched in 10- to 17-Nucleotide "Tiny" RNAs. *The Plant Cell*, *31*(2), 315–324. https://doi.org/10.1105/tpc.18.00872

Bollmann, S. R., Press, C. M., Tyler, B. M., & Grünwald, N. J. (2018). Expansion and Divergence of Argonaute Genes in the Oomycete Genus Phytophthora. *Frontiers in Microbiology*, *9*. https://www.frontiersin.org/articles/10.3389/fmicb.2018.02841

Chen, P. Y., Weinmann, L., Gaidatzis, D., Pei, Y., Zavolan, M., Tuschl, T., & Meister, G. (2008). Strand-specific 5′-O-methylation of siRNA duplexes controls guide strand selection and targeting specificity. *RNA*, *14*(2), 263–274. https://doi.org/10.1261/rna.789808

Dai, X., & Zhao, P. X. (2011). psRNATarget: A plant small RNA target analysis server. *Nucleic Acids Research*, *39*(Web Server issue), W155–W159. https://doi.org/10.1093/nar/gkr319

de la Luz Gutiérrez-Nava, M., Aukerman, M. J., Sakai, H., Tingey, S. V., & Williams, R. W. (2008). Artificial trans-Acting siRNAs Confer Consistent and Effective Gene Silencing. *Plant Physiology*, *147*(2), 543–551. https://doi.org/10.1104/pp.108.118307

Dorrance, A. E. (2018). Management of Phytophthora sojae of soybean: A review and future perspectives. *Canadian Journal of Plant Pathology*, *40*(2), 210–219. https://doi.org/10.1080/07060661.2018.1445127

Dorrance, A. E., Jia, H., & Abney, T. S. (2004). Evaluation of Soybean Differentials for Their Interaction with Phytophthora sojae. *Plant Health Progress*, *5*(1), 9. https://doi.org/10.1094/PHP-2004-0309-01-RS

Elbashir, S. M., Lendeckel, W., & Tuschl, T. (2001). RNA interference is mediated by 21- and 22-nucleotide RNAs. *Genes & Development*, *15*(2), 188–200. https://doi.org/10.1101/gad.862301

Food and Agriculture Organization of the United Nations. *FAOSTAT statistical database*. [Rome]: FAO, c1997-. https://search.library.wisc.edu/catalog/999890171702121

Gao, H., Narayanan, N. N., Ellison, L., & Bhattacharyya, M. K. (2005). Two classes of highly similar coiled coil-nucleotide binding-leucine rich repeat genes isolated from the Rps1-k locus encode Phytophthora resistance in soybean. *Molecular Plant-Microbe Interactions: MPMI*, *18*(10), 1035–1045. https://doi.org/10.1094/MPMI-18-1035

Griffiths-Jones, S., Saini, H. K., van Dongen, S., & Enright, A. J. (2008). miRBase: Tools for microRNA genomics. *Nucleic Acids Research*, *36*(suppl_1), D154–D158. https://doi.org/10.1093/nar/gkm952

Hou, Y., & Ma, W. (2020). Natural Host-Induced Gene Silencing Offers New Opportunities to Engineer Disease Resistance. *Trends in Microbiology*, *28*(2), 109–117. https://doi.org/10.1016/j.tim.2019.08.009

Hou, Y., Zhai, Y., Feng, L., Karimi, H. Z., Rutter, B. D., Zeng, L., Choi, D. S., Zhang, B., Gu, W., Chen, X., Ye, W., Innes, R. W., Zhai, J., & Ma, W. (2019). A Phytophthora Effector Suppresses Trans-Kingdom RNAi to Promote Disease Susceptibility. *Cell Host & Microbe*, *25*(1), 153-165.e5. https://doi.org/10.1016/j.chom.2018.11.007

Hu, X., Persson Hodén, K., Liao, Z., Åsman, A., & Dixelius, C. (2022). Phytophthora infestans Ago1-associated miRNA promotes potato late blight disease. *New Phytologist*, *233*(1), 443–457. https://doi.org/10.1111/nph.17758

Kereszt, A., Li, D., Indrasumunar, A., Nguyen, C. D., Nontachaiyapoom, S., Kinkema, M., & Gresshoff, P. M. (2007). Agrobacterium rhizogenes-mediated transformation of soybean to study root biology. *Nature Protocols*, *2*(4), Article 4. https://doi.org/10.1038/nprot.2007.141

Kis, A., Tholt, G., Ivanics, M., Várallyay, É., Jenes, B., & Havelda, Z. (2016). Polycistronic artificial miRNA-mediated resistance to Wheat dwarf virus in barley is highly efficient at low temperature. *Molecular Plant Pathology*, *17*(3), 427–437. https://doi.org/10.1111/mpp.12291

Koch, A., & Wassenegger, M. (2021). Host-induced gene silencing – mechanisms and applications. *New Phytologist*, *231*(1), 54–59. https://doi.org/10.1111/nph.17364

Kozomara, A., Birgaoanu, M., & Griffiths-Jones, S. (2019). miRBase: From microRNA sequences to function. *Nucleic Acids Research*, *47*(D1), D155–D162. https://doi.org/10.1093/nar/gky1141

Lau, N. C., Lim, L. P., Weinstein, E. G., & Bartel, D. P. (2001). An Abundant Class of Tiny RNAs with Probable Regulatory Roles in *Caenorhabditis elegans*. *Science*, *294*(5543), 858–862. https://doi.org/10.1126/science.1065062

Leevers, S. J., Vanhaesebroeck, B., & Waterfield, M. D. (1999). Signalling through phosphoinositide 3-kinases: The lipids take centre stage. *Current Opinion in Cell Biology*, *11*(2), 219–225. https://doi.org/10.1016/S0955-0674(99)80029-5

Lunardon, A., Johnson, N. R., Hagerott, E., Phifer, T., Polydore, S., Coruh, C., & Axtell, M. J. (2020). Integrated annotations and analyses of small RNA–producing loci from 47 diverse plants. *Genome Research*, *30*(3), 497–513. https://doi.org/10.1101/gr.256750.119

Masanga, J. O., Matheka, J. M., Omer, R. A., Ommeh, S. C., Monda, E. O., & Alakonya, A. E. (2015). Downregulation of transcription factor aflR in Aspergillus flavus confers reduction to aflatoxin accumulation in transgenic maize with alteration of host plant architecture. *Plant Cell Reports*, *34*(8), 1379–1387. https://doi.org/10.1007/s00299-015-1794-9

Masuda, T., & Goldsmith, P. D. (2009). *World Soybean Production: Area Harvested, Yield, and Long-Term Projections*. *12*(4), 20.

Mi, S., Cai, T., Hu, Y., Chen, Y., Hodges, E., Ni, F., Wu, L., Li, S., Zhou, H., Long, C., Chen, S., Hannon, G. J., & Qi, Y. (2008). Sorting of Small RNAs into Arabidopsis Argonaute Complexes Is Directed by the 5′ Terminal Nucleotide. *Cell*, *133*(1), 116–127. https://doi.org/10.1016/j.cell.2008.02.034

Panwar, V., Jordan, M., McCallum, B., & Bakkeren, G. (2018). Host-induced silencing of essential genes in Puccinia triticina through transgenic expression of RNAi sequences reduces severity of leaf rust infection in wheat. *Plant Biotechnology Journal*, *16*(5), 1013–1023. https://doi.org/10.1111/pbi.12845

Rodrigues, N. F., Nogueira, F. C. S., Domont, G. B., & Margis, R. (2020). Identification of soybean trans-factors associated with plastid RNA editing sites. *Genetics and Molecular Biology*, *43*(1 suppl 2), e20190067. https://doi.org/10.1590/1678-4685-gmb-2019-0067

Sang, H., & Kim, J.-I. (2020). Advanced strategies to control plant pathogenic fungi by hostinduced gene silencing (HIGS) and spray-induced gene silencing (SIGS). *Plant Biotechnology Reports*, *14*(1), 1–8. https://doi.org/10.1007/s11816-019-00588-3

Sedivy, E. J., Wu, F., & Hanzawa, Y. (2017). Soybean domestication: The origin, genetic architecture and molecular bases. *New Phytologist*, *214*(2), 539–553. https://doi.org/10.1111/nph.14418

Tyler, B. M. (2007). Phytophthora sojae: Root rot pathogen of soybean and model oomycete. *Molecular Plant Pathology*, *8*(1), 1–8. https://doi.org/10.1111/j.1364-3703.2006.00373.x

Varkonyi-Gasic, E., Wu, R., Wood, M., Walton, E. F., & Hellens, R. P. (2007). Protocol: A highly sensitive RT-PCR method for detection and quantification of microRNAs. *Plant Methods*, *3*(1), 12. https://doi.org/10.1186/1746-4811-3-12

Wang, C., & Fang, J. (2015). RLM-RACE, PPM-RACE, and qRT-PCR: An Integrated Strategy to Accurately Validate miRNA Target Genes. In M. Rederstorff (Ed.), *Small Non-Coding RNAs: Methods and Protocols* (pp. 175–186). Springer. https://doi.org/10.1007/9781-4939-2547-6_16

Wang, W., Chen, L., Fengler, K., Bolar, J., Llaca, V., Wang, X., Clark, C. B., Fleury, T. J., Myrvold, J., Oneal, D., van Dyk, M. M., Hudson, A., Munkvold, J., Baumgarten, A., Thompson, J., Cai, G., Crasta, O., Aggarwal, R., & Ma, J. (2021). A giant NLR gene confers broad-spectrum resistance to Phytophthora sojae in soybean. *Nature Communications*, *12*(1), Article 1. https://doi.org/10.1038/s41467-021-26554-8

Wong, J., Gao, L., Yang, Y., Zhai, J., Arikit, S., Yu, Y., Duan, S., Chan, V., Xiong, Q., Yan, J., Li, S., Liu, R., Wang, Y., Tang, G., Meyers, B. C., Chen, X., & Ma, W. (2014). Roles of small RNAs in soybean defense against Phytophthora sojae infection. *The Plant Journal*, *79*(6), 928–940. https://doi.org/10.1111/tpj.12590

Xia, R., Meyers, B. C., Liu, Z., Beers, E. P., Ye, S., & Liu, Z. (2013). MicroRNA Superfamilies Descended from miR390 and Their Roles in Secondary Small Interfering RNA Biogenesis in Eudicots. *The Plant Cell*, *25*(5), 1555–1572. https://doi.org/10.1105/tpc.113.110957

You, C., Cui, J., Wang, H., Qi, X., Kuo, L.-Y., Ma, H., Gao, L., Mo, B., & Chen, X. (2017). Conservation and divergence of small RNA pathways and microRNAs in land plants. *Genome Biology*, *18*(1), 158. https://doi.org/10.1186/s13059-017-1291-2

Zhang, J., Du, X., Zhou, X., Jin, D., Miao, J., & Liu, X. (2021). An FYVE-Domain-Containing Protein, PsFP1, Is Involved in Vegetative Growth, Oxidative Stress Response and Virulence of Phytophthora sojae. *International Journal of Molecular Sciences*, *22*(12), Article 12. https://doi.org/10.3390/ijms22126601